

Driver's risk field

A step towards a unified driver model

Kolekar, S.B.

DOI

[10.4233/uuid:a118e35c-dec9-4c1f-9ed7-8b65a5ca77a3](https://doi.org/10.4233/uuid:a118e35c-dec9-4c1f-9ed7-8b65a5ca77a3)

Publication date

2021

Document Version

Final published version

Citation (APA)

Kolekar, S. B. (2021). *Driver's risk field: A step towards a unified driver model*. [Dissertation (TU Delft), Delft University of Technology]. <https://doi.org/10.4233/uuid:a118e35c-dec9-4c1f-9ed7-8b65a5ca77a3>

Important note

To cite this publication, please use the final published version (if applicable).
Please check the document version above.

Copyright

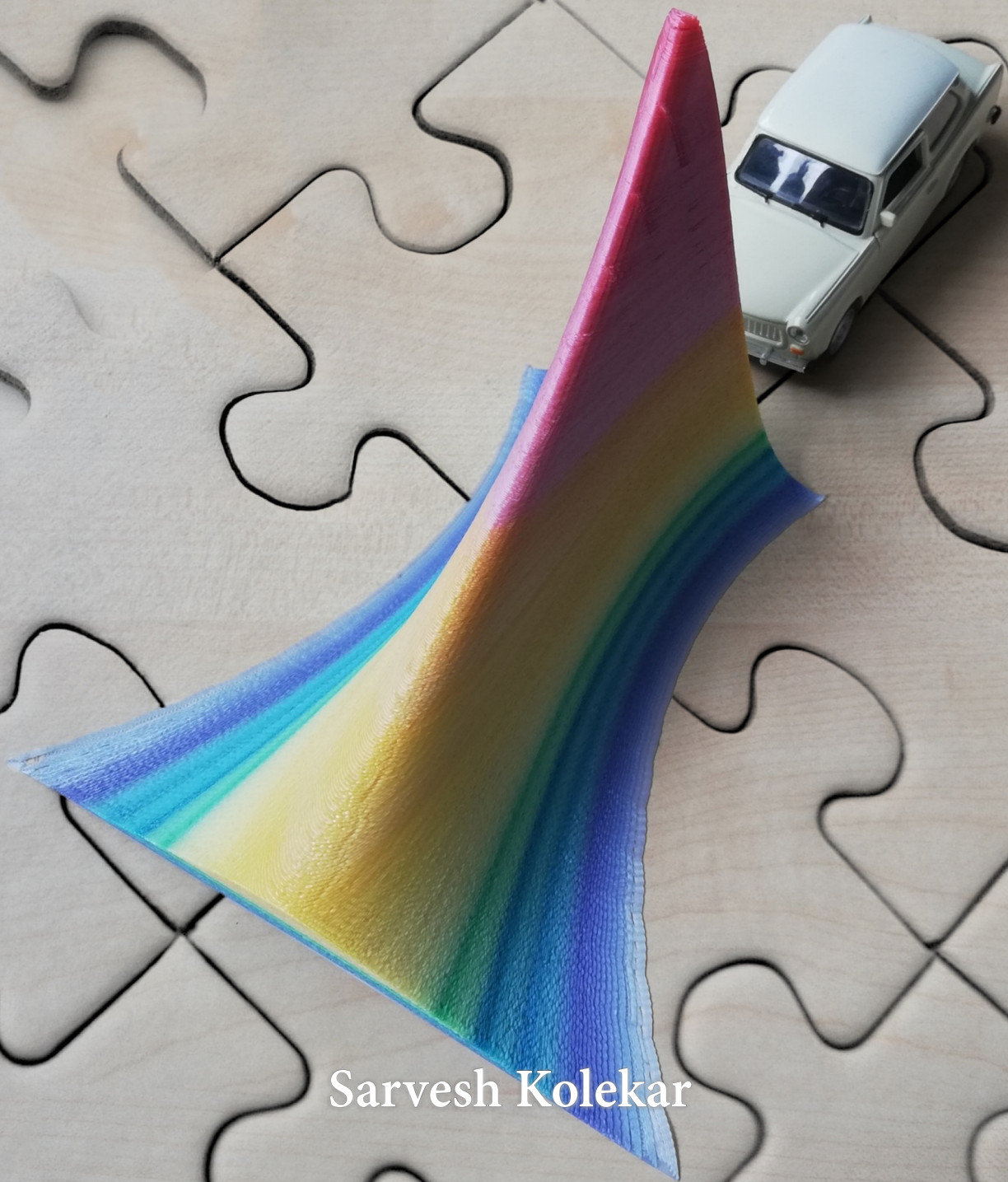
Other than for strictly personal use, it is not permitted to download, forward or distribute the text or part of it, without the consent of the author(s) and/or copyright holder(s), unless the work is under an open content license such as Creative Commons.

Takedown policy

Please contact us and provide details if you believe this document breaches copyrights.
We will remove access to the work immediately and investigate your claim.

Driver's Risk Field

A step towards a unified driver model



Sarvesh Kolekar

DRIVER'S RISK FIELD

A STEP TOWARDS A UNIFIED DRIVER MODEL

DRIVER'S RISK FIELD

A STEP TOWARDS A UNIFIED DRIVER MODEL

Proefschrift

ter verkrijging van de graad van doctor
aan de Technische Universiteit Delft,
op gezag van de Rector Magnificus prof. dr. ir. T.H.J.J. van der Hagen,
voorzitter van het College voor Promoties,
in het openbaar te verdedigen op dinsdag 14 december 2021 om 10:00 uur

door

Sarvesh Budhaji KOLEKAR

Master of Science in Mechanical Engineering,
Technische Universiteit Delft, Nederland,
geboren te Alnavar, India.

Dit proefschrift is goedgekeurd door de promotoren

Samenstelling promotiecommissie is:

Rector Magnificus,	voorzitter
Prof. dr. ir. D.A. Abbink,	Technische Universiteit Delft, promotor
Dr. ir. J.C.F. de Winter,	Technische Universiteit Delft, promotor
Dr. ir. E.R. Boer,	Technische Universiteit Delft, copromotor

Onafhankelijke leden:

Prof. dr. J.D. Lee,	University of Wisconsin–Madison, USA
Dr. T. Victor,	Waymo, USA
Prof. dr. W.A. Ijsselsteijn,	Technische Universiteit Eindhoven, The Netherlands
Prof. dr. ir. B. van Arem,	Technische Universiteit Delft
Prof. dr. ir. M. Mulder,	Technische Universiteit Delft, reservelid



The work presented in this thesis was made possible by the Dutch Technology Foundation STW (VIDI project 14127), which is a part of the Netherlands Organisation for Scientific Research (NWO).

Keywords: Driver modelling, Risk field, Sensorimotor control

Printed by: Glideprint

Front & Back: Designed by Sarvesh Kolekar.
DRF was 3D printed by J.N.P. Giltay.

Copyright © 2021 by S. Kolekar

An electronic version of this dissertation is available at
<http://repository.tudelft.nl/>.

To aai and baba.

CONTENTS

Acknowledgements	ix
Summary	xiii
Samenvatting	xvii
1 Introduction	1
1.1 Background	1
1.2 Problem	3
1.3 Goal of this thesis	5
1.4 Scope and approach	5
1.5 Thesis structure	8
1.6 Applications	9
2 Driver's Risk Field (DRF): an empirical quantification	11
2.1 Background	12
2.2 Experimental methods	14
2.3 Analysis	19
2.4 Results	23
2.5 Discussion	28
2.6 Conclusions.	33
3 DRF-based driver model: operationalizing the risk threshold theory	35
3.1 Background	36
3.2 Methods	37
3.3 Results	48
3.4 Discussion	56
3.5 Conclusion	59
4 DRF-based risk estimate: a validation study in a test-vehicle	61
4.1 Background	62
4.2 Experimental methods	64
4.3 Results	68
4.4 Discussion	76
4.5 Conclusions.	78

5	Conclusions	79
5.1	Background	79
5.2	Three overarching conclusions	81
5.3	Future work and take home message	92
A	Appendix for Chapter 2	93
A.1	Supplementary table	93
A.2	Data availability and supplementary media.	96
B	Appendix for Chapter 3	101
B.1	Supplementary figures	101
B.2	Supplementary tables.	105
B.3	Supplementary notes	109
B.4	Data availability and supplementary media.	111
C	Appendix for Chapter 4	113
C.1	Driver comments during automated driving	113
C.2	Supplementary figure	125
	Curriculum Vitæ	141
	List of Publications	143
	Propositions	145

ACKNOWLEDGEMENTS

I would like to start this thesis with the acknowledgements because I feel the people and the relationships built during this Ph.D. are more valuable than the Ph.D. itself.

David, my promotor (not confined to this Ph.D.)! This thesis owes you a lot. The journey from calling you ‘Prof Abbink’ (in 2012 when you were an Asst. Professor) to calling you ‘David’ (in 2021 when you are a Professor), has been an eventful one. Ever since the first email I sent you in 2012, you have been a constant source of encouragement and guidance through these (in your words) ‘formative years of my life’. Your ability to provide honest feedback while giving me the freedom to pursue my ideas has transformed, what could have been just a collection of papers, into a thesis that I can truly be proud of! I think, all my colleagues from the Delft Haptics Lab will agree that you never made us feel that you were ‘The Professor’, especially with your choice of clothes. Your trousers were as short as your email signature. Thank you for personifying ‘simple living, high thinking’ and being a constant source of inspiration!

Joost, what can I say? Having a promotor who is also known as the ‘walking-talking Google Scholar’ doesn’t hurt. Your ability to gobble up literature and the insatiable appetite for papers from diverse research areas is unbelievable. But what amazed me, and what I tried to learn from you the most, was the clarity with which you could cut through the clutter and get to the heart of the problem. This superpower has had its downsides (mainly affecting me and Mr. T), as you would quickly realise during our update meetings that there was no significant progress made in the last week and gently start your backwards walk towards the exit. Before we knew it, you were gone! This blend of humour and scientific rigour is rare and I am glad I got to witness it in person! Thank you, Joost!

Erwin ‘the Kalman filtering’ Boer, my (long-distance) co-promotor! You never failed to challenge me to think beyond the ordinary. Your breadth of knowledge and skills, from having the most outrageous ideas on how to analyse the data to the nitty-gritty details of the working of a model, has always inspired me. Thank you!

At this point, I would also like to take a moment to thank our *guardians* at Nissan: **Tomohiro-san**, **Bouet-san**, **Takada-san**, and **Sakuma-san** for making the three month visit to Nissan possible, and fulfilling one of my dreams - implementing something in a real car. You made sure that we did not face the slightest amount of inconvenience during our time in Japan. I would also like to thank **Rene van Paassen** for his generous and support. I walked into your office uninvited on several occasions, but you always made time to help me out. Thank you!

Mr. Timo and **de Bastiaan**, without you two this thesis would not have been

even half as fun as it was. Be it the coffee breaks, or the walks, or your ‘practical’ jokes which when viewed out of context by ‘you know who’ could be completely inappropriate; made the atmosphere very lively! De Bas, thank you for being the *big brother*, and the calming figure through the ups and downs of the amazing three months in Japan. Those three months would not have been remotely as fun, without your constant failure to stop extending your arms for a handshake (instead of bowing) to greet our Japanese colleagues. Mr. T, apart from the scientific collaborations and *Healthic*, the support, entertainment, lunches, and of course the unlimited information about Ajax that you provided during these five years, is irreplaceable. The road trip to Belgium, the ping-pong matches in the lab (sorry Bastiaan!), and your ability to assign points to every food item, will be thoroughly missed. Thank you for being the *brother from another mother* throughout this journey!

Sarah, thank you for being constant source of inspiration to work harder, and also the rivetting discussions on some fascinating topics. Your strength and determination, especially during the tough times, was not only inspiring for me, but our entire lab! Your keen eye on details is something that I have always longed to learn. However, the biggest favor you did on all of us at the Haptics Lab was to introduce us to **Mr. Dirk**. Mr. Dirk, without your DUECA skills I don’t think any of our experiments would have seen the light of day. Your uninhibited willingness to help others is very inspiring! Thank you for all the help and all the Easter eggs (apt-get moo)!

Mr. Joris No Problem Giltay, this thesis would have been completed much earlier if it were not for you. However, it would have been a thesis with significantly fewer memories. Be it the *community straw* you built for Bastiaan, or the zoo of mutants you 3D printed (thank you for the 3D print on the coverpage, by the way), or your attempts at flying drones in the office, or adding sambal to basically ever kind of sandwich, or unknowingly stealing the limelight from Niek during the now infamous ‘Almonds’ incident, you were truly *legendaarryyyy*. Thanks for being the heart beat of the office and always keeping things lively!

Stijn and Elco, the only true Mechanical engineers of our group, along with **Frank, Sjors, Wietske, Hugo, Karlijn, Marijke, Roderick, and Ellen**; you drew the blue prints for the culture of our lab, without which it would have been just a collection of desks and chairs. The *Haptics Lab Wall of Fame*, the (either seldom or overly watered) plants, the countless number of pranks, the *broodje leo* lunches, and the *kip-knaks* lunches would not have been possible without you. Thanks for imparting a soul to our lab!

Arkady, Niek, Olger, and Yohei you guys carried forward the baton of the Lab’s culture with the epic lunches that included the debate: *subject vs participant*, the infamous *Almonds* incident (sorry Niek, I can’t help myself bringing it up multiple times), and for starting the tradition of croissants (15 points according to Mr. T) with *Nutella*. The *post-office* hours talks with Arkady and Niek, and the workshops with you, Olger - the Python God, were a lot of fun! Arkady, thanks for keeping an eye out for opportunities for me and being more excited than I was if something seemed like it would work out. Mr. Yohei, thank you for all the help, especially with

the Japan visit and the translations!

Marco, and **Gaia**: the constants since my early days in Delft. Thank you for all the surprise visits, painting sessions, and the surprise lunches. Marco, I still can't believe that the random pen you found in some part of the world was our 'ISO standard' while purchasing the *Sherwani*. **Rik**, and **Tse-Kang** thank you for the lovely evenings and nerdy discussions from cars to C++. The adventures at Zandvoort track were amazing and so was the chocolate curry! Rik, thanks for the tips, tricks, and the list of restaurants you gave me from your stay in Japan. Very helpful!

Talking about Japan, the 3 months spent there would not have been nearly as enjoyable without the colleagues at Nissan! **Sakuma-san**, thank you for being our *guardian* in Japan. Be it, picking me up from the railway station on the first day, or bringing us a van full of utensils and household appliances, you ensured that we never faced any inconvenience. **Aoki-san**, our other *guardian* ensured we never missed out on having fun. The 3pm tea-time walks, you getting me addicted to *Calpis soda* and *Mitsuya cider*, the visit to restaurants in Tokyo, the amazing home-made gyoza, your insistence that the *Otaku* culture originated in your home town and not in Akihabara; everything will be missed. Without you two, **Aoki-san** and **Sakuma-san**, the experiments would have never been possible, especially after the Typhoon! **Seguchi-san** needs a special mention not only for his help during the testing, but also for the amazing frozen chocolate banana! **Ito-san** and **Yokosawa-san**, what can I say? You are living the dream. Thank you for taking us on a road trip in your amazing cars. **Ohsawa-san**, thank you for making me realise that hostel life (complete chaos) is same everywhere in the world, and helping us get the *Hanko!* **Daniel-san** and **Ebina-san**, thank you for the pleasant lunches and enlightening us with talks from a diverse range of topics! Thank you **Hiraizumi-san** and **Taira-san** for enduring the torrential rains and ensuring a safe test-track while we performed experiments. Thank you all for making the visit a truly memorable one!

Now coming to the people who brought an essence of home away from home. **Shrinivas**, **Uddhav**, **Sharadi**, and **Vadhiraj**, thank you for the weekend lunch / dinners, and the discussions that covered such a diverse range of topics that they were borderline incoherent. We cannot forget the precision with which baba chimmal would add the ingredients, and the frequency with which the rest of us would fail to meet his high standards regrading the size and shape of chopped veggies. Then there was the margarine vs butter incident. Apart from these *light* moments, you all were there during the tough times and whenever I needed help. Be it the first move into the new house when Shrini carried tons of stuff from IKEA or the last move out of Delft, when UG helped vacate. Thank you for adding the *spice* to the weekends and always being there for me!

Mr. Rithwick, we have been friends ever since you moved into the adjacent apartment. These 6 years have been quite eventful, but nothing a dash of F1, and a pinch of *Impractical jokers* could not remedy. Thank you for the weekend dinners, and the inspiration to work harder. Your zeal and passion is quite infectious! **Mr. Karun**, and **Akshey**, had an amazing time with you guys. The three musketeers walking with food to lord Krishna's apartment, can never be forgotten!

From the home away from home, I will come to my friends in my hometown - Goa. It still amazes me that none of us have any idea of (or interest in knowing) what each of us does for a living. **Pogo**, aka Scientific Reality, thank you for the impromptu calls for discussing extremely urgent matters of national importance such as Seinfeld and Curb your enthusiasm. **Almas** thank you for the amazing biryani and **Scientist**, for sharing the enthusiasm for hobby electronics since our childhood! **MP**, thanks for the constant morale support, and reinforcing 'nothing is impossible'. **Pingu**, your countless PJs and nerdy talks were a constant source of entertainment! Thank you for being constants in my life while while the scenery around me kept changing.

Talking about constants, **aai** (mom) and **baba** (dad), you are the reason I am even capable of typing this acknowledgement today. Your life long sacrifices to ensure I do not face any hindrances in achieving my life goals have made this thesis and everything else in my life possible. This thesis is dedicated to you. Thank you for being the pillars of strength in my life!

Sarvesh Kolekar

Vasco, Goa - India, May 2021

SUMMARY

The National Highway Transportation Safety Administration (NHTSA) reports that 94-96% of the road accidents involve human error. These statistics make it seem as if humans are terrible drivers. However, a different set of numbers paint a completely different picture. According to the United States Bureau of Transportation Statistics, the failure rate of human drivers is 0.68 fatalities per 100 million kilometres. This number is so low that autonomous vehicle manufacturers are having a hard time proving that their vehicles are safer than human drivers. The safety benefits of Driver Assistance Systems, autonomous vehicles, and other safety systems are not being challenged here. However, it needs to be realised that a non-fatigued, attentive human is one of the safest drivers we can have.

Automotive manufacturers and researchers have realised this fact and are now shifting towards understanding how humans drive, to make their systems more safe, efficient, and acceptable to humans who use them. This has brought the age-old field of driver modelling back into the limelight. Researchers in this field try to understand *why humans drive the way they do* and formulate mathematical models that can replicate human driving behaviour. Unsurprisingly, akin to other fields in science, a *theory of everything* (for driving) has kept researchers busy for decades. Several *unified theories* of driving have been proposed. For example, the risk-threshold theory put forth by Näätänen and Summala proposed that humans try to maintain their perceived risk below a certain threshold. Gibson and Crooks proposed that humans perceive a 'Field of Safe Travel' that comprises of all the possible trajectories that a vehicle could take unimpeded. These motivational theories could *qualitatively* explain driving behaviour in a unified manner, but lack the specificity and operationalizability of *quantitative* mathematical models. *Quantitative* driver models have traditionally adopted two main strategies. First is the data-driven black-box approach, which provides little to no understanding about the underlying motivations for human driving behaviour, and second is by stitching together several models, each of which are based on a different underlying principle and are applicable in a different scenario. This has led to a rather fragmented understanding of the underlying motivations for driving. Hence, to the best of our knowledge, driver models are currently, either unified but qualitative, or fragmented but quantitative.

The goal of this thesis is to take a step towards formulating a unified and quantitative driver model by operationalizing the *qualitative* motivational theories of driving behaviour. One such motivational theory that showed potential to be operationalized was the previously mentioned risk-threshold theory proposed by Näätänen and Summala. According to this theory, drivers try to maintain their perceived risk, which was objectively defined as the product of the *probability* of an event

occurring and the *consequence* of that event, below a threshold level. Here, *probability* refers to the driver's belief about the probability of him/her passing through a location in the upcoming seconds (look-ahead-time), and the *consequence* refers to the 'dangerousness' of being at a particular location (cost map). This definition of risk sounded a lot like the concept of *consequence of noise* in the field of sensorimotor control. More interestingly, researchers in that field had already formulated unified quantified models for simple limb movements. Hence, it was obvious that these models and principles had to be borrowed from sensorimotor control and applied to the field of driving.

In chapter 2, the first step was taken in this attempt to operationalize a motivational theory by using sensorimotor control principles. An experiment was conducted to empirically quantify the *probability* part of the risk equation. In the field of sensorimotor control, the origin of this probability distribution of the future positions the limbs is attributed to the presence of noise in the sensors and actuators of our body. However, in the field of driving there was no such study that empirically quantified the driver's belief about what possible positions the ego-vehicle will occupy in the upcoming time interval. To address this gap, a driving simulator experiment in which eight participants encountered 308 obstacles each, was performed. These identical obstacles appeared at 77 (7 longitudinal positions, 11 lateral positions) different locations in front of the vehicle. The idea was that this experiment would reveal what parts of the road guide obstacle avoidance, and consequently expose where drivers think the ego-vehicle will be in the upcoming seconds. Since, the obstacles at all the 77 locations were identical, the consequence of hitting these obstacles was identical as well. This meant that the magnitude of the subjective and objective response, that constituted the Driver's Risk Field (DRF), could be interpreted as the driver's assumed probability of where the ego-vehicle will be in the next few seconds. The subjective response was a numerical answer to the question "How much steering do you think you need at this moment in time?" and the objective response was calculated as the maximum absolute steering angle. The results showed that the magnitude of the DRF decreased as the distance from the ego vehicle increased, and could be modelled using the Gaussian function in the lateral direction, and the power-law in the longitudinal direction. The results also showed that the propagation of the width of the DRF along the longitudinal direction resembled an hourglass shape, i.e., the DRF widened as the distance from the ego-vehicle increased. More importantly, all participants responded to obstacles that were placed beyond the width of the car. This implied that the DRF is wider than the car-width and suggests the propagation of sensorimotor noise in predicting the future positions of the ego-vehicle.

In chapter 3, the second step: combining the empirically quantified *probability* with the *consequence of the event* i.e., a cost map representing the dangerousness of the different elements in the environment, was taken. However, before this could be done, the static DRF that was estimated in the previous chapter needed to be upgraded to a dynamic DRF so that it could incorporate the effects of the multiplicative sensorimotor noise. Essentially, the dynamic DRF would now elongate in the longitudinal direction with an increase in speed (assuming a constant look

ahead time) and expand in the lateral direction as a function of absolute steering angle. The resultant product was the *risk estimate* and was hypothesised to correlate with the risk perceived by the drivers. This *risk estimate* was then used as a 'cost function' in a threshold-based controller where the controller would only take corrective action (steering and/or speed) when the *risk estimate* exceeded a certain risk-threshold. The behaviour emerging from this DRF-based driver model was compared to human driving behaviour in seven different scenarios (four road scenarios: lane width change, curve driving, obstacle avoidance, and roadside furniture; and three traffic scenarios: car following, overtaking, and negotiating on-coming cars). The results showed that the trends shown by the model were coherent with those exhibited by human drivers (reported in the literature). This suggests that maintaining the 'consequence of the human's perception-action noise' under a threshold level is an underlying principle for driver's adaptations in speed and lateral position to a wide variety of road and traffic conditions.

In chapter 4, the third step: testing the validity of the *risk estimate* in a real vehicle, was taken. Although, human-like behaviour emerged from the driver model that used *risk estimate* as a 'cost function', the hypothesis that the *risk estimate* correlates with the perceived risk of the driver was yet to be tested. To address this an experiment was performed where the participants' actions and comments were compared to the dynamic signal: *risk estimate*. The experiment was performed in a real vehicle since it was essential that the drivers perceived realistic levels of risk. Eight participants drove 5 laps manually and experienced 12 different laps of automated driving on a test track. The test track consisted of three sections: curve driving, parked car, and 90-degree intersections. If the driver verbally expressed risk or performed a takeover, that particular sector was labelled as risky. The results showed that the *risk estimate* could predict manual driving behaviour ($\rho_{steering} = 0.69$, $\rho_{speed} = 0.64$), as well as correlated with the driver's perceived risk in curve driving ($r^2 = 0.98$), and while driving past a car parked outside the lane boundary ($r^2 = 0.59$). No conclusions could be drawn for the 90-degree intersections because all the occurrences in this sector were rated to be safe by the participants, and had a low *risk estimate* value. Hence there were no data points that had a high value of *risk estimate* or a 'risky' rating by the participants. Despite the lack of data for 90-degree intersections, the results showed that the *risk estimate* was predictive of manual driving behaviour, and perceived risk in automated driving.

Three overarching conclusions can be drawn from this thesis: (i) Drivers respond to objects beyond the width of the car and lane boundaries. (ii) The computed *risk estimate* constitutes a signal that correlates with the risk perceived by the driver, and (iii) Human-like adaptations in speed and lateral position behaviour emerge when the consequence of sensorimotor noise is maintained below a threshold level. These results and conclusions point towards the fact that, in line with the goal of this thesis, a unified quantitative driver model can be formulated using a risk-based model (at least for the seven scenarios tested in this thesis).

However, these results and conclusions come with some limitations, which one needs to be aware of before using these mathematical formulations. First, the DRF only accounts for the obstacles in front of the vehicle. Hence it is not capable of

reacting appropriately in a lane change scenario on a highway with multiple lanes. Second, the DRF only responds to the danger posed by an object due to its physical presence, and does not account for the ‘tactical costs’. For example, it won’t anticipate cross-traffic and slow down at an intersection or stop at a traffic light. However, this can be easily resolved by adding artificial barriers at intersections whose costs are context-dependent. Third, the traffic elements used in this thesis, although dynamic, were deterministic and non-interacting. Hence, the model will have to be substantially upgraded before it can start ‘negotiating’ at unprotected intersections and reacting acceptably to other interacting traffic. Finally, the model is computationally inefficient and does not run in real-time. If the model is to be used as a reference trajectory generator for automated systems, this practical aspect will be an essential upgrade that will have to be made.

Despite these limitations, the DRF based driver model, and the *risk estimate* are a step towards a *theory of everything* for driving. We hope that the mathematical formulations proposed in this thesis become a part of larger theories (e.g., predictive processing theory) of driving and enhance not only *quantitativeness* of these unifying theories but also the scientific understanding of human driving behaviour. Regardless of the future evolution of this DRF-based model, one thing is for sure: we humans are aware of the consequence of noise in our sensorimotor system and account for it while driving, similar to while performing simple movement tasks.

SAMENVATTING

De National Highway Transportation Safety Administration (NHTSA) meldt dat 94-96% van de verkeersongevallen te maken heeft met menselijke fouten. Door deze statistieken lijkt het alsof mensen vreselijke chauffeurs zijn. Een alternatieve statistiek geeft echter een heel ander beeld: Volgens het Amerikaanse Bureau of Transportation Statistics is de faalbaarheid van menselijke bestuurders 0,68 doden per 100 miljoen kilometer. Dit aantal is zo laag dat fabrikanten van autonome voertuigen het moeilijk vinden om te bewijzen dat hun voertuigen veiliger zijn dan menselijke bestuurders. De veiligheidsvoordelen van rijhulpsystemen, autonome voertuigen en andere veiligheidssystemen worden hier niet in twijfel getrokken. Men moet zich echter realiseren dat een niet-vermoeide, oplettend mens een van de veiligste chauffeurs is die we kunnen hebben.

Autofabrikanten en onderzoekers hebben dit feit ingezien en zijn nu bezig met het begrijpen van hoe mensen rijden, om hun systemen veiliger, efficiënter, en acceptabeler te maken voor mensen die ze gebruiken. Dit heeft het eeuwenoude veld van bestuurdersmodellering weer in de schijnwerpers gezet. Onderzoekers op dit gebied proberen *waarom mensen rijden zoals ze doen* te begrijpen en wiskundige modellen te formuleren die menselijk rijgedrag kunnen nabootsen. Het is niet verwonderlijk dat, net als andere wetenschapsgebieden, een *theorie van alles* (voor autorijden) onderzoekers decennia lang heeft bezig gehouden. Er zijn verschillende *uniforme theorieën* over autorijden voorgesteld. De risicodrempeltheorie die werd voorgesteld door N äät änen en Summala stelde bijvoorbeeld voor dat mensen proberen hun waargenomen risico onder een bepaalde drempel te houden. Gibson en Crooks stelden voor dat mensen een 'veld van veilig reizen' dat alle mogelijke trajecten omvat die een voertuig onbelemmerd zou kunnen afleggen, waarnemen. Deze motivatietheorieën zouden het rijgedrag *kwalitatief* op een uniforme manier kunnen verklaren, maar missen de specificiteit en bruikbaarheid van *kwantitatief* wiskundige modellen. *Kwantitatieve* bestuurdersmodellen hanteren van oudsher twee hoofdstrategieën: Ten eerste de datagestuurde black-box-benadering, die weinig tot geen inzicht geeft in de onderliggende motivaties voor menselijk rijgedrag, en ten tweede door verschillende modellen die elk gebaseerd zijn op een ander onderliggend principe en derhalve toepasbaar zijn in een ander scenario. Dit heeft geleid tot een nogal gefragmenteerd begrip van de onderliggende motivaties voor autorijden. Voor zover wij weten, zijn de bestuurdersmodellen daarom momenteel ofwel uniform maar kwalitatief, ofwel kwantitatief maar gefragmenteerd.

Het doel van dit proefschrift is om een stap te zetten in de richting van het formuleren van een uniform en kwantitatief bestuurdersmodel door de *kwalitatieve* motivatietheorieën over rijgedrag te operationaliseren. Een van die motivatiethe-

orieën die het potentieel toonde om te worden geoperationaliseerd, was de eerder genoemde risicodrempeltheorie. Volgens deze theorie is risico een product van de *waarschijnlijkheid* dat een gebeurtenis plaatsvindt en het *gevolg* van die gebeurtenis, en dat bestuurders proberen dit risico onder een drempelniveau te houden. Deze definitie van risico leek veel op het concept van *consequentie van ruis* op het gebied van sensorimotorische controle. Interessanter is dat onderzoekers op dat gebied al uniforme gekwantificeerde modellen hadden geformuleerd voor eenvoudige bewegingen van ledematen. Het was dus duidelijk dat deze modellen en principes moesten worden ontleend aan sensorimotorische besturing en toegepast op het rijgedrag.

In hoofdstuk 2 was de eerste stap die werd gezet in deze poging om een motiethoorie te operationaliseren met behulp van sensorimotorische controleprincipes, het empirisch kwantificeren van het *waarschijnlijkheidsdeel* van de risicovergelijking. Op het gebied van sensorimotorische controle wordt de oorsprong van deze kansverdeling van de toekomstige posities die de ledematen zullen innemen, toegeschreven aan de aanwezigheid van ruis in de sensoren en actuatoren van ons lichaam. Op het gebied van autorijden was er echter geen studie die de overtuiging van de bestuurder over de mogelijke posities die hij/zij in het komende tijdsinterval zal innemen, empirisch kwantificeert. Om deze kloof te dichten, werd een rijnsimulator-experiment uitgevoerd waarbij acht deelnemers elk 308 obstakels tegenkwamen. Deze identieke obstakels verschenen op 77 verschillende locaties voor het voertuig (7 lengteposities, 11 laterale posities). Het idee was dat dit experiment zou onthullen voor welke delen op de weg bestuurders obstakels vermijden en bijgevolg blootlegt waar de bestuurders denken dat het ego-voertuig zich de komende seconden zou kunnen bevinden. Aangezien de obstakels op alle 77 locaties identiek waren, was het gevolg van het raken van deze obstakels ook identiek. Dit betekende dat de omvang van de subjectieve en objectieve respons, die het Driver's Risk Field (DRF) vormde, kon worden geïnterpreteerd als het door de bestuurder aangenomen waarschijnlijkheid van waar het ego-voertuig de komende seconden zal zijn. De subjectieve reactie was een cijfermatig antwoord op de vraag "Hoeveel stuurinput denkt u op dit moment nodig te hebben?" en de objectieve respons werd berekend als de maximale absolute stuurhoek. De resultaten toonden aan dat de omvang van de DRF afnam naarmate de afstand tot het ego-voertuig groter werd, en kon worden gemodelleerd met behulp van de Gaussische-functie in de laterale richting en een machtsfunctie in de longitudinale richting. Interessant is dat de resultaten toonden dat de voortplanting van de breedte van de DRF in de lengterichting leek op een zandlopervorm en dat alle deelnemers reageerden op obstakels die buiten de breedte van de auto waren geplaatst. Dit impliceerde dat het Driver's Risk Field breder is dan de wagenbreedte en suggereert de voortplanting van sensorimotorisch ruis bij het voorspellen van de toekomstige posities van het ego-voertuig.

In hoofdstuk 3 werd de tweede stap genomen om de empirisch gekwantificeerde *kans* te combineren met het *gevolg van de gebeurtenis*, d.w.z. een kostenkaart die de gevaarlijkheid van de verschillende elementen in de omgeving weergeeft. Voordat dit kon worden gedaan, moest de statische DRF die in het vorige

experiment werd geschat, worden geüpgraded naar een dynamische DRF zodat deze de effecten van de multiplicatieve sensorimotorische ruis kon opnemen. In wezen zou de dynamische DRF nu langer worden in de lengterichting met een toename in snelheid (uitgaande van een constante vooruitkijktijd) en uitbreiden in de laterale richting als functie van de absolute stuurhoek. Het resulterende product was de *risicoschatting* en werd verondersteld te correleren met het door de bestuurders waargenomen risico. Deze *risicoschatting* werd vervolgens gebruikt als een 'kostenfunctie' in een drempelgebaseerde controller waarbij de controller alleen corrigerende maatregelen zou nemen (sturen en/of snelheid) wanneer de *risicoschatting* een bepaald risico overschreed. drempel. Het gedrag dat voortkwam uit dit op DRF gebaseerde bestuurdersmodel werd vergeleken met menselijk rijgedrag in zeven verschillende scenario's (vier wegsenario's: verandering van rijstrookbreedte, rijden in bochten, vermijden van obstakels en wegkantmeubilair; en drie verkeersscenario's: auto volgen, inhalen en onderhandelen tegen tegenliggers). De resultaten toonden aan dat de trends die door het model werden getoond, coherent waren met die van menselijke bestuurders (gerapporteerd in de literatuur). Dit suggereert dat het onder een drempelwaarde houden van het 'gevolg van het waarnemingsruis van de mens' een onderliggende principe is voor de aanpassing van de snelheid en de laterale positie van de bestuurder aan een grote verscheidenheid aan weg- en verkeersomstandigheden.

In hoofdstuk 4 werd de geldigheid van de *risicoschatting* getest in een echt voertuig. Hoewel mensachtig gedrag voortkwam uit het bestuurdersmodel dat *risicoschatting* als 'kostenfunctie' gebruikte, moest de hypothese dat de *risicoschatting* correleert met het gepercipieerde risico van de bestuurder nog worden getest. Om dit aan te pakken werd een experiment uitgevoerd waarbij de acties en commentaren van de deelnemers werden vergeleken met het dynamische signaal: *risicoschatting*. Het experiment werd uitgevoerd in een echt voertuig, aangezien het essentieel was dat de bestuurders realistische risiconiveaus ervaarden. Acht deelnemers reden 5 ronden handmatig en beleefden 12 verschillende ronden geautomatiseerd rijden op een testbaan. De testbaan bestond uit drie secties: rijden in bochten, geparkeerde auto, en kruisingen van 90 graden. Als de bestuurder het risico verbaal uitsprak of een overname uitvoerde, werd die specifieke sector als risicovol bestempeld. De resultaten lieten zien dat de *risicoschatting* handmatig rijgedrag kan voorspellen ($\rho_{steering} = 0,69$, $\rho_{snelheid} = 0,64$), en ook correleert met het door de bestuurder gepercipieerde risico bij het rijden in bochten ($r^2 = 0,98$) en tijdens het passeren van een auto die buiten de rijstrookgrens geparkeerd stond ($r^2 = 0,59$). We konden geen conclusies trekken voor de 90-graden-kruising, omdat alle voorvallen in deze sector door de deelnemers als veilig werden beoordeeld en een lage *risico-inschatting* waarde hadden. Daarom waren er geen datapunten met een hoge waarde van *risicoschatting* of een risicovolle beoordeling van de deelnemers. Ondanks het gebrek aan gegevens voor 90-graden kruispunten, toonden de resultaten aan dat de *risicoschatting* voorspellend was voor handmatig rijgedrag en waargenomen risico bij geautomatiseerd rijden.

Drie overkoepelende conclusies kunnen worden getrokken uit dit proefschrift:
(i) Bestuurders reageren op objecten buiten de breedte van de auto en de rijstrook-

grenzen. (ii) De berekende *risicoschatting* is een signaal dat correleert met het door de bestuurder waargenomen risico, en (iii) Menselijk rijgedrag komt naar voren wanneer het gevolg van sensorimotorische ruis onder een drempelwaarde wordt gehouden. Deze resultaten en conclusies wijzen erop dat een uniform kwantitatief driver-model kan worden geformuleerd met behulp van een risicogebaseerd model (althans voor de zeven scenario's die in dit proefschrift zijn getest).

Deze resultaten en conclusies hebben echter enkele beperkingen waarvan men op de hoogte moet zijn alvorens deze wiskundige formuleringen te gebruiken. Ten eerste houdt de DRF alleen rekening met obstakels voor het voertuig. Daarom is het niet in staat om op de juiste manier te reageren bij een rijstrookwisselscenario op een snelweg met meerdere rijstroken. Ten tweede reageert de DRF alleen op het gevaar van een object vanwege zijn fysieke aanwezigheid en houdt geen rekening met de 'tactische kosten'. Het anticipeert bijvoorbeeld niet op kruisend verkeer en vertraagt niet op een kruispunt of stopt bij een verkeerslicht. Dit kan echter eenvoudig worden opgelost door kunstmatige barrières toe te voegen op kruispunten waarvan de kosten contextafhankelijk zijn. Ten derde waren de verkeerselementen die in dit proefschrift werden gebruikt, hoewel dynamisch, deterministisch en niet interactief. Daarom zal het model substantieel moeten worden geüpgraded voordat het kan beginnen met 'onderhandelen' op onbeschermde kruispunten en acceptabel kan reageren op ander reagerend verkeer. Ten slotte is het model rekeninefficiënt en werkt het niet in realtime. Wil het model worden gebruikt als referentietrajectorgenerator voor geautomatiseerde systemen, dan zal dit praktische aspect een essentiële upgrade zijn die aan het model moet worden doorgevoerd.

Ondanks deze beperkingen zijn het op DRF gebaseerde bestuurdersmodel en *risicoschatting* een stap naar een *theorie van alles* voor autorijden. We hopen dat de wiskundige formuleringen die in dit proefschrift worden voorgesteld, een onderdeel worden van grotere theorieën (bijv. Voorspellende verwerkingstheorie) over autorijden en niet alleen *kwantitativiteit* van deze verenigende theorieën versterken, maar ook het wetenschappelijk begrip van menselijk rijgedrag. Ongeacht de toekomstige evolutie van dit op DRF gebaseerde model, één ding is zeker: wij mensen zijn ons bewust van de gevolgen van ruis in het sensorimotorische systeem en houden er rekening mee tijdens het rijden, vergelijkbaar met het uitvoeren van eenvoudige bewegingstaken.

1

INTRODUCTION

1.1. BACKGROUND

THE quest for a *theory of everything* has tempted scientists since time immemorial. Be it in the fields of biology and psychology where humans try to understand humans, or the fields of physics and chemistry where humans try to understand the nature of nature. There seems to be some beauty in trying to explain the complexity of the world through simple underlying principles. Research in the field of driving, which has become an important part of our lives ever since the introduction of the automobile, has not escaped this allure of an all explaining unified theory of driving.

1.1.1. UNIFIED QUALITATIVE THEORIES OF DRIVING

Researchers have proposed different theories about what motivates humans to drive like they do. Gibson and Crooks (1938) [1], for example, proposed that drivers perceive a *Field of Safe Travel* (FoST) - a field of all the safe paths the car can take unimpeded. The main idea was that locomotion through the FoST is similar to walking or running, except that in this case the locomotion was performed using a tool - the car. Others, for example, Näätänen and Summala [2] proposed that drivers try to maintain their perceived risk below a certain threshold and perform (steering and/or speed) corrections only when this threshold is exceeded.

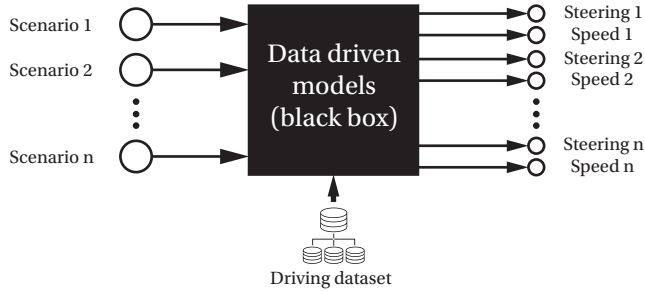
Motivational theories proposed by Fuller [3] and Wilde [4], similar to the ones mentioned above, focused on the low-level control behaviour of the driver and aimed to explain human driving behaviour qualitatively (Fig. 1.1 [a]). They provide a good theoretical framework, but lack the specificity of mathematical models [5].

1.1.2. QUANTITATIVE DRIVER MODELS

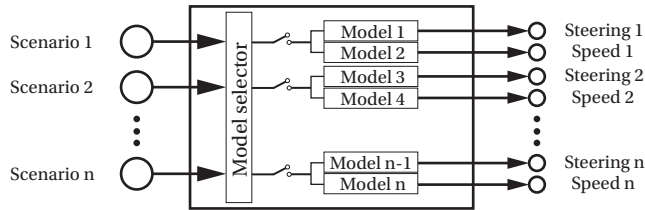
For any practical use, we need mathematical models that can generate quantifiable outputs, for given inputs. They find use in applications ranging from the design



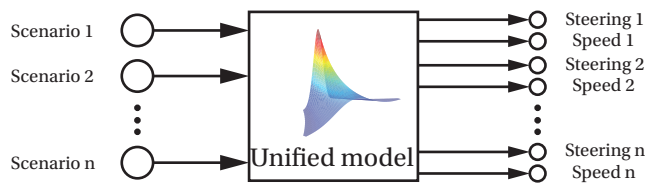
(a) Qualitative driver models



(b) Quantitative driver models: data driven approach



(c) Quantitative driver models: approach based on underlying principles



(d) Proposed quantitative driver model: unified and based on underlying principles

Figure 1.1: Approaches to driver modelling: Scenario, Steering, and Speed 1,2,...,n represent the scenarios and the corresponding lateral and longitudinal control actions, respectively. **(a)** Qualitative driver models propose theories that explain human driving behaviour without mathematical specificity. Quantitative driver models either take a data-driven (black-box) approach **(b)** or a fragmented approach **(c)** where several models based on different underlying principles (explainable) for different scenarios are combined. **(d)** In this thesis, the formulation a unified model based on underlying principles (hence explainable), that also offers the diversity similar to the black-box approach, is proposed.

and construction of roads to the development of automated systems for vehicles. Quantitative driver models are being used as reference models for automated systems, since an attentive non-fatigued human driver is one of the best drivers we can have. In fact, automated vehicle manufacturers are having a hard time proving their systems are safer than a human driver [6]. These quantitative driver models, which are being used as reference models could also help in generating human-acceptable trajectories for the automated systems. For example, that driver's prefer a system that they think drives like them [7].

Researchers have developed several quantitative models of driver behaviour and these have been formulated using one of the following two main approaches:

1. **Data driven approach:** In this approach, a large dataset is used to estimate the parameters of a standard model (e.g., neural network). This approach can deliver models of driving behaviour in scenarios that were used for estimating the parameters, but cannot easily generalise to previously unseen scenarios [8]. This is partly solved by introducing more scenarios in the training dataset. However, the most important drawback of this approach is that, these models provide little to no understanding of *why humans drive like they do*. This makes such models a black-box which is not only scientifically not satisfying but also largely unexplainable, which is not desirable in critical applications like driving, where an error could lead to a life-altering event [9] (Fig. 1.1 [b]).
2. **Approach based on underlying principles:** In this approach, researchers formulate models based on the understanding of some underlying principles. This approach has the presumed advantage of being generalizable to previously unseen scenarios but the models are typically fragmented. What we mean by fragmentation is that the task of driving is divided into sub-tasks, each of which is modelled separately. Fragmentation has occurred because it is difficult to systematically conduct rigorous research of the driving task as a whole. It also allows the freedom to base each sub-task on a different theoretical underpinning [10]. For example, longitudinal behaviour has been modelled using the optical edge rate [11] on open roads, the time to extended tangent point [12] in curves, time to collision (TTC) [13] [14] while approaching obstacles and time headway (THW) [15] during car following. Lateral positioning has been modelled using heading perception in two-point (i.e., anticipatory vs. compensatory) [16] models in normal driving, and open-loop steering [17] corrections in emergency scenarios.

1.2. PROBLEM

1.2.1. DRAWBACKS OF A FRAGMENTED APPROACH

A fragmented set of models, each performing a different sub-task is efficient and practical for implementing Driver Assistance Systems, since they aim to automate parts of the driving task. Practically, a unitary model can be *stitched* together from

several models (Fig. 1.1 [c]), but this fragmented approach has several drawbacks. A few of them are listed below:

1. An appropriate *switching* model that determines which model to use in which scenario, will be needed [18].
2. Switching between the models needs to be smooth and stable. For example, if we switch from a car following to an overtaking task, the parameter settings of the respective models need to be such that the transition is smooth and stable [19].
3. The low-level control behaviour, which this thesis focuses on, is affected by higher-level factors (e.g., familiarity of the driver to a road). If the effects of such high-level behaviour (e.g., drives more aggressively on a familiar road, and cautiously on an unfamiliar road) are to be incorporated, the parameter setting of all the different models will have to be changed *homogeneously* so as to not cause any abrupt changes [5].
4. It is also unclear how the occurrence of multiple scenarios simultaneously will be handled. For example, how will the models of overtaking and negotiating oncoming traffic be combined when we encounter an oncoming vehicle while overtaking.
5. Although, each of the models are generalizable, they can be generalised to previously unseen scenarios within their scope (that particular sub-task). For example, a car following model cannot be generalised to perform a curve driving task. This means that the *stitched* model will not be able to execute appropriate actions in scenarios that have not been specifically incorporated in it.
6. Since, the fragmented models use different theoretical underpinnings for each sub-task, it becomes difficult to develop a unified scientific understanding of the motivations for driving behaviour [10].

The above points highlight the need for a unified quantitative driver model. To the best of our knowledge, there exist unified *qualitative* driver behaviour theories, but there are no unified *quantitative* driver models based on underlying principles. Optimal Preview Control models such as that proposed by Peng and Tomizuka [20] used both feedforward and feedback components to control the steering. However, their main limitation was that they considered driving as a lane-centre tracking task, which does not allow for *satisficing* [21]: a behaviour exhibited by human drivers. Some algorithms from the field of robotics do offer the possibility of performing trajectory planning in a wide range of scenarios [22][23][24][25]. However, these algorithms having been developed for robots do not account for the subtleties of human driving. For example, they can perform path planning and even re-plan in real-time, in case of dynamic obstacles. However, they are not concerned with slowing down more, and cutting a curve more, while negotiating a sharp corner, as compared to a shallow corner, which human drivers would do [26].

1.3. GOAL OF THIS THESIS

The goal of this thesis is to formulate a unified quantitative driver model that can predict human behaviour, in terms of speed and lateral position adaptations, in a multitude of scenarios. More importantly, the model needs to be based on a single underlying principle, from which human-like adaptations are expected to emerge in different scenarios. The by-product of this driver model could be a mathematical representation of the underlying motivation for *why humans drive the way they do* and could also be used as a *feature* in the ‘data-driven’ approach.

1.4. SCOPE AND APPROACH

It is important to note that, in this thesis, the focus will be on modelling the effect of road geometry (e.g., curvature, lane width) and non-interacting deterministic traffic (e.g., car following, overtaking). The modelling of interactive behaviour of traffic elements, or the process of conscious decision making during driving (e.g., which route to take) will not be studied in this thesis. Essentially, the focus will be on modelling the effect of the physical presence of different (static and dynamic) road elements, on driver behaviour.

To achieve the goal of this thesis, inspiration was drawn from the fields that study basic human movements. The thought being that the mathematical formulations developed for simple human movements could be extended to the more complex field of driving (Fig. 1.2).

The *Optimal Feedback Control* (OFC) theory for sensorimotor control proposed by Todorov and Jordan in 2002 [27] successfully unified several characteristics of human movements (e.g., Gaussian velocity profiles [28], reduction in movement variability in the vicinity of constraints) across a range of movements (e.g. hitting a ping-pong ball, grasping an object). The essence of this model lies in its two main features:

1. **Multiplicative noise:** The noise in the sensors and actuators (e.g., muscles) of our body contains multiplicative noise. In essence, the noise increases as the mean value of the signal increases [29]. This means that a faster movement leads to a larger inaccuracy and hence affects the chances of achieving the goal (e.g., moving your arms to a circular target). The Fitts’ Law emerges from this model, since humans slow down their arm movements when the target gets smaller. This ‘target reaching task’ in motor control is analogous to a car slowing down for a narrow road.
2. **Managing the *relevant* consequences of noise:** The noise in the sensors and actuators can lead to a deviation from the intended action and hence result in undesirable consequences. It appears that the brain tries to find a trade-off between the *reward* (intended action) and the *cost* (undesired consequences) [30]. More importantly, the Optimal Feedback Controller uses a ‘goal oriented’ cost function i.e., it only penalises the states that deviate from the goal. This is different from a ‘reference trajectory’ approach where the cost function penalises any deviation from a reference trajectory. What this

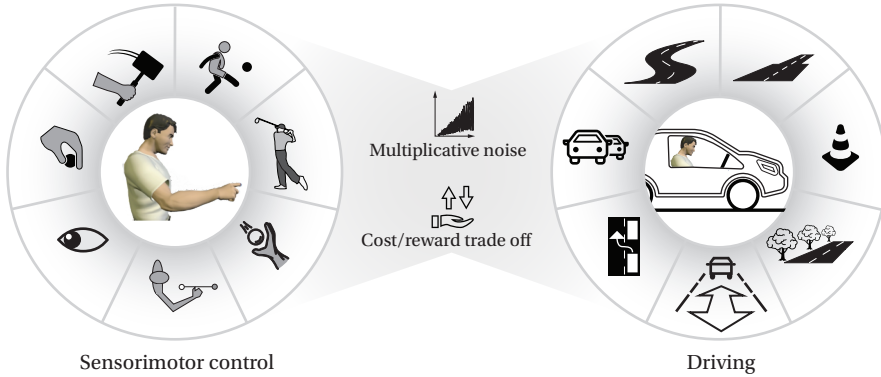


Figure 1.2: **Research approach:** The field of sensorimotor control provides principles, and a unified approach (Optimal Feedback Control theory) that can quantitatively model human movements in a wide range of scenarios. The aim is to extract the essence of these principles and apply them to the field of driving, to formulate a unified model for driving behaviour in a multitude of scenarios. The following two principles were borrowed: (i) Human sensorimotor system has multiplicative noise, and (ii) Humans balance the cost and reward due to the consequence of the noise *relevant* to the goal.

leads to is a controller from which human-like behaviour emerges in terms of remarkable consistency in achieving the goal while rarely replicating the trajectory in its details. This is analogous to the concept of satisficing [21] in driving, where drivers do not try to follow a reference trajectory (e.g., centre of the road), but are satisfied with being within certain bounds on the road.

Such similarities between simple motor tasks and driving, and the ability of the Optimal Feedback Controller to quantitatively model sensorimotor tasks in a unified manner make it a great candidate to be extended to the field of driving. Kolekar et al. [31] attempted this for a driver steering model but manifesting the OFC into a receding horizon controller, but soon ran into mathematical complexity while extending it to speed control and dynamic traffic related tasks. Hence, this thesis aims to extract the essence of this sensorimotor control theory and implement it in a mathematically simplistic way to probe if an approach similar to the Optimal Feedback Control can be successful in modelling speed and lateral position adaptations in driving.

One of the essential elements of the OFC that we are interested in extracting is the cost function it uses. The *cost* referred to above, is a product of the *probability* of an event occurring and the *consequence of that event* occurring (Fig. 1.3). The *probability* of the event occurring is determined by the probability distribution of the possible locations of the limb due to the multiplicative noise in the sensorimotor system. The *consequence of the event* is dependent on the task (e.g., hitting a ping-pong ball correctly gives you a point, whereas missing it costs you a point) and essentially, defines the goal of a particular movement. Incidentally, this product of probability and consequence has been termed *risk* in the field of driving [2]. This thesis proposes the *risk estimate* signal that aims to quantify this *risk* during

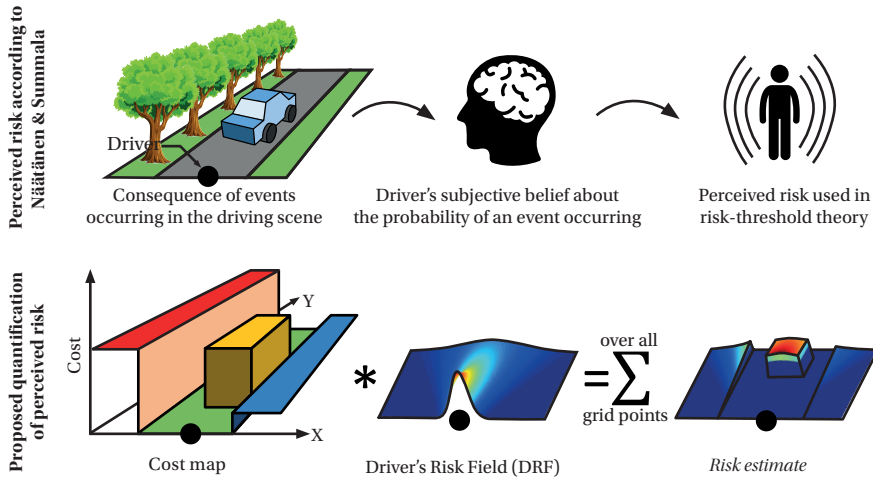


Figure 1.3: **Proposed risk estimate:** The first row visualises the definition of risk proposed by Näätänen and Summala. They proposed that the risk perceived by a driver is the production of the consequence of being in a particular location and the driver's belief about he/she passing through that location. The second row illustrates the method proposed in this thesis to quantify the risk.

driving. The *probability of an event* and the *consequence of an event* in the context of driving are defined as follows:

1. **Probability of an event:** This is similar to a probability distribution function, with input being the state of the ego-vehicle (x-y position) and the output being the driver's belief about how probable it is that he/she will pass through that point in the next few seconds (look-ahead-time).
2. **Consequence of an event:** This is similar to a 'cost map' that defines the 'dangerousness' of each state in the environment (x-y position). For example, the value of this cost map will be very low (or even zero) for the road and very high for the tree besides the road.

In the definitions provided above, **an event** refers to the act of being present at a particular location. A collision occurs when the position of the ego-vehicle coincides with the position of an obstacle in the environment.

This approach of conceptualizing the *probability* and the *consequence* as a probability field and a cost map, respectively, draws inspiration from the field based approach adopted by Gibson and Crooks [1] in their Field of Safe Travel theory. Their theory could explain, in a unified manner, driving in several scenarios. Hence, it was decided to integrate the concept of *risk* and the *field* based approach to propose the new *Driver's Risk Field* quantitative formulation. One of the novelties of our field based approach, is that we aim to define the shape of the field from human driving data as opposed to an artificial potential field which was created based on thoughtful insights of the researcher [32].

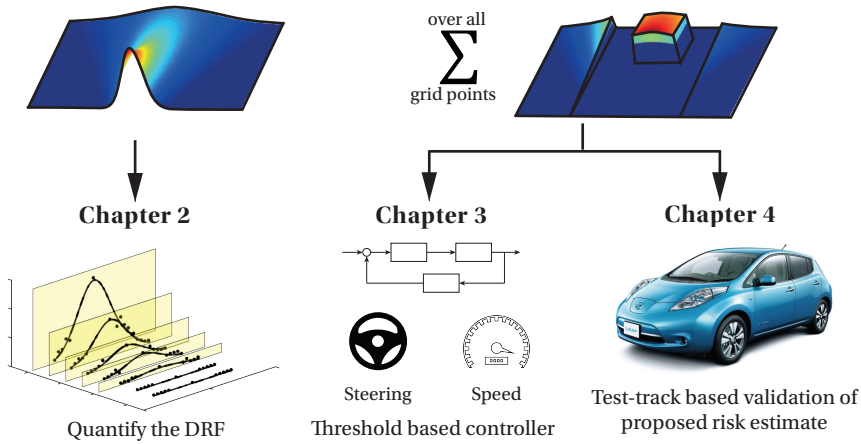


Figure 1.4: **Thesis structure:** In chapter 2, the shape of the DRF is quantified. In chapter 3, the *risk estimate* is used as a cost function in a risk threshold-based controller to formulate a driver model. The output of the driver model (speed and steering) is validated by comparing it to driving behaviour reported in literature. In chapter 4, it is tested if the proposed risk estimate corresponds to the subjective feeling of risk of the driver while driving manually and in an automated vehicle on a test track.

1.5. THESIS STRUCTURE

The details of the proposed Driver's Risk Field (DRF) and the steps taken to achieve the goals of this thesis are explained in the upcoming chapters that are structured as follows (Fig. 1.4):

- **Chapter 2:** Since the field-based approach proposed by Gibson and Crooks was qualitative, the first step was to try and empirically quantify the shape of the field. Essentially, it would reveal which parts of the road, in front of the driver incite a response from the driver. The field derived in this chapter is called the *Driver's Risk Field* (DRF) and represents the *probability* component of the *risk*.
- **Chapter 3:** In this chapter, the principles learned from sensorimotor control are used to upgrade the static DRF derived in chapter 2, to a dynamic DRF. This dynamic DRF, essentially, morphed its shape and size with the steering angle and speed of the ego-vehicle. The DRF when used in conjunction with 'consequence' map of the environment, yielded an estimate of the perceived risk of the driver. The *risk estimate* when used in a risk threshold-based controller, human-like driving behaviour emerged in several driving (road and traffic) scenarios. The model's behaviour was validated using the experimentally measured driving behaviour published in the literature.
- **Chapter 4:** The *risk estimate* calculated in the previous chapter could generate *human-like* behaviour in different scenarios. But it was not known if this *risk estimate* that was proposed, actually corresponded to the risk perceived by the human drivers. To test this, conditions where the drivers perceived

realistic levels of risk were needed. Hence, the validation experiments were conducted in a real car on a test-track. The validity of the proposed *risk estimate* was tested in both: manual and automated driving conditions.

In short, the single unifying principle that was focused on in this thesis is: Do human-like adaptations in speed and lateral position behaviour emerge, when the consequence of noise (*risk estimate*) is attempted to be maintained below a certain threshold?

1.6. APPLICATIONS

The findings of this thesis are not only aimed to improve the scientific understanding of *why humans drive like they do*, but also have applications in partially and fully automated vehicles. For example, a unified driver model can be a very potent tool for the automotive industry to run (virtual) 'driver-in-the-loop' simulations in a variety of scenarios. The unified model could also generate human-acceptable trajectories for automated systems in fully or partially automated vehicles [7]. The *risk estimate* proposed in this thesis could be used as a metric to evaluate *how risky* a particular trajectory of an automated vehicle is, or to add constraints to the operational domain of an automated system, as proposed by Mobileye [33]. Moreover, since this thesis aims to understand the underlying principles that motivate drivers' speed and lateral position adaptations, its findings can be a valuable tool for applications in the field of human-machine interaction. For example, the Symbiotic Driving project [34], which aims to develop an adaptive Haptic Shared Controller, can incorporate the driver model that will be developed in this thesis to generate predictions about where, when, and how drivers will adapt to the environment. This information can then be used to generate appropriate torque commands on the steering wheel and gas pedal to *share* the control of the vehicle with the driver.

2

DRIVER'S RISK FIELD (DRF): AN EMPIRICAL QUANTIFICATION

Gibson and Crooks (1938) argued that a 'field of safe travel' could qualitatively explain drivers' steering behaviour on straights, curved roads, and while avoiding obstacles. This chapter aims to quantitatively explain driver behaviour while avoiding obstacles on a straight road, and quantify the 'Driver's Risk Field' (DRF). In a fixed-based driving simulator, 77 (7 longitudinal and 11 lateral) positions of the obstacles were used to quantify the subjectively perceived and objectively (maximum absolute steering angle) measured DRF for eight participants. The subjective response was a numerical answer to the question "How much steering do you think you need at this moment in time?" The results show that the propagation of the width of the DRF along the longitudinal distance, resembled an hourglass shape, and all participants responded to obstacles that were placed beyond the width of the car. This implies that the Driver's Risk Field is wider than the car-width.

The contents of this chapter have been published in:
S. Kolekar, J.C.F. de Winter, and D. Abbink, *Which parts of the road guide obstacle avoidance? Quantifying the driver's risk field*, [Applied ergonomics](#) 89 (2020), 103196

2.1. BACKGROUND

MANY car manufacturers worldwide are developing highly automated driving systems that are expected to contribute to driver comfort and safety [35]. Before automated driving systems can be deployed on a large scale, various technological challenges still need to be resolved. One specific challenge is that current automated driving systems are conservative, strictly obedient to the traffic rules, and unable to exhibit natural driving behaviours, rendering them, at present, slow and inefficient [36]. A second challenge is that until fully (SAE Level 5) autonomous cars are introduced, there will be a need for automated systems that keep the human involved in the driving task. Such systems may have to interact with the driver in a human-like manner [37][38][39], for example via a shared control system [40].

This need for effective interaction, and the inefficiencies of (partially and highly) automated vehicles provides an impetus for developing automated cars that drive in a human-like manner, with acceptable safety margins towards other road users and road boundaries [41]. At present, however, there is no generally accepted model that quantitatively captures human driving behaviour [10][42][43]. As early as 1970, a driver task analysis by McKnight and Adams [44] identified over 1,000 characteristics (vehicle, roadway, traffic, and environment characteristics) of the highway transportation system to which the driver must respond. The sheer complexity of driving makes it impractical to rely on separate heuristics for every driving situation, which is why it would be beneficial to identify the general principles that govern human driving behaviour.

So far, attempts at identifying the underlying principles of human driving behaviour have resulted in a rather fragmented understanding of the driving task, where specific visual cues are used to predict the driver's behaviour in specific driving tasks [10]. For example, the optical edge rate has been used to predict the speed at which drivers drive [11], whereas Lee (1976) [13] showed that time to collision (TTC) is predictive of human braking behaviour while approaching a static or moving obstacle. Godthelp and colleagues provided evidence that time-to-lane-crossing (TLC) can describe the positioning of a vehicle in a lane while driving on straights and curves [45][46]. The TLC model of Godthelp was extended by Boer, to account for the variability of lateral position (satisficing) while driving in curves [47]. Additionally, models based on a 'potential-field' have tried to solve the path planning problem by assigning different costs to different obstacles and finding the path of least cost [48]. However, these potential-field models have not been tested for human-likeness.

The first attempt of creating a unified model of human driving behaviour can be found in Gibson and Crooks' 1938 paper, where they proposed the concept of 'field of safe travel' [1]. They defined the field of safe travel as the "field of possible paths which the car may take unimpeded" (p. 454); it was described as comprising both subjective elements ("subjective experience of the driver", p. 455) and objective elements ("it exists objectively as the actual field within which the car can safely operate", p. 455). Gibson and Crooks illustrated the field with various drawings of driving situations (e.g., straight-line driving, curve driving, moving pedes-

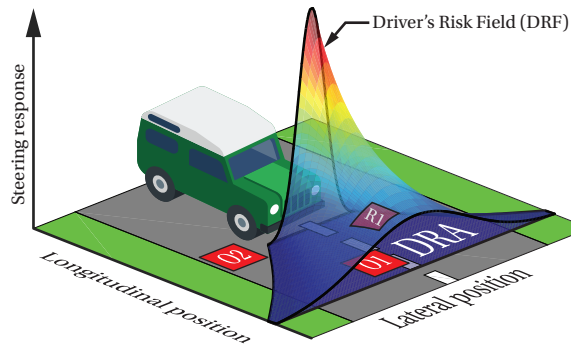


Figure 2.1: **Visualising the Driver's Risk Field (DRF)**: The height of the surface represents the magnitude of the steering response to an obstacle (subjective or objective). Obstacle O1 stimulates a response of magnitude R1, whereas obstacle O2 does not stimulate any response from the driver.

trian, moving obstacle, overtaking a parked car, blind corner). The study, however, was qualitative and based on discussions between a psychologist and a student of driving. Thus, although the field of safe travel is introspectively plausible and highly influential, it lacks operationalization and has limited empirical validation [49].

In recent years, some automated cars have been based on concepts similar to that of Gibson and Crooks'. These concepts used 'tentacle-like' algorithms that allowed for driving on straights and curves while negotiating obstacles [23] [50]. These algorithms generated the possible future paths originating from the current state of the vehicle (based on several different methods such as rapidly-exploring random trees (RRT) and trajectories of maximum lateral acceleration at different speeds) which resembled tentacles extending from the front of the vehicle. These algorithms scanned the driver's preview area and used that information for planning the path through the environment. Despite the fact that these algorithms were not intended to be human-like, their success in navigating through several scenarios indicates that area-based models could potentially provide an understanding of human driving behaviour in several scenarios [51].

As indicated above, the use of field-based approaches is promising in modelling human driving behaviour and for using it in the controllers of automated vehicles. However, so far, there appears to be no experimental evidence as to whether such a field is perceived and used by humans while driving. In this study, we take a step towards operationalizing the field of safe travel [1] by measuring the 'Driver's Risk Field' (DRF): a quantification of the driver's steering response as a function of the region (area) in front of the vehicle. It is important to point out that the DRF defined in this study and the field of safe travel are two different concepts. To put it in the context of other literature, Näätänen and Summala (1976) [2] suggest that a driver's perceived risk is the product of (i) the driver's belief about the probability of a hazardous event occurring and (ii) the consequences of that event. In this chapter, we hold the second part (consequence of the event) constant by perform-

ing obstacle avoidance tasks with identical obstacles. We assume that when the drivers think that they may collide with the obstacle they respond proportionally to the perceived risk. With this assumption, the DRF represents the first part: the driver's belief about the probability of him/her colliding with an obstacle appearing (hazardous event) in his/her preview. The DRF can be used to estimate the driver's perceived risk, which will be a function of the car and driver state. The optimal values of this estimated risk (with respect to the yaw rate, heading, speed, etc. apart from the position of the vehicle), when plotted as a function of the position of the vehicle in the environment, will result in Gibson and Crooks' field of safe travel. The field of safe travel can hence be seen as the solution space of a path planning problem, whereas the DRF can be viewed as a component that helps generate this solution space.

To determine the shape of the DRF, different positions in the preview of the driver needed to be probed. For this study, we chose an obstacle avoidance task on a straight road, where an obstacle appeared at a specific lateral and longitudinal location. The experiment was conducted in a driving simulator instead of in a real car for safety and experimental control. The shape of the DRA (the 2D projection of the DRF on the road surface) was hypothesised to expand (i.e., widen) as the longitudinal distance from the vehicle increases (Fig. 2.1). This hypothesis was based on neurophysiological studies that have provided evidence for the presence of noise in the human sensors (vision, proprioception, etc.) and actuators (muscles) [29]. It is also known that humans try to minimise the effect of noise present in their sensorimotor control system [30][52]. In the field of driving, it has been established that humans look ahead (preview) while driving [53]. If predictions of positions of the vehicle are made, the noise/uncertainty will propagate and will result in an expanding region as the longitudinal distance increases [54]. Furthermore, we hypothesised that the height of the DRF decays as the lateral and longitudinal distance from the vehicle increase. This hypothesis is based on findings in the literature that show that with higher time margins, the response of the driver decreases. Jurecki and Stanczyk [55] found that the driver became more relaxed (higher reaction times) as the risk of colliding with a pedestrian decreased (time to collision (TTC) to pedestrians increased). Lewis-Evans et al. [56] found that the perceived risk and task difficulty increased when the time headway during car-following increased. In our study, we aimed to quantify these observations by finding the functions that describe these relationships.

2.2. EXPERIMENTAL METHODS

2.2.1. APPARATUS

Participants (N = 8) drove in a fixed-base simulator (Fig. 2.2) at the Control and Simulation Department at the faculty of Aerospace Engineering, Delft University of Technology. Self-aligning torques of the front wheels were provided by a MOOG FCS ECO18000 S steering motor running at 2500 Hz. A single-track model (heavy sedan of 1.8 m width) was used to simulate the vehicle dynamics. The environment was shown using three digital light processing (DLP) projectors (BenQ W1080ST

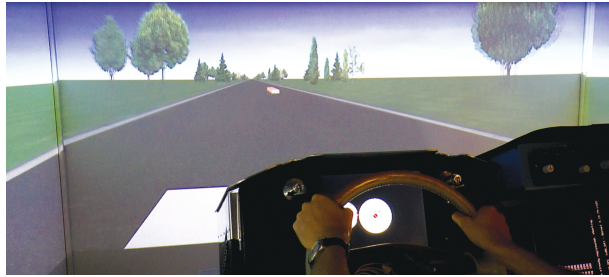


Figure 2.2: **Fixed base driving simulator:** A snapshot of the driving scene from the simulator, at the moment the obstacle appeared in front of the driver. The participants drove a 1.8 m wide car on a 7 m wide road with no centre lane markings, at a constant speed of 25 m s^{-1} .

1080p Full HD), together providing a horizontal and vertical field-of-view of 180° and 40° , respectively. The visuals were displayed with a frame rate of 60 Hz, and the data was logged at 100 Hz. The (front) bonnet/hood of the car was visualised to facilitate a more accurate perception of the car's position relative to the road boundaries.

2.2.2. PARTICIPANTS

Since, our goal was to examine the functional relationships at the level of individual participants, it was decided to follow a design in which a large number of observations were made on a relatively small number of participants (Smith, 2018). Eight participants (7 male, 1 female) with normal or corrected-to-normal vision volunteered for this study and performed 308 obstacle avoidance trials. Participants had the following characteristics (Mean \pm SD) [units]: age (25.4 ± 1.7) [years], driving experience (6.1 ± 2.0) [years], driving frequency in the last 12 months (2.1 ± 1.8) [trips/week], and distance driven in the past 12 months (4712 ± 688) [km].

2.2.3. EXPERIMENTAL SETUP

Participants had to avoid an obstacle that appeared at one (randomly chosen) of the 77 positions. Each obstacle position was encountered 4 times, once per block of 77 trials. In total, each participant performed 308 obstacle avoidance trials. The experiment was spread out over two separate (not necessarily consecutive) days, with each day consisting of 2 blocks of approximately 30 minutes each. Each block consisted of 3 sub-blocks of approximately 8 minutes each. Sub-blocks 1, 2, and 3 consisted of 26, 26, and 25 trials, respectively, which resulted in each block making up 1 repetition of 77 trials. The trials were randomly ordered among the sub-blocks to ensure that participants could not anticipate the position of the obstacles.

In the experiment we had 78 obstacle positions, but the 78th position was not used for analysis in this study. It appeared as the 26th obstacle of every sub-block 3 and was positioned on the lane centre (lateral position = 0 m) at a longitudinal distance of 350 m. This obstacle was implemented for analysis which will be performed in a follow up study, and has not been considered for analysis in this study.

2.2.4. ROAD AND OBSTACLE DESIGN

ROAD DESIGN

Participants drove on a straight single-lane 7-m wide road, with no centre lane markings, and no traffic. The road was designed to be wide, to minimise the cues that participants would get from the lane boundaries with respect to the obstacle positions.

OBSTACLE POSITIONS

The 77 obstacle positions formed a grid that was used to determine the shape of the DRF. There were 7 columns of obstacle positions, and each column consisted of 11 positions. The distances were calculated from the centre of the obstacle to the centre of the vehicle, with longitudinal and lateral directions being parallel and perpendicular to the heading of the road, respectively. The 7 columns were at longitudinal distances of 25 m, 50 m, 75 m, 100 m, 125 m, 150 m, and 175 m in front of the vehicle centre. In each of the columns, the obstacles were positioned at lateral distances of 2.05 m, 1.85 m, 1.65 m, 1.45 m, 1.25 m, 0 m, -1.25 m, -1.45 m, -1.65 m, -1.85 m, and -2.05 m, from the lane centre. A positive value indicates that the obstacle was to the left of the lane centre, negative to the right, and zero indicates that the obstacle was on the lane centre.

As can be noticed, the 5 obstacles to the left and right of the lane centre were laterally positioned 20 cm apart, but the distance between the obstacle at ± 1.25 m and the obstacle at 0 m is 1.25 m. The vehicle used in the simulator is 1.8 m wide, and hence, any obstacle positioned within 1.025 m ($1.8/2 + 0.25/2$) of the lane centre would have to be always avoided. All the obstacles beyond 1.025 m, theoretically, do not need to be avoided, as they are beyond the width of the car. Accordingly, in our experiment, 70 out of 77 obstacles (i.e., all obstacles except the 7 in the centre row) did not have to be avoided. The participants were not made aware of this information.

OBSTACLE PROPERTIES

Each obstacle was a cuboid with a rectangular cross-section (height x width = 12.5 cm x 25 cm) and length of 15 m. The obstacle laid flat on the road with its long axis parallel to the road heading. The obstacle was relatively long to encourage participants not to steer back immediately after they have passed the front of the obstacle.

2.2.5. DRIVING TASK

The experiment was conducted at a constant vehicle speed (25 m s^{-1}) since the intention was to measure the response of the driver solely by means of steering. If speed control would be handed over to the driver, it could be expected that the response of the driver would get distributed over steering and speed control. Additionally, it was necessary to ensure that, in every trial, the relative distance between the vehicle and the obstacle is realised, as per the design (Fig. 2.3). Therefore, guidance torques were exerted on the steering wheel, which guided the vehicle to the

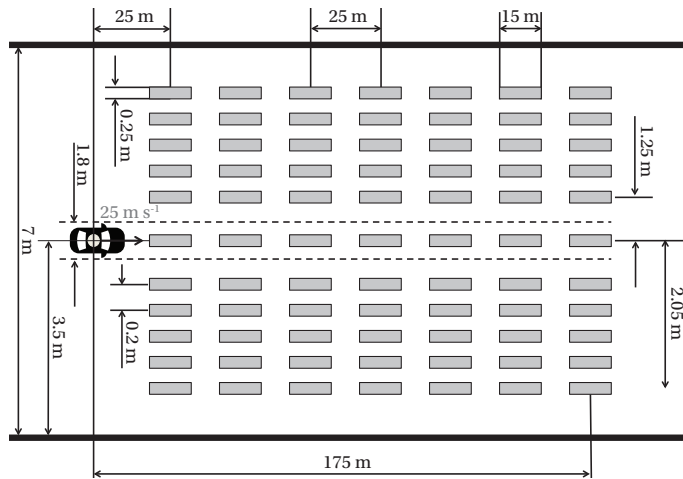


Figure 2.3: **Obstacle positions:** The representation (not to scale) of the grid of obstacle positions. During each trial, an obstacle would appear at one of these 77 positions (11 lateral and 7 longitudinal positions). If driven straight, only the centre row of obstacles obstructed the vehicle. All other obstacles were at a lateral distance (at least 0.225 m) greater than the width of the car.

lane centre, before the start of each trial. A small buzzing vibration was also added to the steering wheel to convey to the driver that the vehicle is guiding itself to the lane centre. Each trial was assigned a road section of 350 m, and the obstacle would appear at the start of this section (Fig. 2.4). As soon as the obstacle would appear, the lane centring guidance would deactivate. The driver would perform the manoeuvre, and then 50 m after the obstacle centre had been passed by the vehicle centre, the guidance torques would come into effect. As soon as the next obstacle would appear, the guidance torques would deactivate, and the experiment would continue with the subsequent trial.

Because the obstacles appeared at random positions and the lane centring guidance system took over after the obstacle was passed, the duration for which the guidance system was on was also random. This random duration mitigated the problem of participants anticipating the obstacle appearance based on the duration for which the guidance was on.

2.2.6. MEASURING THE DRIVER'S RESPONSE

Whether the DRF is subjective (only perceived) or objective (visible in the driver's actions) is an important point that needs to be investigated. If the DRF is subjective but not objective, then it could be a quirk of human perception, where people subjectively experience the DRF but do not act accordingly. Conversely, if it is objective but not subjective, then apparently people perform their steering actions subconsciously, without necessarily being aware of what they are doing. These, however, are extreme cases. Different shapes of DRF for subjective and objective steering responses could provide insights into the driver's awareness and perception of the

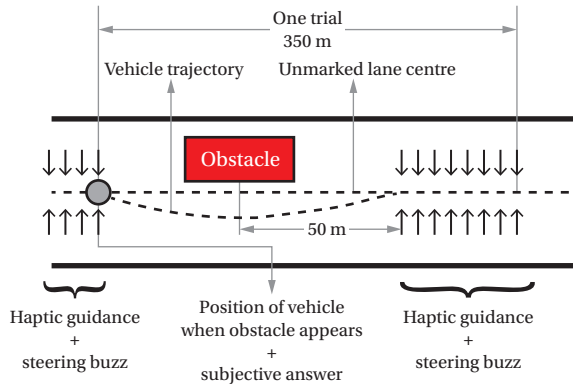


Figure 2.4: **Driving task:** A trial commenced when the obstacle appeared. The participant was expected to provide a numerical value (subjective response) and perform (or not perform) a steering manoeuvre to avoid the obstacle. Fifty meters after the vehicle centre had passed the obstacle centre, the lane centring guidance forces took over and guided the participant to the lane centre, in preparation for the next trial. The guidance deactivated, as soon as the next obstacle appeared, which also marked the beginning of the next trial.

driving scene. Thus, the experiment measured both the subjective and the objective steering responses of the participants during an obstacle avoidance task, and the results are analysed independently without assuming any dependency of one on the other.

OBJECTIVE RESPONSE

The objective measure was calculated as the maximum of the absolute value of the steering angle applied from the instant the obstacle appears to the point when the vehicle centre travelled 25 m (1 s, since speed of vehicle = 25 m s^{-1}). In Fig. 2.5, this is indicated from 0 longitudinal distance until the dotted vertical line. This ensured that we captured the initial response of the participants since we were interested in quantifying the shape of the DRF at the “current instant in time”.

SUBJECTIVE RESPONSE

For each trial, participants had to say aloud a non-negative real number as soon as the obstacle appeared. The number was an answer to the question: “How much steering do you think you need, at this moment?”. The words “at this moment” are an important part of the question since the DRF, as previously defined, relates to the perceived risk at the current time instant. Participants were instructed to report zero if they did not feel the need to steer at the current time instant. The question was stated at the beginning of the experiment (on each day) and was not repeated for each trial. The participants were expected to respond as soon as the obstacle appeared. They were trained for this with a 6 minute trial at the start of each day. No scale or reference values related to the subjective response were provided to the participants [57]. This approach was used to prevent the saturation

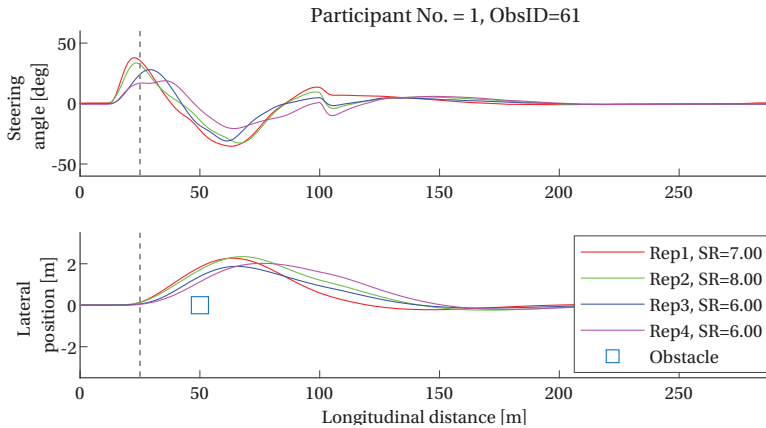


Figure 2.5: **Driver's response:** The figure shows the steering angle applied by a participant and the lateral position of the vehicle on the road as a function of the longitudinal distance along the lane centre. In this particular example, the obstacle appeared on the lane centre (lateral position 0 m) at a longitudinal distance of 50 m. The four lines represent the four repetitions for this particular obstacle position (Rep1 = first repetition). SR = subjective response of the participant for the corresponding trial.

of subjective answers towards the extremes of a predefined scale, which is important in our experiment because the participants did not know the lowest or highest level of the stimulus beforehand. Also, this approach provided more freedom to the participants, as it did not require them to multiply, divide, etcetera to scale their responses to the given reference value (Stevens, 1975 [57], p 28).

2.3. ANALYSIS

In this chapter, the analysis and results are reported for each participant independently. For each trial, we calculated a subjective and an objective measure, as described in the methods section. Three-hundred-eight responses were recorded per participant for the subjective and objective measure, each. All participants were instructed to report a subjective response of '0' to indicate "no steering needed at this instant in time". A similar threshold that distinguishes between a 'steering action' and 'no steering action' is needed for the objective measure (since the objective measure will never be exactly 0). A steering angle of ± 2 degrees was used as a threshold for the objective measure since literature indicates that angles greater than $|\pm 2 \text{ degrees}|$ represents a conscious steering action [58][59][60]. This means that if the maximum of the absolute of the steering angle applied by the participant was less than 2 degrees, the objective measure was set to 0, for that particular trial. Following this, for both subjective and objective measures, the 4 repetitions for the 77 obstacle locations were averaged and rearranged in an 11×7 matrix (11 lateral positions and 7 longitudinal positions). It is important to note that we performed the experiment at a constant speed and we expect speed to have a significant effect on the DRF (which will have to be quantified in future studies). Hence, to avoid the

speed dependency, we report our results in terms of distances and not in terms of time-based measures such as time to collision (TTC) or time headway (THW).

2.3.1. SHAPE OF THE DRIVER'S RISK FIELD (DRF)

We investigated the relationship between the position of the obstacle and the steering responses (subjective and objective) to determine the shape of the DRF with respect to the 3 axes:

1. **y-axis:** Effect of the lateral position of the obstacle on steering response (subjective and objective)
2. **x-axis:** Effect of the longitudinal position of the obstacle on steering response (subjective and objective)
3. **z-axis:** Contours of constant steering response (subjective and objective)

For each of these 3 axes, the data was fit to a function (Gaussian, power curve, or parabolic), and the R^2 index was calculated to assess the goodness of fit. A non-linear least-squares method with the Trust-Region algorithm was used to find the optimal parameters [61]. The analysis is identical for the subjective and the objective steering response, and is performed independently for each participant.

EFFECT OF THE LATERAL POSITION OF THE OBSTACLE ON THE STEERING RESPONSE

The effect of lateral position on the steering response was studied by using the 11 data points per longitudinal position (Fig. 2.6, Row 1). Each row of 11 data points (in cutting planes parallel to the y-z plane) was used to fit a Gaussian function (equation 2.1).

$$z = a_1 \exp\left(\frac{-y^2}{a_2^2}\right) \quad (2.1)$$

where a_1 and a_2 are the parameters to be estimated. The steering responses had their maximum value at the lane centre and decayed to zero on either side of the lane centre, for each of the 7 longitudinal positions. Accordingly, the continuous and differentiable Gaussian function was chosen over other simple functions such as linear functions or parabolas. The R^2 index was calculated per participant by taking a mean of the R^2 index of each of the 7 (longitudinal positions) curves.

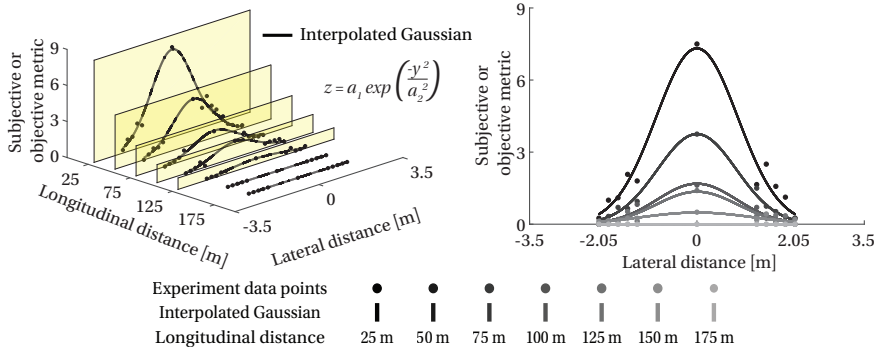
EFFECT OF LONGITUDINAL POSITION OF THE OBSTACLE ON THE STEERING RESPONSE

The effect of longitudinal position on the steering response was studied by using the 7 data points per lateral position (Fig. 2.6, Row 2). Each column of 7 data points was then used to fit a power function (equation 2.2).

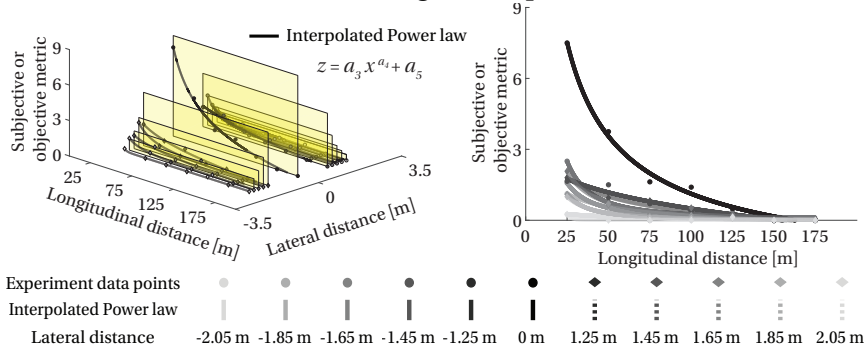
$$z = a_3 x^{a_4} + a_5 \quad (2.2)$$

where a_3 , a_4 , and a_5 are the parameters to be estimated. A power curve was fit to the experimental data because, from visual inspection, it could be seen that the steering response decays as the longitudinal position increases, an effect that bears

1. Effect of lateral position



2. Effect of longitudinal position



3. Steering response contours

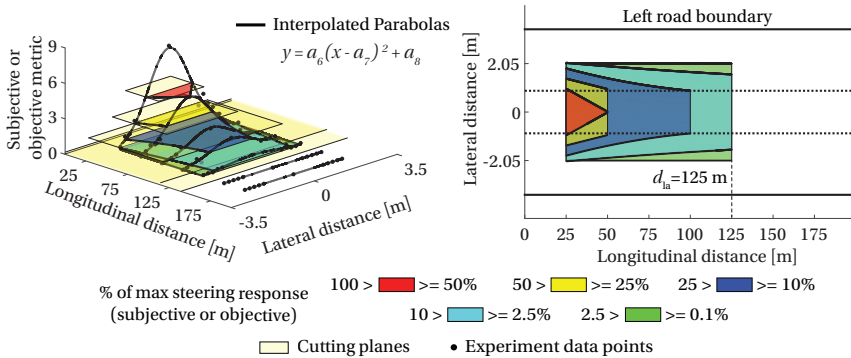


Figure 2.6: **Analysing the shape of the DRF:** Shape of the DRF was analysed along the y (lateral position) and x (longitudinal position) axes. Constant steering response contours were analysed along the z axis. The left column illustrates the analysis performed on the experimental data (black circles) using the (pale yellow) cutting planes, to arrive at the results shown in the right column. The look ahead distance (d_{la}) was the distance along the longitudinal axis, beyond which the steering response of the driver was zero.

a resemblance to the relationship between an objective stimulus and a subjective response studied by Stevens (1975). The R^2 index is calculated, per participant, by taking a mean of the R^2 of each of the 11 (lateral positions) curves.

SHAPE OF CONTOURS REPRESENTING CONSTANT STEERING RESPONSES

The interpolated Gaussian functions (previous subsection) are 'sliced' (parallel to the x-y plane) at 5 levels of steering response (0.1%, 2.5%, 10%, 25%, 50% of the maximum value of the measure). The maximum value is calculated per participant, separately for the subjective and objective measure. The points at which these cutting planes intersect the interpolated Gaussians are calculated and used to fit a second-order polynomial (equation 2.3)

$$y = a_6 (x - a_7)^2 + a_8 \quad (2.3)$$

where a_6 , a_7 , and a_8 are the parameters to be estimated and x is the longitudinal distance. A parabolic function was chosen because it is the lowest degree of the polynomial capable of estimating curvature. The number of data points available for curve fitting was a factor of consideration because we probed seven longitudinal distances (25 m to 175 m), but participants could have lower look ahead distances (d_{la}), resulting in a smaller (than 7) number of data points available for interpolation. Hence, a polynomial of the second order was chosen. If the cutting plane intersected only two Gaussians, then linear interpolation (equation 2.4) was used because interpolating a parabola is not feasible with less than three points.

$$y = a_6 x + a_7 \quad (2.4)$$

If the cutting plane intersected less than two Gaussians, a region could not be calculated, and hence is not shown in the plots. The R^2 index was calculated per participant by averaging the R^2 index of each curve. There are five cutting planes and each plane results in two boundary curves (left and right), which are mirror images of each other about the longitudinal distance (x) axis since the Gaussian function is centred at a lateral position of 0 (equation 2.1).

2.3.2. WIDTH OF THE GAUSSIAN CROSS-SECTION ALONG THE LONGITUDINAL DISTANCE

In the previous subsection, we proposed to quantify the cross-section of the DRF with a Gaussian function whose height decays as a power-law function of the longitudinal distance. However, the propagation of the width of the Gaussian function along the longitudinal distance is not quantified. For this, we fit a 2nd order polynomial to the a_2 parameter (from equation 2.1) of the Gaussian function at each longitudinal distance.

$$\sigma = a_9 (x - a_{10})^2 + a_{11} \quad (2.5)$$

The 3 parameters for (a_9 , a_{10} , a_{11}) of the second-order polynomial (equation 2.5) define the shape of the propagation of the width of the DRF along the longitudinal distance (x). Parameter a_9 dictates the curvature of the boundary ($a_9 > 0$,

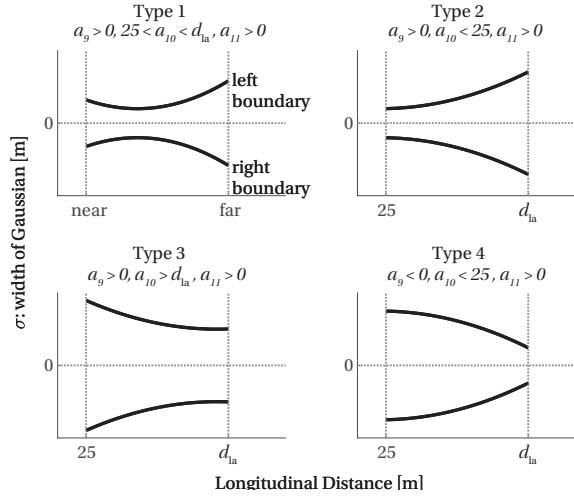


Figure 2.7: **Width of the Gaussian cross-section as a function of longitudinal distance:** The three parameters (a_9 , a_{10} , a_{11}) can form 12 different shapes, 4 of which are shown. The direction of travel of the vehicle is along the positive x-axis, and the near and far end are located at 25 m and d_{la} (look ahead distance) in front of the vehicle, respectively.

curves upwards and $a_9 < 0$, curves downwards). Parameter a_{10} defines the position along the longitudinal distance, at which the curve reaches its inflection point (slope = 0). Parameter a_{10} can be classified into three regions: (i) $a_{10} < 25$ (in front of the near end), (ii) $25 < a_{10} < d_{la}$ (between the near and far end), and (iii) $a_{10} > d_{la}$ (beyond the far end). d_{la} is the look ahead distance of a particular participant. If the obstacles appear beyond the d_{la} , the participant does not feel the need to steer immediately (Fig. 2.6). Parameter a_{11} defines the lateral position of the inflection point of the curve. Hence, a_9 is classified in 2 ways ($a_{10} > 0$, $a_{10} < 0$), a_{10} is classified in 3 ways ($a_{10} < 25$, $25 < a_{10} < d_{la}$, $a_{10} > d_{la}$), and a_{11} is classified in 2 ways ($a_{11} > 0$, $a_{11} < 0$). Hence, there are 12 ($2 \times 3 \times 2$) possible shapes, 4 of which are shown in Fig. 2.7. The Type 1 shape resembles an hourglass, which widens at the ends and narrows in the middle. Type 2 looks like a funnel which widens from one end to the other, and Type 3 is ‘opposite’ of Type 2, where the funnel narrows as the longitudinal distance increases. Type 4 bulges outwards while narrowing from the near end to the far end. We plot the left boundary using (equation 2.5) ($a_2 > 0$) and its ‘mirror image’ ($-a_2 < 0$) about the longitudinal axis to provide better visualisation and understanding of the shape that would propagate (Fig. 2.7).

2.4. RESULTS

2.4.1. SHAPE OF THE DRIVER’S RISK FIELD (DRF)

EFFECT OF THE LATERAL POSITION OF THE OBSTACLES ON THE STEERING RESPONSE

The effect of lateral position of the obstacles on the steering response of all eight participants (individually) is shown in Fig. 2.8 (subjective: top two rows, objec-

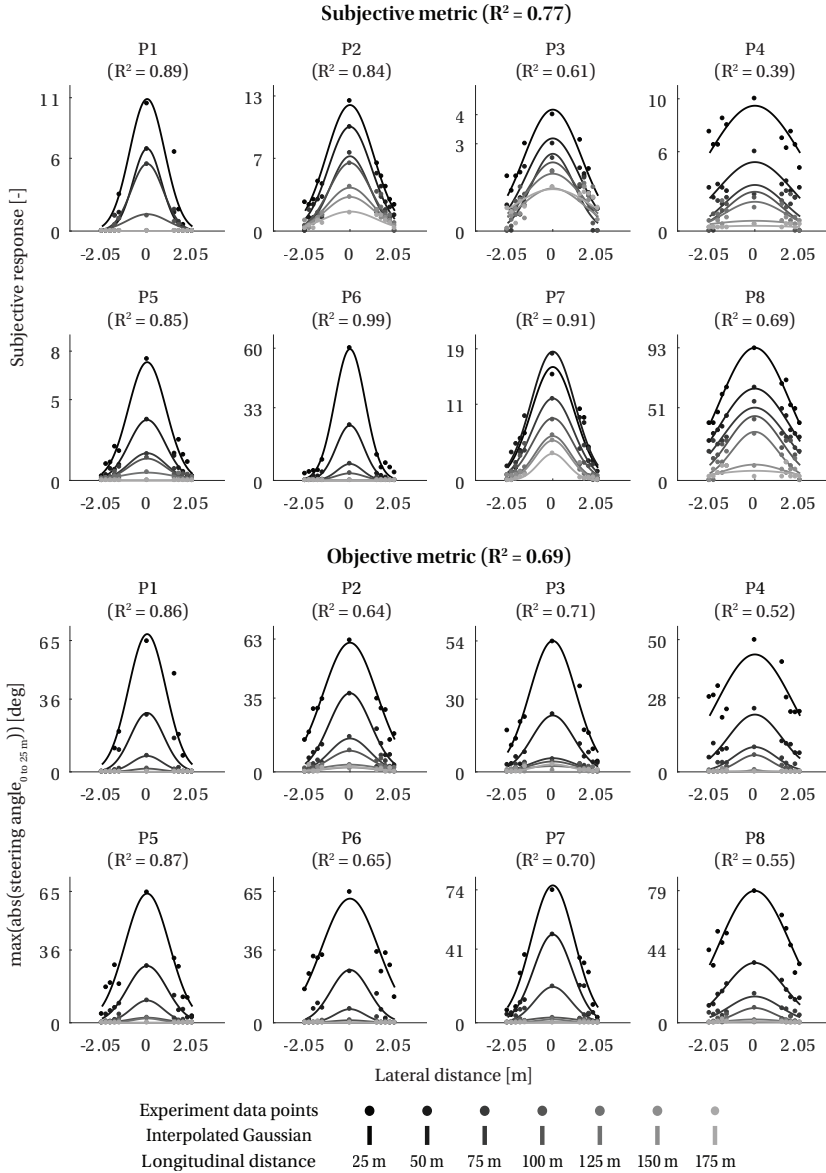


Figure 2.8: **Effect of lateral distance:** The figure shows the effect of lateral distance (of the obstacle centre from the lane centre) on the steering response for the eight participants (P1–P8). The x-axis represents the lateral distance of the obstacle from the lane centre (left of lane centre is positive), and the y-axis represents the subjective response (top 2 rows) and the objective measure of maximum absolute steering angle (bottom 2 rows).

tive: bottom two rows). As hypothesised, the magnitude of steering response decreased as the lateral distance of the obstacle from the lane centre increased (on either side). All participants responded to obstacles beyond the width of the car (± 0.9 m), indicating that the area in the driver's preview that stimulates a steering correction is wider than the width of the vehicle and that drivers prefer to adopt a lateral safety margin to the obstacles. Individual differences can be found in the height and width of the Gaussians. For example, P1 and P5 have narrow Gaussians, whereas P4 and P8 have wide Gaussians. As the longitudinal distance of the obstacle to the vehicle increases, the magnitude of steering response decreases (as shown by the grayscale gradient lines in Fig. 2.8). The range of angles applied by the participants (objective measure) was quite similar (in the range of 0–80 deg), while the subjective responses had widely varying ranges. For example, P8 had a range from 0 to 100, while P3 had a range from 0 to 4. A Gaussian function accurately described the effect of lateral position on subjective ($R^2 = 0.77$) and objective ($R^2 = 0.69$) steering responses.

EFFECT OF THE LONGITUDINAL POSITION OF THE OBSTACLES ON THE STEERING RESPONSE

The effect of the longitudinal position of the obstacles on the steering response is shown in Fig. 2.9 (subjective: top two rows, objective: bottom two rows). As the longitudinal distance of the obstacle from the vehicle increases, the magnitude of steering response decreases. Individual differences can be found in the height and the rate at which the responses decline as a function of longitudinal distance. For example, P3 and P7 have gradual rates of descent of steering response, whereas P5 and P6 have steep rates of descent. As the lateral distance to the lane centre increases, the magnitude of steering response decreases (as shown by the grayscale gradient lines in Fig. 2.9). A Power law was used to describe the effect of the longitudinal position of the obstacle, on subjective ($R^2 = 0.86$) and objective ($R^2 = 0.98$) steering responses.

CONTOURS OF CONSTANT STEERING RESPONSES

The results in Fig. 2.10 show the regions in the DRF that correspond to different intervals of steering response. The intervals were defined relative to the maximum steering response (subjective and objective) of each participant. There are clear individual differences in the way participants responded to obstacles. For example, P2 has a very wide DRF compared to P1. As the magnitude of steering response increases (0.1% to 50%), the area of the corresponding contour region shrinks towards the vehicle. It is also evident that the participants used different look ahead distances (d_{la}). Most participants (P1, P2, P4, P5, P6, P8) have the same look ahead distance for subjective and objective measures.

Participants P3 and P7 have a shorter look ahead distance calculated from the objective measure as compared to that calculated from the subjective measure. This means that participants consciously decided to make a correction, but the steering corrections were smaller than the 2 deg steering angle threshold that we set (to differentiate a conscious steering action from noise). Some of the subplots

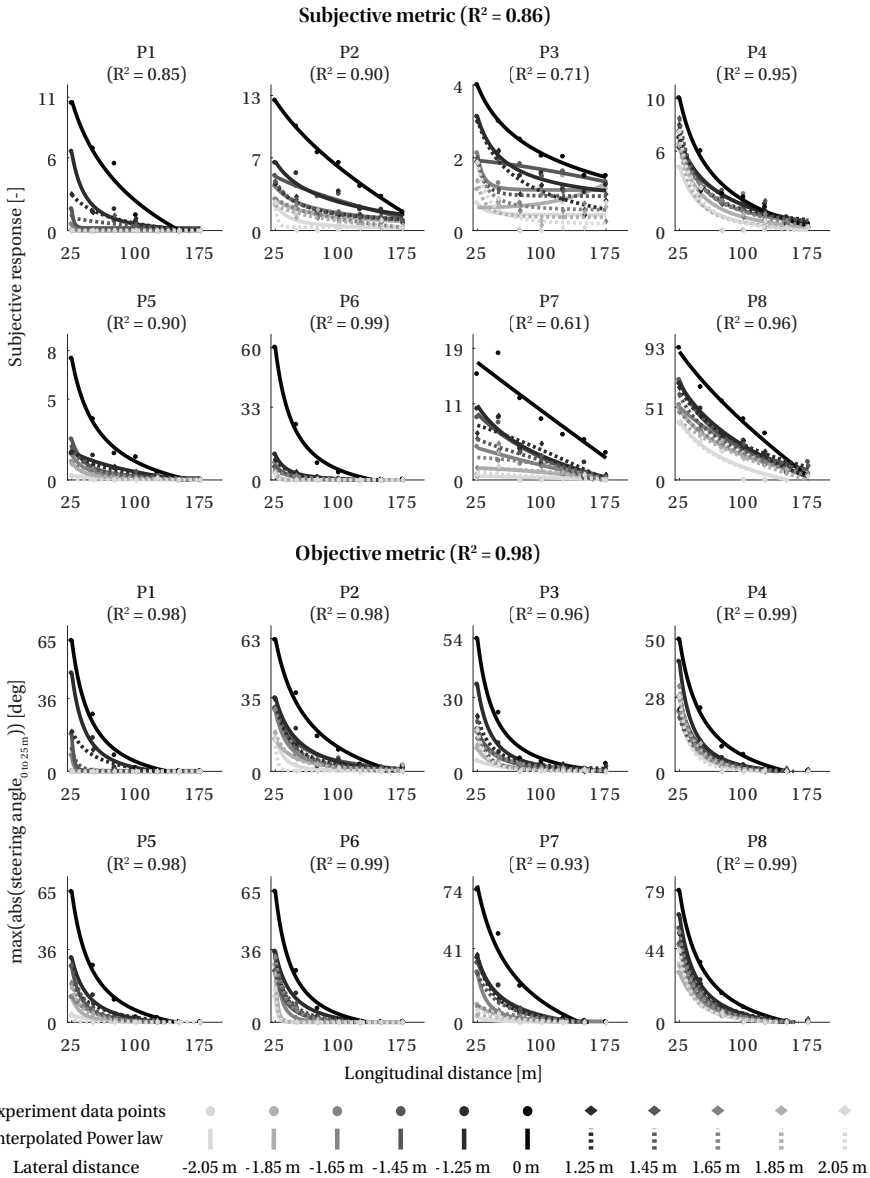


Figure 2.9: **Effect of longitudinal distance:** The figure shows the effect of longitudinal distance (of the obstacle centre from the vehicle centre) on the steering response for the eight participants (P1-P8). The x-axis represents the longitudinal distance of the obstacle from the vehicle (the vehicle is travelling in the positive x-direction), and the y-axis represents the subjective response (top 2 rows) and the objective measure of max absolute steering angle (bottom 2 rows).

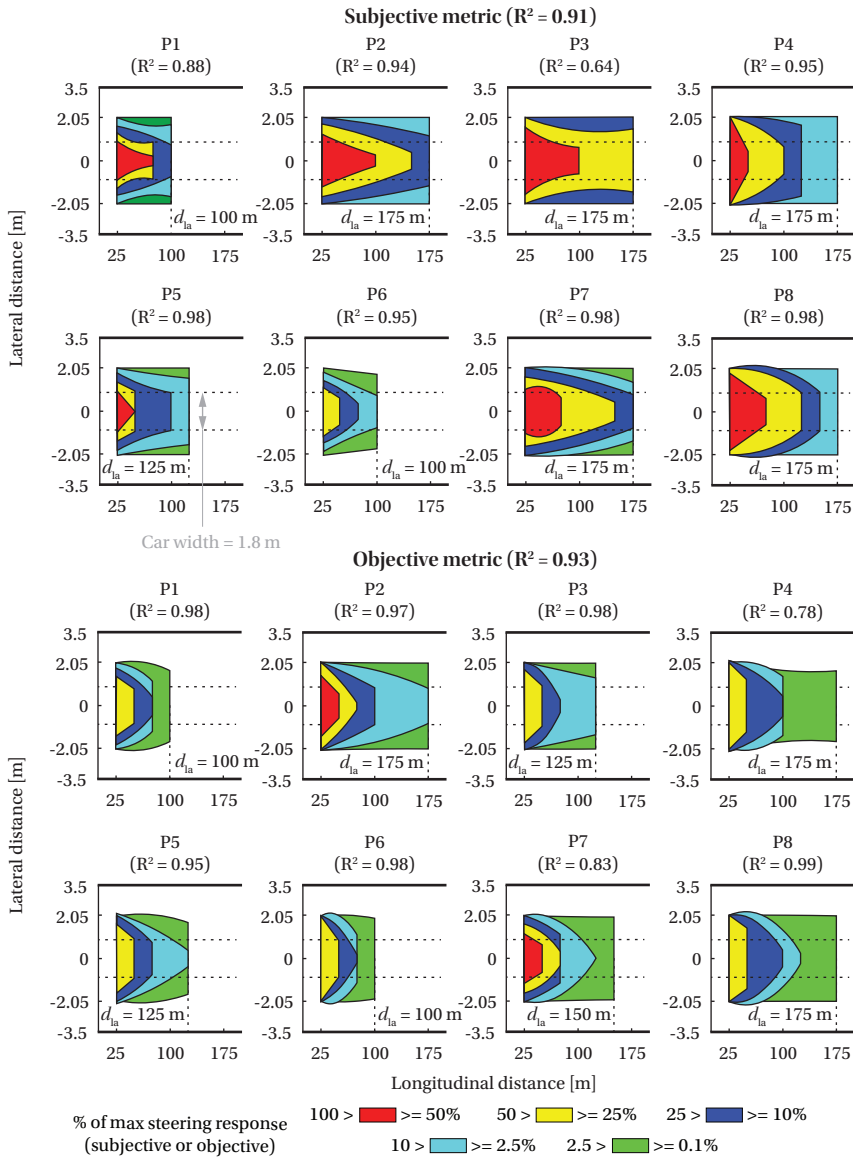


Figure 2.10: Constant steering response contours: The figure shows the regions of constant steering response at different intervals, for the eight participants (P1-P8). The different intervals (0.1%, 2.5%, 10%, 25%, 50%) are of the maximum value of the measure (subjective and objective, respectively), per participant. The x-axis represents the longitudinal distance of the obstacle from the vehicle (the vehicle is travelling in the positive x-direction), and the y-axis represents the lateral distance of the obstacle from the lane centre. All participants exhibit a DRF that is wider than the width of the car (horizontal dotted lines).

do not have the 50% (red) plane plotted (subjective: P6, objective: P1, P3, P4, P6, P8) since the 50% cutting plane intersected with less than two Gaussians.

2.4.2. WIDTH OF THE GAUSSIAN CROSS-SECTION ALONG THE LONGITUDINAL DISTANCE

The width of the Gaussian function (a_2) for each longitudinal distance was used to interpolate a parabola to determine the shape of the propagation on the DRF (Fig. 2.11). The 95% confidence interval of the estimation of a_2 is shown in grey markers.

The shape was quantified by the parameters of the parabolic boundaries (a_9 , a_{10} , and a_{11}) as explained in the analysis section (reported in Table A.1: Appendix A), and was classified into Type 1, 2, 3, or 4 (Fig. 2.7), according to the parameter values. The interpolated Gaussian functions with height (a_1) = 0 were not used for fitting the parabolas since 0 steering response indicated 'no immediate steering required'. Most of the shapes (six of eight for subjective, and seven of eight for objective) resemble an hourglass shape (Type 1). Participants P1 and P3's objective measure narrows as the longitudinal distance increases and hence is classified as Type 3, whereas the subjective measure of P7 narrows (with a bulge) and hence is classified as Type 4.

2.4.3. THE RELATION BETWEEN SUBJECTIVE AND OBJECTIVE MEASURES

When the subjective responses were compared against the corresponding objective responses, for each participant (Fig. 2.12), the Pearson correlation coefficients (r) indicated a strong association between them. This result shows that the DRF was not only perceived by the humans (subjective measure) but also acted upon (objective measure). However, there were a considerable number trials (especially for participant 4, $N_{obj0} = 30$) where participants reported a non-zero subjective response but did not perform a steering action within 1 s of the obstacle appearing. This effect can also be seen in Fig. 2.10, where the subjective contours (Fig. 2.10 top 2 rows) with higher values (red, yellow, deep-blue) cover larger areas of the DRF, compared to their area in the objective contours (Fig. 2.10 bottom 2 rows). This indicates that even if the participants perceive the risk at the current instant in time, they do not necessarily act immediately.

2.5. DISCUSSION

This study aimed to experimentally investigate the shape of the 'Driver's Risk Field' (DRF) by quantifying the steering response in an obstacle avoidance task, at a constant speed. The results (Fig. 2.8, Fig. 2.9) show that the effect of lateral and longitudinal position of the obstacle on steering response can be quantified by the Gaussian function and the Power law, respectively. Hence, the DRF constitutes a function (Fig. 2.13 [b]) that describes the driver's risk along the direction of movement of the vehicle, where the risk decreases in the lateral direction according to a Gaussian function, and according to the Power law in the longitudinal direction.

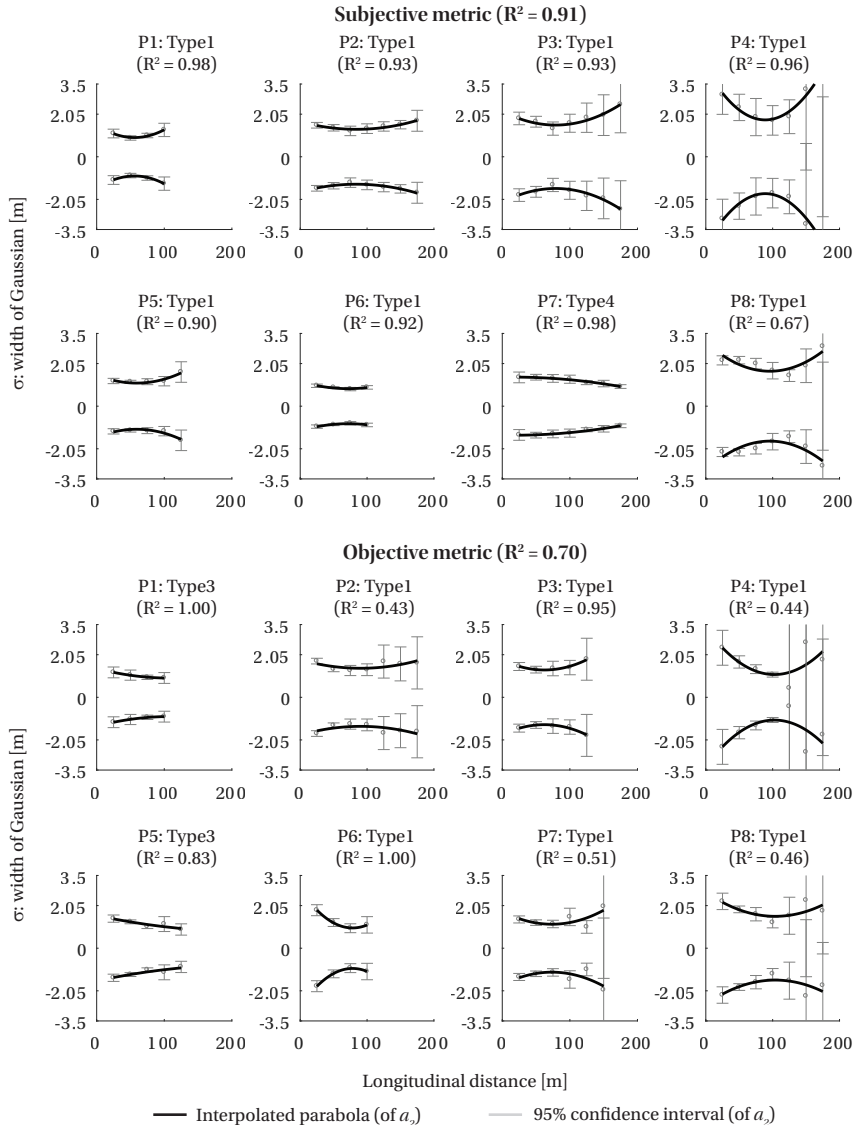


Figure 2.11: **Width of Gaussian cross-section:** The figure shows the effect of longitudinal distance on the width of the Gaussian cross-section of the DRF for the eight participants (P1-P8). The x-axis represents the longitudinal distance of the obstacle from the vehicle (the vehicle is travelling in the positive x-direction), and the y-axis represents the width of Gaussian. A parabolic function is fit to the width of Gaussian (parameter a_2 in equation 1) at every longitudinal distance. The 95% confidence interval (calculated using the *confint* function in MATLAB) are shown with the grey markers.

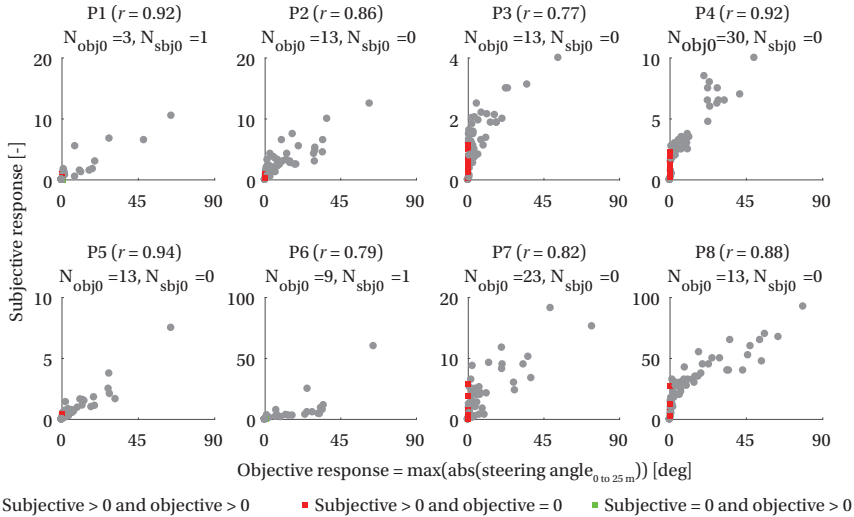


Figure 12: **Relation between subjective and objective measures:** The figure shows the correlation between the subjective response on the y-axis and the objective response (maximum of the absolute steering angle applied by the driver) on the x-axis. The Pearson correlation coefficient (r) is reported for each participant and indicates a high correlation between the subjective and objective measures (average of all participants: $r = 0.86$). N_{obj0} is the number of times (out of 77) that the objective measure was 0 and the subjective measure was non-zero (red squares), and N_{sbjo} is the number of times the subjective measure was 0 and the objective measure was non-zero (green squares).

The top-down projection of the function visualises the Driver's Risk Field projected around the vehicle, and the propagation of the width of the risk field follows an hourglass shape (for most participants). We hypothesised that the shape of the DRF would expand as the longitudinal distance increased (Type 2 shape), but the results show that the DRF is shaped like an hourglass (Type 1 shape) for most of the participants (Fig. 2.11). The Type 1 and 2 shapes are both wide at the far end, but the hourglass shape (Type 1) we observed for most subjects also widens at the near end. This widening at the near end could be due to startle, because of an obstacle appearing suddenly in front of the participant. This startle could initiate an open-loop steering action, without completely processing the position of the obstacle. This open-loop type of steering response in emergency scenarios was also observed in a previous study by Van Auken et al. (2011) [17].

We hypothesised that the steering response would decrease as the distance between the obstacle and the vehicle increases. This hypothesis was confirmed by the results in Fig. 2.8 and Fig. 2.9. The decrease in steering response magnitude for increasing longitudinal distance to an obstacle corresponds to previous studies. For example, Gold et al. [62], the steering response (and hence the trajectory of the vehicle) became smoother as the take-over 'time budget' was increased (Fig. 4 in Gold et al., [62]). Other researchers found a decrease in subjective ratings of risk as the time headway (to a leading vehicle) increased, confirming our

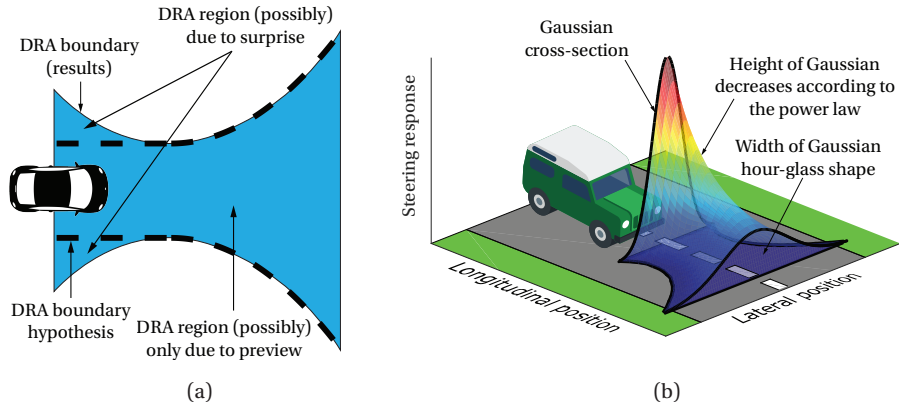


Figure 2.13: **Shape of the DRF:** (a) The results of our study show that the DRF is hourglass-shaped (Type 1), whereas the hypothesis (marked by the dashed black lines) is funnel-shaped (Type 2). We argue that the widening towards the vehicle is due to the startle open-loop correction caused by an obstacle suddenly appearing at a short distance. (b) Three-dimensional representation of the shape of the DRF. The height and width of the Gaussian cross-section follow the power law and the hourglass shape, respectively.

subjective results [56][63][64]. An important contribution of this chapter is that we captured this decrease in steering response as a function of increasing longitudinal distance by means of a Power law function for both subjective and objective steering response. The shape of the DRF in this study is quantified at a constant speed. However, to fully understand the nature and properties of the DRF, experiments at different fixed vehicle speeds and with speed control handed over to the driver need to be carried out. However, the challenge here will be to derive a single DRF based on both lateral and longitudinal control since the driver's response is expected to be distributed over steering and braking/acceleration. We expect that the size of the DRF will scale with the speed of the vehicle, but maintain its shape. This prediction is based on the fact that drivers tend to maintain a constant look ahead time, and hence the look ahead distance, and in turn, the DRF scales with speed [65].

The shape of the DRF, as quantified in this study, is based on the steering response magnitude as a function of the position of the obstacles. All the obstacles presented in this study were identical. This was done to study only the effect of the position of the obstacle and not its dangerousness. However, in the real world, obstacles pose different levels of risk. For example, a stone is less harmful as compared to a rock (effect of size), a sheet of paper on the road is less dangerous than a pothole of the same size (effect of material), a static obstacle like road work equipment causes different response compared to dynamic obstacles such as pedestrians and vehicles (effect of speed). Future experiments should be done using obstacles posing different levels of hazard.

In this study, we measured the subjective and objective responses of the par-

ticipants to examine if the risk field is perceived and/or acted upon. The results showed that the participants perceived (subjective response) and acted (objective response) on the risk. However, Fig. 2.12 showed that some participants perceived the risk at the current instant in time but did not act immediately. This means that sometimes the perceived risk is not large enough to elicit an immediate action (or any action at all). The relationship between the delay in responding to perceived risk and the position of the obstacle will be studied in the future.

One of the limitations of measuring subjective and objective response simultaneously is that there can be an interaction between the two responses. We tried to minimise this interaction by making the task 'subconscious' so that the participants did not consciously link their subjective and objective responses. We trained and motivated the participants to provide us their subjective response as soon as they saw the obstacle. Secondly, the participants could respond with any non-zero number and did not have to adhere to any predefined scale. This reduced the mental effort of consciously performing arithmetic calculations to provide a subjective response. Future studies could measure the subjective and objective measure separately and examine the interaction effect.

The DRF proposed in this study, which represents the belief of the driver regarding the *probability* of a hazardous event occurring, can be combined with the *consequences of the event* to calculate the perceived risk [2]. This perceived risk could be used as a novel 'cost function' in controllers of automated driving/assistance systems. Fajen et al. [66] performed a similar study with participants walking in an area strewn with obstacles and reported that such a field-based approach could predict participant's path. The 'tentacle-like' algorithms in the field of robotics make use of the information from a vehicle's preview and show resemblance to the DRF. These similarities and the success of the area-based approaches in the field of robotics to negotiate a variety of scenarios indicates that the DRF can potentially be useful in several curve negotiation and obstacle avoidance scenarios [67][23][50][68]. However, the main difference between the existing algorithms and the present DRF is that the former are derived from a control-theoretic point of view, whereas the DRF, as shown in this study, is perceived and acted upon by humans. We expect that our human-factors based approach can serve to improve the anthropomorphism of automated vehicles. In recent years, 'human-like' driver models [69][31][70][71][72] and personalised driver models that can describe and adapt to the behaviour of individual drivers [73][74] have gained increasing attention. An important aspect of such models is the use of a function, the parameters of which can be modified to individualise driving behaviour [75]. The DRF in our experiment had an hourglass shape (for most participants), but its size was different for each tested individual. These individual differences can be captured by manipulating the parameter values and hence provide a means to individualise the DRF and make personalised driver models. Note that in this study, we do not provide a unifying model or theory based on the quantified DRF. Such model development will have to be explored in future research, along with experimental studies to test the generalisability of the shape of the DRF for different driving scenarios. We hope that this study thereby contributes to the development of automated vehicles that

understand and interact with humans in a safer and more efficient manner.

2.6. CONCLUSIONS

In order to quantify the Driver's Risk Field (DRF) which is subjectively perceived and objectively acted upon by the drivers, we performed a driving simulator study where drivers needed to avoid suddenly appearing objects on a straight road at a constant speed. For the experimental conditions studied, we conclude the following:

- Objective and subjective response of the drivers decreased as the lateral distance of the obstacle from the vehicle increased, and this relationship could be described by the Gaussian function (Fig. 2.8: Subjective $R^2 = 0.77$, Objective $R^2 = 0.69$).
- Objective and subjective response of the drivers decreased as the longitudinal distance of the obstacle from the vehicle increased, and this relationship could be described by the Power law (Fig. 2.9: Subjective $R^2 = 0.86$, Objective $R^2 = 0.98$).
- All participants responded to obstacles that were placed beyond the width of the car, meaning that the quantified DRF exceeds car-width. (Fig. 2.10).
- For most of the participants, the propagation of the width of the DRF along the longitudinal distance resembled an hourglass shape (Fig. 2.11).

3

DRF-BASED DRIVER MODEL: OPERATIONALIZING THE RISK THRESHOLD THEORY

Current driving behaviour models are designed for specific scenarios, such as curve driving, obstacle avoidance, car-following, or overtaking. However, humans can drive in diverse scenarios. Can we find an underlying principle from which driving behaviour in different scenarios emerges? We propose the Driver's Risk Field (DRF), a two-dimensional field that represents the driver's belief about the probability of an event occurring. The DRF, when multiplied with the consequence of the event, provides an estimate of the driver's perceived risk. Through human-in-the-loop and computer simulations, we show that human-like driving behaviour emerges when the DRF is coupled to a controller that maintains the perceived risk below a threshold-level. The DRF model predictions concur with driving behaviour reported in literature for seven different scenarios (curve radii, lane widths, obstacle avoidance, roadside furniture, car-following, overtaking, oncoming traffic). We conclude that our generalizable DRF model is scientifically satisfying and has applications in automated vehicles.

The contents of this chapter have been published in:
S. Kolekar, J.C.F. de Winter, and D. Abbink, *Human-like driving behaviour emerges from a risk-based driver model*, [Nature communications 11.1 \(2020\), 1-13](#)

3.1. BACKGROUND

WITH the introduction of automated vehicles, humans will increasingly need to interact with automated systems. One of the factors that influences human-automation interaction is the trust that users have in the system [76][77]. Research suggests that the more technology seems to have human-like capacities, the more people are expected to trust it to perform its intended function competently [78]. For example, when recorded vehicle trajectories were played back to drivers, the drivers preferred a driving style they thought was their own [7]. To impart human-like capabilities in automated systems, understanding and modelling the human driver is essential.

Despite many efforts in the field of driver modelling (for surveys see [79][80][81]), driver models are typically developed for specific scenarios. For example, longitudinal behaviour has been modelled using the optical edge rate on open roads [11], the time to extended tangent point in curves [12], time to collision (TTC) while approaching obstacles [13], and time headway (THW) during car-following [65]. Lateral positioning has been modelled using two-point (i.e., anticipatory vs. compensatory) models [16][70] in normal driving, and open-loop steering corrections [17] in emergency scenarios. To the best of our knowledge, the literature does not include a model of human driver behaviour that is applicable to a multitude of scenarios.

Practically, a unitary model could be developed by including a switch that selects a sub-model (or model parameters) based on the current driving scenario. However, this would require a-priori identification of all possible scenarios, linked to appropriately parameterized models, and smooth transitions between them. Such an approach has two main problems: Firstly, the fragmented approach will not perform satisfactorily for driving situations where there is an inappropriate switch between tasks, or for driving situations that have not been addressed a-priori, a problem also reported for machine learning techniques [8]. Secondly, this fragmented approach is not scientifically satisfying since it does not elucidate the underlying principles governing driving behaviour. These principles can be seen as a 'cost function' that human drivers try to minimise. Such cost functions have been proposed in the area of human motor control and have demonstrated emergent motor control behaviour in different tasks and environments [27]. The present study explores whether a similar generalizable model can be made for driving in different scenarios.

Essential to generalizable models is a cost function that is based on existing theories that aim to explain driving behaviour in a unified manner. The first attempt to such a unified theory was made by Gibson and Crooks [1]. They proposed that drivers perceive the qualitative concept of a 'field of safe travel', which is comprised of the possible paths that the car can take unimpeded. This theory paved the way for 'motivational driver models' such as the risk homeostasis and task difficulty homeostasis theories by Wilde [4] and Fuller [82], respectively. However, these theories have two drawbacks: Firstly, they lack specificity regarding their internal mechanisms, which makes it difficult to operationalize and vali-

date them [83][84][85]. Secondly, homeostasis theories cannot account for an important characteristic of human driving behaviour, namely satisficing. Drivers do not optimise their states (e.g., they do not try to follow the centre-line of the road perfectly) but try to maintain their state within acceptable limits (e.g., within lane boundaries) [21]. Models based on homeostasis theories maintain a certain risk or task-difficulty level, and hence will always follow a reference trajectory (for example, centreline of the road), which is not coherent with satisficing behaviour.

Näätänen and Summala [2] addressed satisficing behaviour by introducing the concept of a risk threshold. According to their theory, drivers do not maintain a certain level of risk but make corrective actions only when the risk they perceive increases beyond a threshold. This means that any vehicle state is acceptable, as long as the driver's risk is within his/her individualised threshold. However, to the best of our knowledge, the risk threshold theory has not been operationalized and tested in different driving scenarios.

In this chapter, we propose a novel metric - the *risk estimate*, which is based on published empirical data. We then formulate a driver model that utilises the proposed *risk estimate* as a cost function, simulate it in different driving scenarios, and compare its predictions about adaptations in speed and lateral position behaviour with the driver behaviour reported in literature. The results exemplify that, in driving, similar to motor-control tasks, a cost function that accounts for the consequence of noise (in human's perception and actions) seems to be the underlying principle governing speed and lateral position adaptations of drivers. In short, we propose the *risk estimate* that operationalizes human-like behaviour in a unified manner, for different driving scenarios.

3.2. METHODS

3.2.1. QUANTIFYING PERCEIVED RISK

According to Näätänen and Summala [2], perceived risk is the product of the subjective *probability* that an event will occur and the *consequence of that event* (Fig. 3.1 [a]). In this chapter, we operationalize these components (Fig. 3.1 [b]). The consequence of an event is the dangerousness of being in a particular state. We quantified this by assigning a cost to objects in the driving scene according to the danger they pose. These values need to be identified experimentally and are independent of the driver. A representation of the driver's belief about the probability of an event occurring was quantified in chapter 2. They measured drivers' subjective (self-reported) risk levels and objective (steering angle) steering responses in an obstacle avoidance task. The Driver's Risk Field (DRF), as we called it in chapter 2, has a high value near the ego car and decays as the lateral and longitudinal distance from the ego car increases. The DRF hence indicates that the driver believes that there is a higher probability of being in a position near their current position, in the next t_a seconds (preview time), than at further away points. The DRF, in essence, is assumed to capture the driver's uncertainty in his/her perception and actions.

The *risk estimate* is a scalar value which is the product of the 'cost of an event'

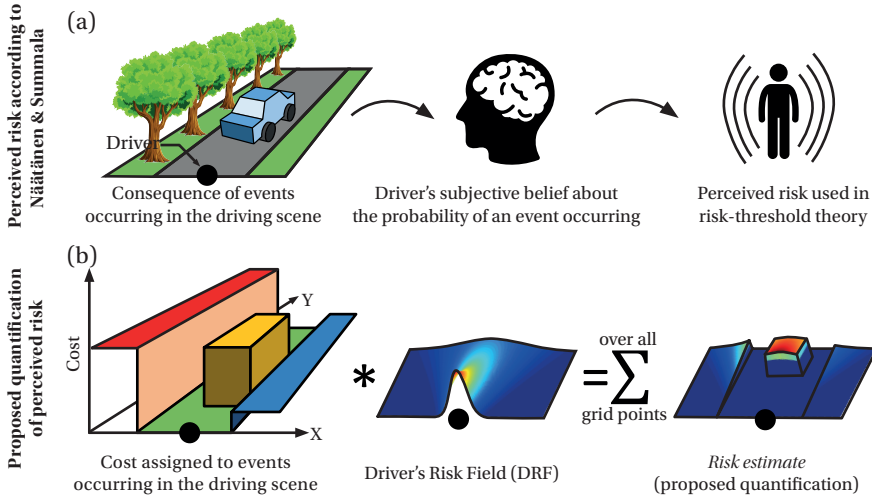


Figure 3.1: **Visualising the quantification of driver's perceived risk:** (a) This row illustrates Näätänen and Summala's [2] formulation of perceived risk. The consequence of an event (e.g., colliding with a tree) and the driver's subjective belief about the probability of that event occurring, form the driver's perceived risk. The driver in the ego car is indicated using the black marker. (b) This row illustrates the proposed quantification of this perceived risk. The cost of each element in the driving scene is multiplied with the Driver's Risk Field (DRF) that represents the driver's belief of the probability of being in a position. This product summed over all grid points generates the *risk estimate*.

and the DRF, summed over all the grid points. In essence, the *risk estimate* quantifies the 'consequence of noise/variability in our perception and actions', which is similar to the unifying cost functions proposed in motor control [27][30].

3.2.2. MODELLING THE DRIVER'S RISK FIELD

The DRF has been previously quantified for a fixed speed on a straight road [86]. In this section, we provide the mathematical formulation of a DRF that moves with the driver and changes its shape with speed and steering angle. In this chapter, the predicted vehicle path is calculated using a kinematic car model. The position (x_{car} , y_{car}), heading (ϕ_{car}), and steering angle (δ) determine the radius of the arc (R_{car}) in which the car is predicted to travel, assuming a constant steering angle (equation (3.1)).

$$R_{\text{car}} = \frac{L}{\tan(\delta)} \quad (3.1)$$

L is the wheel-base of the car. Using x_{car} , y_{car} , ϕ_{car} , and R_{car} , the centre of the turning circle (x_c , y_c) is determined, which is used to calculate the arc-length (s), measured along the predicted path (Fig. 3.2 [a]). The DRF is modelled as a torus with a Gaussian cross-section (equation (3.2)). The height (a) and width (σ) of the

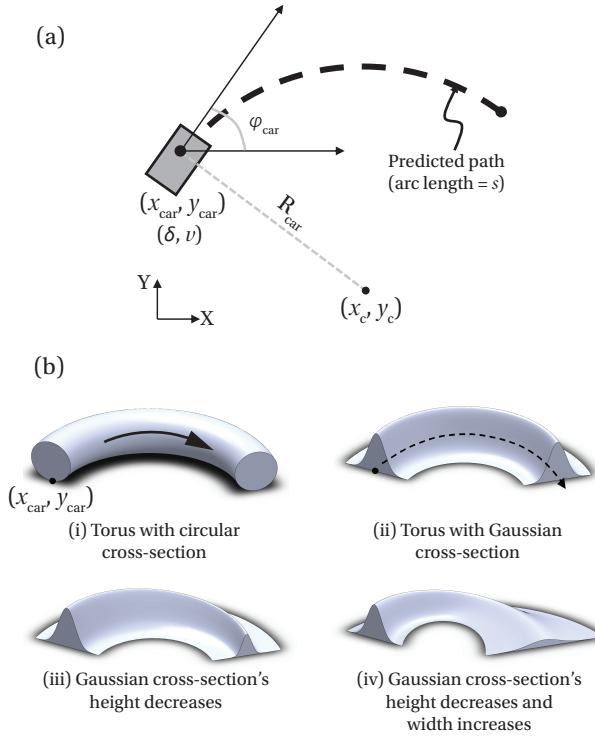


Figure 3.2: **Modelling the Driver's Risk Field:** (a) The 'predicted path' is calculated using the trajectory of vehicle kinematics, assuming constant steering angle (δ) and speed (v) for a fixed look ahead time (t_{la}). (b) The DRF is modelled as a modified torus. Four steps are taken to form the DRF from (i) A torus that curves along the 'predicted path'. (ii) Cross-section of torus is modified to a Gaussian. (iii) Height (a) and (iv) width (σ) of the Gaussian become functions of arc length (s), equations (3.3) and (3.4), respectively.

Gaussian are a function of the arc length (s) (Fig. 3.2 [b]).

$$z(x, y) = a \exp\left(\frac{-\left(\sqrt{(x-x_c)^2 + (y-y_c)^2} - R_{car}\right)^2}{2\sigma^2}\right) \quad (3.2)$$

The height of the Gaussian (a), is modelled as a parabola (equation (3.3)).

$$a = p(s - v t_{la})^2 \quad (3.3)$$

With a fixed look ahead time (t_{la}), the look ahead distance is assumed to increase linearly with speed (v). Parameter (p) defines the 'steepness' of the parabola (Fig. 3.3 [a][b]).

The width of the Gaussian (σ) is modelled as a linear function of arc length (s) (equation (3.4)), which is a simplification of the parabolic function (Fig. B.1 [a]:

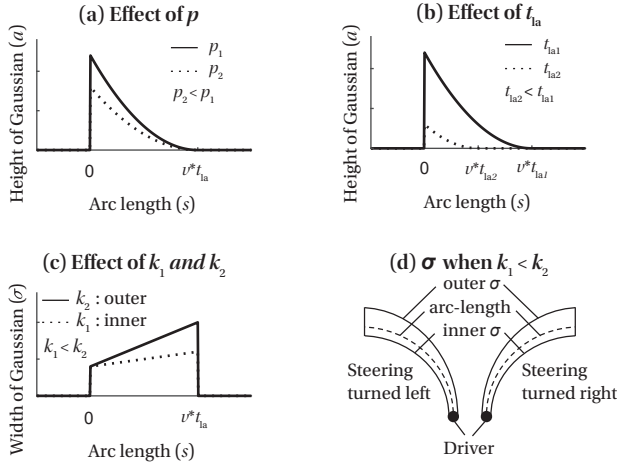


Figure 3.3: **Driver's Risk Field (DRF) parameters** The DRF is parameterized by 6 parameters: p , t_{la} , k_1 , k_2 , m , c . The effect of p (steepness of the parabola) and t_{la} are shown in (a) and (b) and emerge from equation (3.3). The maximum height of the Gaussian is determined by p , t_{la} , and speed. (c) Parameters k_1 and k_2 link the steering angle to the width of the Gaussian. The DRF widens (if $k_1, k_2 > 0$) or narrows (if $k_1, k_2 < 0$). (d) k_1 and k_2 correspond to the inner and outer Gaussian widths, respectively. So, if $k_1 < k_2$, the inner Gaussian is narrower than the outer, which enables 'corner cutting' in curves.

Appendix B) used in Chapter 2 and includes the following parameters: (i) c defines the width of the DRF at the location of the vehicle and is related to the car-width. In this chapter, c is equal to car-width/4 ($\pm 2\sigma$ of Gaussian distribution accounts for 95%). (ii) m defines the slope of widening (or narrowing for negative values) of the DRF when $\delta = 0$ (driving straight). (iii) k_1 and k_2 increase (or decrease, for negative values) the width of the DRF proportional to the (absolute) steering angle ($|\delta|$). This is based on the rationale that variability in steering angle increases linearly with the intended steering angle [65][31]. It is similar to the empirically confirmed signal-dependent noise present in the human sensorimotor system [30][29]. k_1 and k_2 represent the parameters for the inner and outer edges of the DRF, respectively, and allow for an asymmetric DRF (Fig. 3.3 [c][d]). The expansion of DRF proportional to $|\delta|$ results in the accumulation of a higher risk for a curve with a smaller radius. The asymmetric expansion (k_1 and k_2) provides flexibility to exhibit curve-cutting ($k_1 < k_2$), centreline ($k_1 = k_2$), or curve overshooting ($k_1 > k_2$) behaviour.

$$\sigma_i = (m + k_i |\delta|) s + c \quad (3.4)$$

$$i = 1(\text{inner } \sigma), 2(\text{outer } \sigma)$$

In short, the Driver's Risk Field (DRF) is parameterized by p , t_{la} , m , c , k_1 , k_2 , and is only dependent on driver's state, not the environment (Fig. 3.4).

To test if the proposed *risk estimate* can operationalize human-like behaviour in a unified manner, we used the *risk estimate* as an input for a simple driver model (Fig. 3.5 and Fig. 3.6) and simulated it on a virtual track (Fig. 3.7).

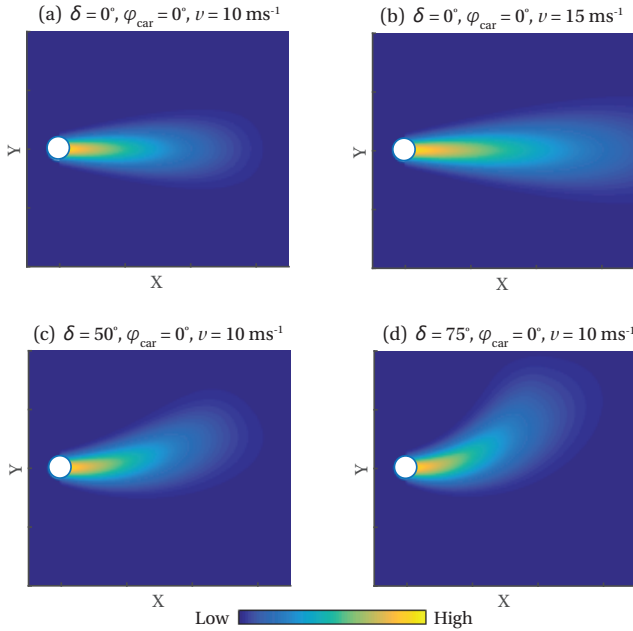


Figure 3.4: **Effect of steering and speed on the DRF:** The figure shows the shape and magnitude of DRF as a function of the position in the driving scene (global X and Y coordinates). The DRF is a dynamic field that expands with an increase in speed (compare (a)–(b)), and steering angle (compare (a)–(c) and (c)–(d)).

3.2.3. DRF-BASED DRIVER MODEL

DRIVER MODEL CONTROL STRUCTURE

To generate model predictions on human driving behaviour, the *risk estimate* calculated using the DRF needs to be connected to a controller that converts the *risk estimate* into control actions. We chose a simple control algorithm over more complex ones for two reasons: (i) we wanted to avoid the ambiguity in attributing the driver model’s behaviour to the complex algorithm instead of the DRF, and (ii) we wanted to avoid unnecessary complexity in formalising the optimisation problem. The DRF is an analytically calculable non-linear function (of the driver’s states). However, since the environment is represented as a discretized (grid) cost map, the *risk estimate* needs to be calculated numerically. Moreover, we need a controller that maintains the cost below a certain threshold and not one that minimises it. Hence, formulating the optimisation problem with the necessary constraints would itself be a separate study and is beyond the scope of this study. The main characteristic of the DRF driver model is that it does not minimise the cost function. Instead, it tries to achieve a certain goal (in this study, a desired speed V_{des}), while maintaining the cost (*risk estimate*: \hat{r}) below an individualised threshold (R_t).

The basic control structure (Fig. 3.5 [a]) includes a driver model that uses the

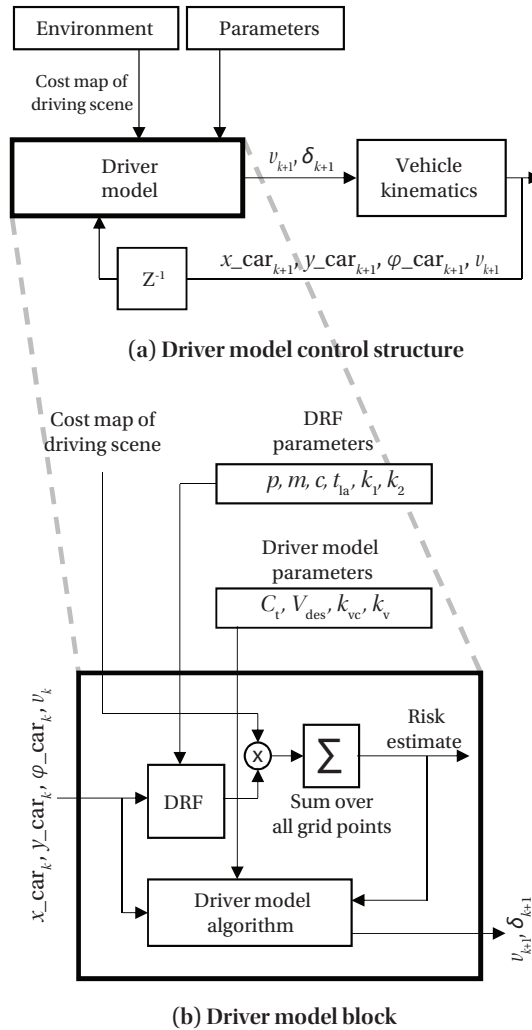


Figure 3.5: **Driver model:** A simple driver model that utilises the proposed *risk estimate* to generate control actions is shown. **(a)** Driver model control structure: The driver model uses the cost map of the driving scene (information about the environment), and the vehicle states (position (x_{car} , y_{car}), heading (φ_{car}), and speed (v) at k^{th} time step to generate the steering angle (δ), and speed (v) for $k+1^{\text{th}}$ time step. **(b)** The zoomed-in driver model block: The DRF is a dynamic field and changes its shape with vehicle state, which are inputs to the driver model block. The DRF is multiplied with the cost map of the driving scene and summed over all grid points to generate the *risk estimate* (cost function). The driver model algorithm uses the computed cost function, and the vehicle states to generate the speed (v) and steering angle (δ) for next time step. The DRF model algorithm is based on the risk threshold theory and compares *risk estimate* (\hat{r}) with risk threshold (R_t). The DRF can be individualised based on DRF parameters while the Driver model parameters determine how the cost (*risk estimate*) is converted to control actions (speed and steering).

information from the environment and the feedback from the vehicle kinematics to generate control actions (v_k : speed, and δ_k : steering angle) at the k^{th} time step. The inner workings of the driver model block are shown in Fig. 3.5 [b]. The DRF is multiplied with the cost map of the driving scene, and summed over all points to provide us with the *risk estimate* (cost). This cost is then used by the driver model algorithm, which is based on the risk threshold theory, to generate the control actions.

DRIVER MODEL ALGORITHM

The *risk estimate* (\hat{r}), in combination with the risk threshold (R_t) and desired speed (V_{des}), is used to formulate the DRF-based driver model. V_{des} is the speed at which the driver wants to drive on an open straight road, uninhibited.

In accordance to the risk threshold theory, the model tries to maintain the *risk estimate* (\hat{r}) below the risk threshold (R_t), and hence does not provide a specific trajectory, but rather a range of safe trajectories (satisficing). To avoid the ‘bouncing’ behaviour exhibited by satisficing controllers (Fig. B.1 [b]: Appendix B), the DRF model is complemented by a heading controller for the steering (equation (3.5)).

$$\delta_{k+1} = \delta_k + k_h (\phi_{\text{road}} - \phi_{\text{car}}) \quad (3.5)$$

where ϕ_{road} and ϕ_{car} are the heading of the road and car t_{lah} seconds in the future, respectively. The gain of the heading controller is k_h . The predictions about the future position and orientation of the car are made using the ‘predicted path’ calculations explained earlier.

The driver model algorithm (Fig. 3.6), at each time step (k), compares the *risk estimate* (\hat{r}_k) to risk threshold (R_t), and speed (v_k) to the goal (V_{des}). This results in four distinct cases of inequality. We do not consider the equality relations (e.g., if $\hat{r}_k = R_t$) because, practically they rarely occur.

1. If ($\hat{r}_k < R_t$ and $v_k < V_{\text{des}}$): This condition generally occurs when you start the journey. The model speeds up at a rate proportional to $(V_{\text{des}} - v_k)$. The parameter k_v (specific for each driver) represents how aggressively the model accelerates. The steering is determined by the heading controller (δ_{head}). Hence, $\delta_{k+1} = \delta_{\text{head}}$ and $v_{k+1} = v_k + k_v (V_{\text{des}} - v_k)$.
2. Else if ($\hat{r}_k > R_t$ and $v_k < V_{\text{des}}$): In this condition, the incurred cost (*risk estimate*) is more than the threshold (R_t), and the goal of desired speed has also not been achieved. In this case, we first check if the steering alone can help the model reduce the *risk estimate* below the threshold. This check is performed by using the *fmin_bound* function which finds the steering angle δ_{op} (within the bounds of $[\delta_k - 180^\circ, \delta_k + 180^\circ]$) that minimises the *risk estimate* (\hat{r}_k) assuming a speed of v_k . It also calculates the *risk estimate* (R_{op}) at this δ_{op} .
 - (a) If the model can find a δ_{op} such that $R_{\text{op}} < R_t$, then we continue to accelerate (to achieve our goal) and steer using δ_{opt} that reduces \hat{r}_k to

R_t (and not δ_{op} that reduces \hat{r}_k to R_{op}). This is done so that the model does not 'over correct'. If we were to use δ_{op} to minimise \hat{r}_k to R_{op} , it would always take the model to the lane centre. Hence the model tries to apply a steering that is just enough to reduce \hat{r}_k and get it below the threshold (R_t). Hence $\delta_{k+1} = \delta_{opt}$ and $v_{k+1} = v_k + k_v(V_{des} - v_k)$.

- (b) If the model cannot find a δ resulting in $R_{op} > R_t$, then the model slows down proportional to $R_{op} - \hat{r}_k$ (and not $R_{op} - R_t$) since the steering applied = δ_{op} is expected to reduce \hat{r}_k to R_{op} . This is done so that we do not slow down more than what is required. Hence, $\delta_{k+1} = \delta_{op}$ and $v_{k+1} = v_k + k_{vc}(R_{op} - \hat{r}_k)$.

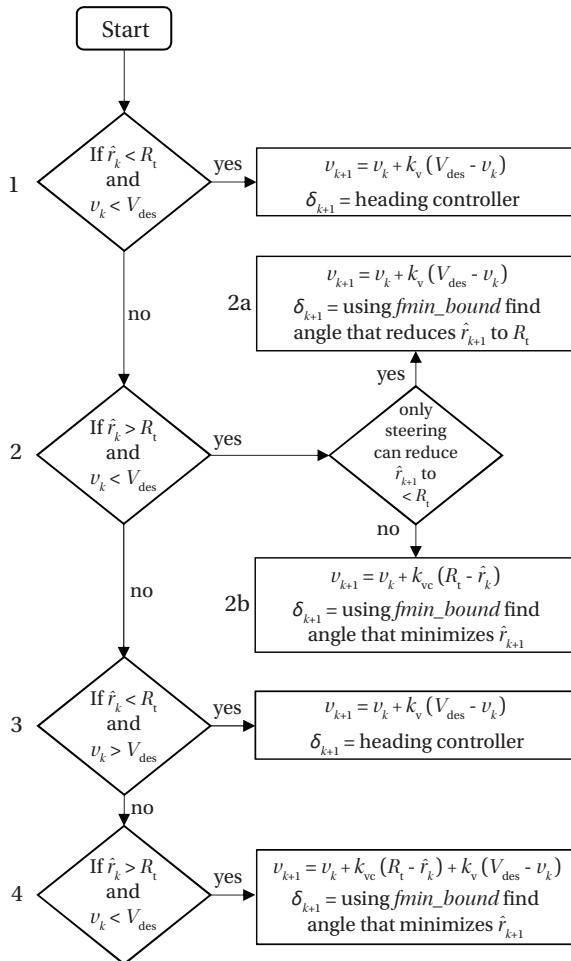


Figure 3.6: **Driver model algorithm:** At each time step (k), we compare the cost (*risk estimate*) (\hat{r}_k) to risk threshold (R_t), and speed (v_k) to the goal (V_{des}). This results in four distinct cases of inequality.

3. Else if ($\hat{r}_k < R_t$ and $v_k > V_{\text{des}}$): In this case the model slows down, while being steered by the heading controller since the *risk estimate* is lower than the threshold, and speed is higher than what is desired. Hence, $\delta_{k+1} = \delta_{\text{head}}$ and $v_{k+1} = v_k + k_v (V_{\text{des}} - v_k)$.
4. Else if ($\hat{r}_k > R_t$ and $v_k > V_{\text{des}}$): In this case both the speed and risk are over the desired limits and hence the model slows down while steering with δ_{op} that minimises \hat{r}_k . Hence $\delta_{k+1} = \delta_{\text{op}}$, and $v_{k+1} = v_k + k_{vc} (R_t - \hat{r}_k) + k_v (V_{\text{des}} - v_k)$.

PARAMETER ESTIMATION

The parameters of the DRF model were estimated from the experimental data ($N = 1$). To identify realistic parameter values for the driver model, we replicated the track used to simulate the model (Fig. 3.7), in a fixed base driving simulator. The experiment was approved by the Human Research Ethics Committee (HREC) - TU Delft, and a signed informed consent was obtained from the 25-year-old male volunteer. The video of the experiment in the fixed base driving simulator is shown in Supplementary Movie 1 (Appendix B). Simulations of the DRF model in normal and sport parameter settings are shown in Supplementary Movies 2 and 3 (Appendix B), respectively.

The participant drove ten times with the instruction, “drive as you normally would” and ten times with, “drive faster”. This was meant to emulate ‘normal’ and ‘sport’ driving behaviour. A section of the track (Fig. 3.7 and Fig. 3.8) was used for parameter estimation. The speed and lateral deviation trajectories estimated by the DRF model showed a close resemblance to the trajectories of the participant who also drove faster in sport setting than in normal setting. Also, the trajectories remained, for most parts, within the $\pm 2\sigma$ bound of the human trajectories. These results show that the DRF driver model can operationalize driving behaviour and remain within the human-like trajectory bounds ($\pm 2\sigma$). These were necessary, but not sufficient checks. To verify if the proposed quantified risk is indeed human-like, we compare the predictions of the DRF model with the results published in human driving behaviour studies in the literature (Results section).

The parameters can be segregated into three types: (i) the DRF parameters that determine the shape of Driver’s Risk Field, and are specific to each person, (ii) the Driver model parameters that connect the *risk estimate* calculated using the DRF to the control inputs of the vehicle, and (iii) the Environment parameters that define the cost map and describe the consequences of being in a particular state (position, velocity, etc.), and are constant for all drivers.

DRF parameters (Table 3.1): As explained in the results section, the six parameters ($p, t_{1a}, m, c, k_1, k_2$) define the driver’s risk field (DRF). Parameter c , which represents the initial width of the DRF can be directly calculated from the width of the ego car (2.0 m). The remaining five parameters were estimated using the grid search algorithm.

Driver model parameters (Table 3.2): The driver model parameters include the speed controller gains (k_{vc}, k_v), the risk threshold (R_t), and the desired speed (V_{des}). Parameters V_{des} and k_v can be directly estimated by driving on a long straight

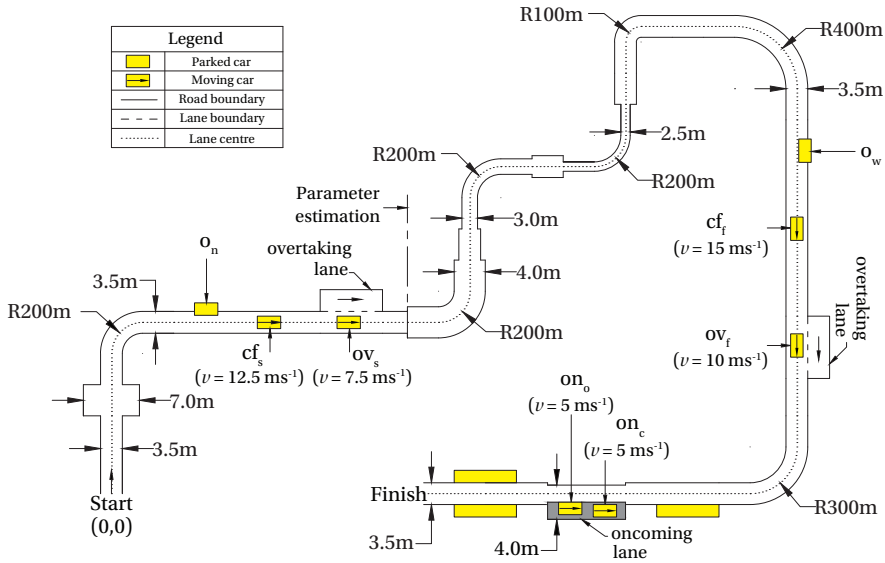


Figure 3.7: **Track used for testing the driver model:** The track contains four road and three traffic scenarios. The four road scenarios are (1) Curve radii: R100m, R200m, R300m, and R400m, (2) Lane widths: 2.5, 3.0, 3.5, and 4.0 m, (3) Obstacle avoidance: A car was parked on a 3.5 m wide straight section such that 0.9 m or 1.4 m of the car-width encroached on the road to simulate narrow (o_n) and wide (o_w) obstacles, respectively. (4) Roadside furniture: A 200 m long row constituting of 10 cars was placed either outside the left lane boundary (asymmetric) or outside both lane boundaries (symmetric). The three traffic scenarios are (1) Car-following: Two cars travelling at a constant speeds of 12.5 m s^{-1} (cf_s) and 15 m s^{-1} (cf_f) along the lane centre on different straight sections were followed. (2) Overtaking: Two cars travelling at constant speed of 7.5 m s^{-1} (ov_s) and 10 m s^{-1} (ov_f) were overtaken using a 3.5 m overtake lane. (3) Oncoming traffic: Two cars, travelling at a constant speed of 5 m s^{-1} on the 2 m wide oncoming lane, approached the ego car. The first oncoming car drove on the lane centre (on_c). The second car was offset 0.3 m towards the ego car.

section of a wide road, where the driver reaches his/her unbounded desired speed (V_{des}) while accelerating (proportional to k_v) from a standstill. k_{vc} and R_t were estimated using the grid search algorithm.

Environment parameters (Table 3.3): The environment parameters define the consequence of being in a particular state (restricted to position, in this study). These parameters are independent of the driver and hence are same for everyone. Personalised driving behaviour is obtained by changing the DRF parameters and the Driver model parameters. In this chapter, we assumed the cost (consequence) of being in the ‘ego lane’ (C_{road}) = 0, and outside the lane boundary (C_{env}) = 500. The costs of all other objects in the environment were identified relative to C_{env} . Different objects have different costs; for example, a car in traffic may be assigned a cost of 4000, and a roadside tree may be assigned a cost of 8000. However, since the focus of this chapter is to demonstrate the working of the model, and not identifying the costs of different obstacles, all the obstacles in our simulation were identical: a sedan (1.8 m wide and 5 m long). This ‘obstacle car’ traversed with differ-

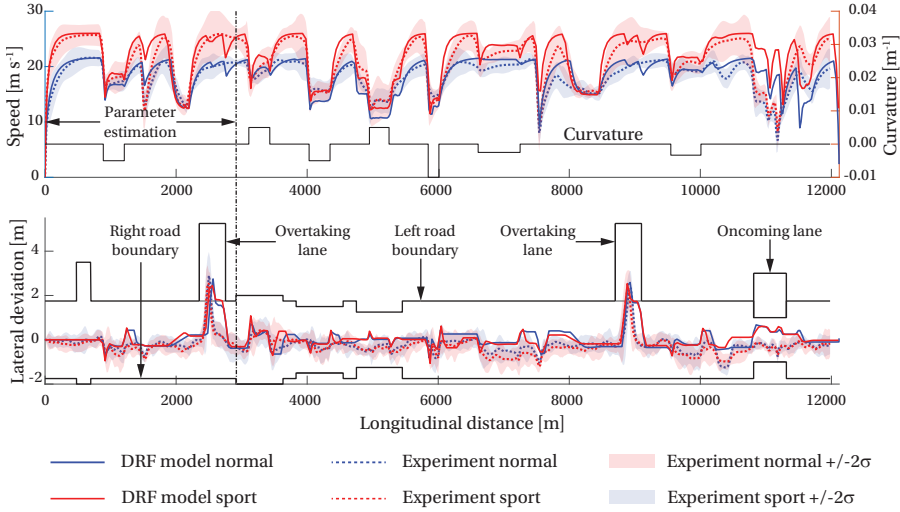


Figure 3.8: **Parameter estimation:** To identify realistic values for the parameters of the DRF driver model, we replicated the track in a driving simulator and one volunteer drove 10 times ‘normally’ (blue) and 10 times in a ‘sporty manner’ (red). Speed and lateral deviation from the lane centre are plotted as a function of the distance travelled along the lane centre of the track. The speed and lateral deviation trajectories of the DRF driver model, for the most part, lie within the $\pm 2\sigma$ limits of the experimental trajectories. The ‘sport’ parameter setting consistently drives faster than the ‘normal’ setting and in both cases shows similar trends in acceleration braking as shown by the human. The driver model maintains itself within the lane boundaries, while exhibiting satisfying (i.e., not always following the lane centre), even in conditions that were not experienced during parameter estimation (oncoming traffic scenario).

ent speeds (for overtaking, oncoming, and car-following scenarios), or was parked alongside the road (for obstacle avoidance, asymmetric and symmetric road furniture). In all these scenarios the same cost (C_{obs}) was assigned to the car, as identified using the grid search algorithm. The overtaking lane (C_{ovt}) was ‘modelled’ as rectangular obstacles with a ‘very low cost’ (identified using grid search), while the oncoming lane was assumed to be four times as dangerous (four times the cost) as the overtaking lane.

The grid search algorithm tried to minimise $\sum_{i=1}^3 (y_i \text{ model} - y_i \text{ experiment})^2$, where $i = 1$: steering angle, $i = 2$: speed, $i = 3$: lateral deviation from the lane centre. All the signals were a function of the distance travelled along the lane centre. Tables 3.1, 3.2, and 3.3 report the estimated parameter values for the ‘normal’ and ‘sport’ condition. It has to be noted that to personalise the DRF model to an individual, only six parameters need to be estimated (p , t_{la} , m , k_1 , k_2 , c). Driver’s Risk Field parameters (Table 3.1) and the Driving scene parameters (Table 3.3) were estimated only from the ‘normal’ condition and were used for ‘normal’ and ‘sport’ parameter setting of the DRF driver model, since neither the driver nor the driving scene changed. Only the task instruction had changed, due to which (we assume) that the manner in which the driver translates his/her perceived risk into steering and

Table 3.1: Driver's Risk Field parameters

	p	t_{1a}	m	k_1	k_2	c
Normal & Sport	0.0064	3.5	0.001	0	1.3823	0.5

Table 3.2: Driver model parameters

	C_t	V_{des}	k_{vc}	k_v
Normal	3000	21.6	1.5×10^{-4}	0.14
Sport	5200	26.0	1.5×10^{-4}	0.30

Table 3.3: Driving scene parameters

	C_{road}	C_{env}	$C_{ovt\ lane}$	C_{car}
Normal & Sport	0 (Assumed)	500 (Assumed)	3.5	2500

speed - control actions changes, which are represented by the Driver model parameters (Table 3.2).

3.3. RESULTS

To validate the DRF model, we selected papers from literature that investigated driver behaviour as a function of road and traffic conditions in terms of speed and lateral position. Since no single study fully replicates our scenarios, we chose different studies from literature, to compare with the respective DRF model predictions. Wherever possible, we chose a naturalistic driving study in similar conditions as simulated.

3.3.1. EFFECT OF ROAD SCENARIOS

We tested four road scenarios: different curve radii, different lane widths, obstacle avoidance, and roadside furniture.

CURVE RADIUS

The effect of curve radius on driving behaviour was examined by investigating the lateral position (curve-cutting behaviour) and speed while driving through curves.

Lateral position: Research has shown that drivers exhibit 'curve-cutting', that is, they do not follow the centreline of the lane but try to increase the effective radius of travel [87][88][89]. For model validation, we selected the on-road study by Xu et al. [26] because it provides the largest sampling of curve radii (0–200 m). They found that the amount of curve-cutting reduced as the curve radius increased (Fig. 3.9 [b]), which is coherent with the predictions of the DRF driver model (Fig. 3.9 [a]). They quantified curve-cutting behaviour using the 'Trajectory Transction Rate' (TTR), which normalises the lateral deviation from the lane centre with respect to the lane width, in curves. The DRF model exhibits curve-cutting behaviour due to its asymmetric shape defined by parameters k_1 and k_2 (Fig. 3.3 [c][d]). The DRF model also predicts that curve-cutting is higher in sport setting than in normal setting.

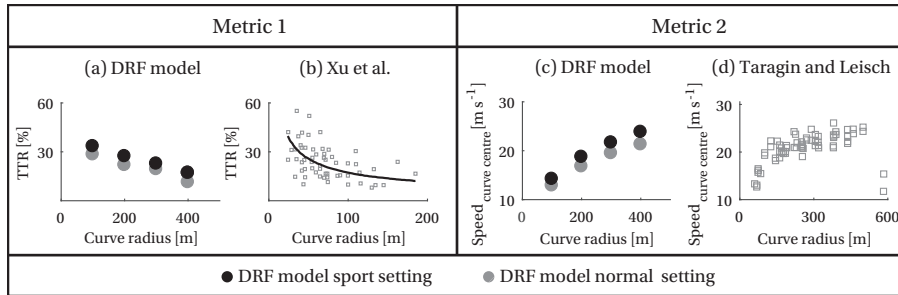


Figure 3.9: **Road scenario 1 - curve radius:** In the two columns (Metric 1 and Metric 2), two different metrics are used to compare the DRF model predictions to those from literature (Xu et al. [26], Taragin and Leisch [90]). Subfigures (a) and (b) show that the DRF model predicts the decrease in ‘curve-cutting’ (quantified using TTR) as curve radius increases. Subfigures (c) and (d) show that the DRF model could predict the increase in speed, at the curve centres, with increasing radius. The sport setting of DRF cuts the curves more (a) and drives at higher speeds (c) compared to the normal setting.

Speed: Several studies report that the speed at which a curve is taken increases non-linearly with the curve radius, in driving simulator [91][92] and on-road tests [65] [91][93]. The paper from Taragin and Leisch [90] was chosen (Fig. 3.9 [d]) because their on-road study provided data on curve radii range (60 to 714 m) and lane width range (2.6 to 4.3 m) which are similar to that simulated for the DRF model. The DRF model predicts that the speed increases with curve radius, asymptotically approaching straight road speed for a large radius (Fig. 3.9 [c]), which is similar to the experimental results of Taragin and Leisch [90] (Fig. 3.9 [d]). The DRF model exhibits this speed dependency on curvature because the width of the DRF changes with steering angle (equation (3.4)).

LANE WIDTH

The effect of lane width was examined using the standard deviation of lateral position (SDLP) and speed.

Lateral position: SDLP, which represents the swerving behaviour of a car, is reported to increase with lane width, in a simulator study by Godley et al. [94]. They examined the SDLPs of participants on three different lane widths (2.5, 3.0, 3.6 m) (Fig. 3.10 [b]). Similar results are reported in other simulator [95][96] and on-road studies [97] which are coherent with the predictions of the DRF model (Fig. 3.10 [a]). On a wider road, the DRF model has wider areas of low cost and hence, can use a larger width of the road without steering corrections (exhibit satisficing), resulting in higher SDLP.

Speed: It is reported that the speed at which drivers negotiate roads increases as the lane width increases, in simulator [94][99][98][42] and on-road studies [97][100]. The DRF model also showed a similar increase in speed with lane width (Fig. 3.10 [c]) and is compared to the results from a (moving base) simulator study of Liu et al. [98] (Fig. 3.10 [d]). On a wider road, there is a larger area of ‘no risk’, which means that the model can reach higher speeds before exceeding the risk threshold.

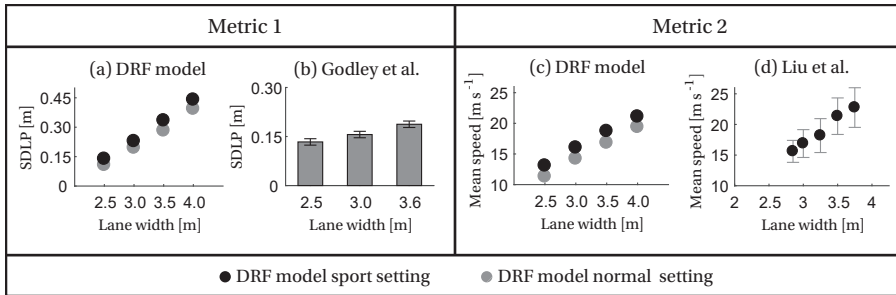


Figure 3.10: **Road scenario 2 - lane width:** In the two columns (Metric 1 and Metric 2), two different metrics are used to compare the DRF model predictions to those from literature (Godley et al. [94], Liu et al. [98]). In the 'DRF model' subfigures, the black and grey markers represent the sport and normal parameter settings, respectively. Subfigure (b) shows that the (mean \pm SE) Standard Deviation of Lateral Position (SDLP) of the vehicle increases as the lane width increases. The DRF model (a) can predict this trend. Subfigure (d) plots the (mean \pm SD) mean speed on different lane widths. Subfigures (c) and (d) show that the DRF model can predict that the speed at which drivers negotiate a road increases as the lane width increases.

ON-ROAD OBSTACLES

Obstacle avoidance was simulated for the DRF model by parking a car partially on the road, which led to a temporary 'narrowing' of the street. The 'narrow' and 'wide' obstacles (Fig. 3.11 [a][b][d][e]) were created by placing the same (1.8-m wide) car such that 0.9 m, and 1.4 m of the car-width encroached over (the left boundary of) the 3.5-m wide lane, respectively. The effect of this temporary narrowing was examined by analysing the lateral deviation and speed of the ego vehicle. Several researchers have reported, in on-road studies, that on-street parking induces 'traffic calming' by reducing the average speed [101][102][103]. We selected the simulator study of Edquist et al. [104] because they measured the effect of on-street parking on lateral position and speed.

Lateral deviation: Edquist et al. [104] reported that the mean lateral position of the vehicles shifted away from the parked cars (Fig. 3.11 [c]). The DRF model yields a similar trend, where the ego car deviates away from the parked car (Fig. 3.11 [b]).

Speed: A reduction in mean speed was reported in the presence of parked cars (Fig. 3.11 [f]) [104], which is coherent with the behaviour shown by the DRF model (Fig. 3.11 [e]). It should be noted that Edquist et al. [104] reported the mean speed since they had a row of parked cars. However, we had only one parked car, which means we can only report the minimum speed. The DRF model successfully avoided on-road obstacles by steering and braking.

ROADSIDE FURNITURE

Road shoulders, guard-rails, vegetation, and parked cars have been reported to affect a vehicle's lateral position and speed [89][105]. The DRF model was simulated in an 'asymmetric' case where a 200 m long row of cars was parked outside the left lane boundary, and a 'symmetric' case where they were parked outside both lane

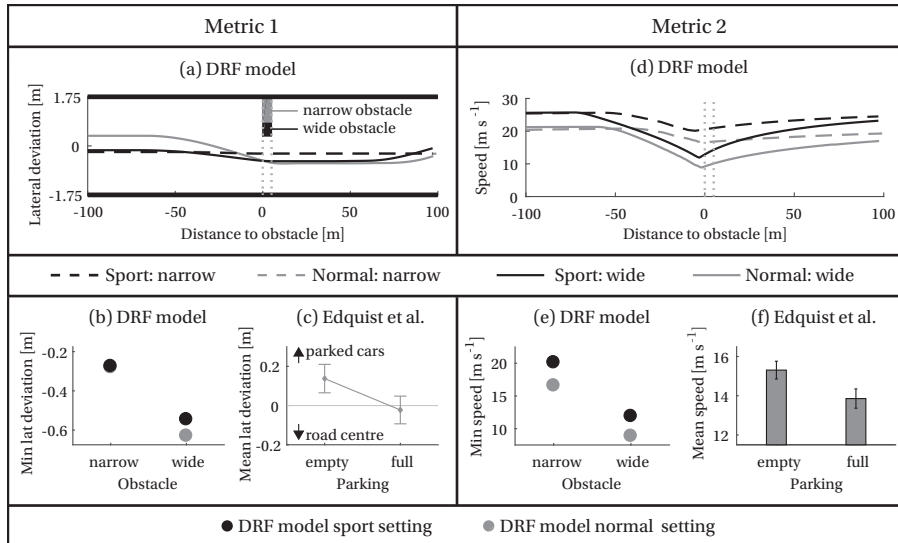


Figure 3.11: **Road scenario 3 - on-road obstacles:** In the two columns (Metric 1 and Metric 2) two different metrics are used to compare the DRF model predictions to those from literature (Edquist et al. [104]). In subfigure (b), the ‘wide’ obstacle encroaches more onto the road compared to the ‘narrow’ obstacle. The minimum lateral deviation (b) is calculated from the trajectories in subfigure (a). Drivers moved away from the parked cars, as shown in subfigure (c). In subfigure (c) lane centre = 0 and the bars indicate 95% confidence interval. Subfigure (b) shows that the DRF model showed a similar trend of moving away from the obstacle. Drivers drove slower when there were parked cars, as compared to when there were no parked cars encroaching the road, as shown in subfigure (f). Here also the bars indicate the 95% confidence interval. Subfigure (e) shows that the DRF model slows down for obstacles covering the road partially.

boundaries. Dunning et al. [106] examined ‘asymmetric’ (with water (more risk) on one and grass (less risk) on the other side of lane boundary), and ‘symmetric’ (with water on both sides) conditions in their experiment.

Lateral position: Dunning et al. [106] reported that the lateral position of the participants shifted towards the less dangerous grass in the asymmetric case and remained in the centre in the symmetric case (Fig. 3.12 [c]). Similar results are seen in the behaviour of the DRF model where the ego car moves away from the parked cars (at lateral position = +2.75 m) and remains in the centre of the lane in the symmetric case (Fig. 3.12 [b]).

Speed: Dunning et al. [106] reported that participants, on average, drove slower in the symmetric case (Fig. 3.12 [f]). The DRF model also shows similar behaviour where the ego car drove faster in the asymmetric case as compared to the symmetric case. This is because in the asymmetric case, the DRF model steered away from the ‘risky’ parked cars and could maintain a higher speed without exceeding the risk threshold. In the symmetric case, driving on the centreline was not enough to reduce the risk below the threshold and hence the model had to slow down. In both conditions, the sport setting drove faster than the normal setting of the DRF

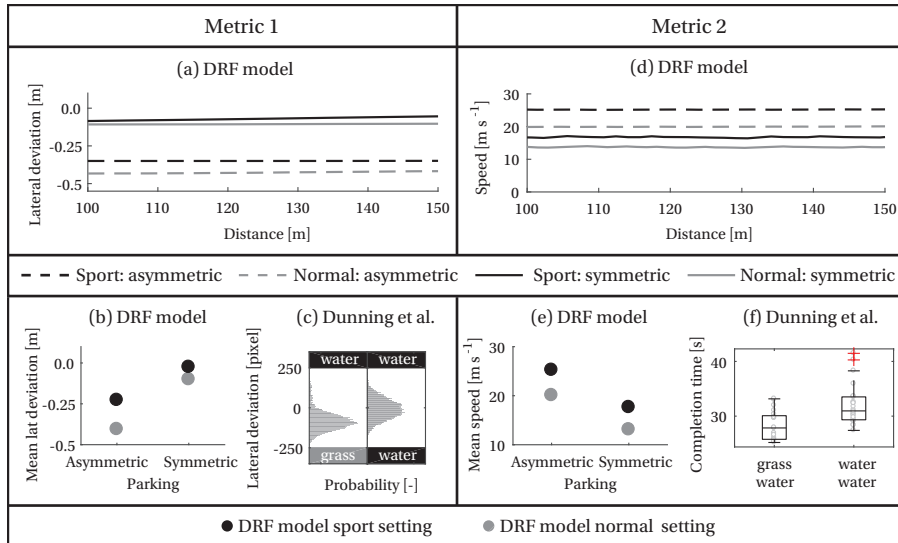


Figure 3.12: **Road scenario 4 - roadside furniture:** In the two columns (Metric 1 and Metric 2) two different metrics are used to compare the DRF model predictions to those from literature (Dunning et al. [106]). In the asymmetric case, the mean lateral deviation from the lane centre is away from the parked cars (b) and away from water (more dangerous than grass) in (c). Subfigure (c) shows the distribution of lateral position of the participants. Subfigures (e) and (f) show that in symmetric condition with ‘danger’ on both sides of the lane, the DRF model correctly predicted that the drivers drove slower than in the asymmetric case. The mean lateral deviation (b) and mean speed (e) are calculated from the trajectories in subfigures (a) and (d), respectively.

model. The DRF model could react to roadside furniture by steering and braking since the DRF spreads beyond the lane boundaries.

3.3.2. EFFECT OF TRAFFIC SCENARIOS

We tested three traffic scenarios, namely: car-following, overtaking, and interaction with oncoming cars.

CAR-FOLLOWING

We tested the effect of lead car speed on Time Headway (THW) and braking intensity during car-following. We simulated ‘slow’ and ‘fast’ car-following with lead cars that maintained constant speeds of 12.5 m s^{-1} and 15 m s^{-1} , respectively.

Time Headway (THW): THW during car-following represents the time available to the driver of the following vehicle to reach the same level of deceleration as the lead vehicle, in case the lead vehicle brakes. Several studies in literature examined the effect of lead vehicle speed on THW [107][108][109] and reported that (for lead car speed above 10 m s^{-1}) the preferred time headway under steady-state car-following (THW_{pref}) is almost constant and independent of the lead car speed. The DRF model also predicts an almost constant THW_{pref} (Fig. 3.13 [b]). The DRF model, with the current parameter values, behaved more conservatively (higher

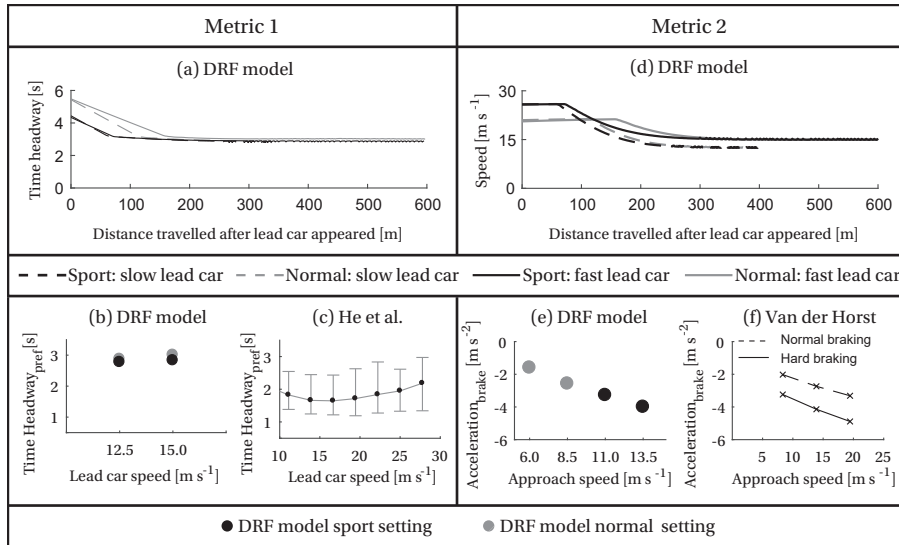


Figure 3.13: **Traffic scenario 1 - car-following:** In the two columns (Metric 1 and Metric 2), two different metrics are used to compare the DRF model predictions to those from literature (He et al. [109] and Van der Horst [111]). Subfigures (b) and (c) indicate that the preferred time headway is independent of the speed. In subfigure (c), the circular markers indicate median and the whiskers indicate 25th and 75th percentile. Subfigures (e) and (f) show that the braking intensity (represented by the acceleration at brake initiation) increases as the approach speed to the obstacle increases.

THW_{pref}) than the average human driver, as reported by He et al. [109] in their on-road study (Fig. 3.13 [c]). Additionally, the THW_{pref} for the sport parameterization was smaller than that for the normal parameterization of the DRF model. This concurs with the findings in the literature, where sensation-seeking drivers were reported to maintain lower THW_{pref} compared to sensation avoiding individuals [108][110].

Braking intensity: Another aspect of car-following that is widely studied is the braking intensity of the car in response to the separation to the lead car. In a test-track study, Van der Horst [111] reported that the braking intensity (deceleration at the onset of braking) increased as the approach speed increased (Fig. 3.13 [f]), which corresponds to the DRF model’s results (Fig. 3.13 [e]). The study also reported that with ‘hard braking’ instruction, participants’ braking intensity was higher than in normal braking condition. The DRF model also predicts that a sport parameter setting (black markers) will yield higher deceleration than the normal setting (grey markers: Fig. 3.13 [e]). The DRF model exhibits this behaviour since the lead car encroached the DRF at a higher rate when the approach speed was high and at a lower rate when the approach speed was low. This ‘rate of encroachment’ translated into velocity reduction at a proportional rate.

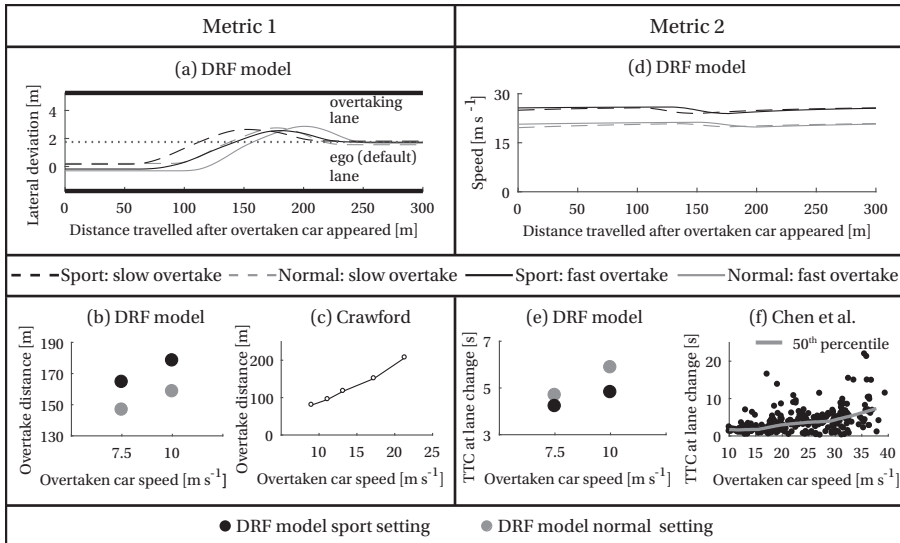


Figure 3.14: **Traffic scenario 2 - overtaking:** In the two columns (Metric 1 and Metric 2), two different metrics are used to compare the DRF model predictions to those from literature (Crawford [112] and Chen et al. [113]). Subfigures (b) and (c) show that the DRF model could correctly predict that the overtake-distance increases as the speed of the overtaken car increases. In the sport setting, the model covers larger distance than in normal setting, indicating ‘smoother’ trajectories in the sport setting. However, the DRF model does not come back to its own lane sufficiently (a). Subfigures (e) and (f) show that the predictions of the DRF model agree with the results in literature that show the Time to collision (TTC) at the start of the overtake manoeuvre increases, as the speed of the overtaken car increases.

OVERTAKING

We studied the effect of lead vehicle speed on overtake-distance (distance covered during the overtaking manoeuvre) and on the time to collision (TTC) at which the overtaking manoeuvre is initiated. To test the DRF model, we simulated a ‘flying overtake manoeuvre’ in which there are no oncoming cars on the adjacent lane. Figure 3.14 [a]) illustrates one of the major drawbacks of the DRF model: it overtakes the car but does not return to its own lane after the overtake. This is the drawback of using a cost threshold-based satisficing controller. Since the model perceives the road to be twice as wide (ego + overtaking lane), it comes back (to its lane) just enough to bring the risk below its threshold (satisficing). Secondly, the DRF model would not be able to perform an ‘accelerative overtake’ since its speed is limited by the V_{des} parameter.

Overtake-distance: Crawford [112] reported that the overtake-distance increased with the speed of the overtaken car (Fig. 3.14 [c]). This corresponds to the DRF model’s behaviour, where the overtake-distance was higher for the 10 m s^{-1} overtaken car than for the 7.5 m s^{-1} overtaken car. Additionally, note that the sport setting of the DRF model had larger overtake-distances than the normal setting.

TTC at overtake initiation: Several studies investigate time to collision (TTC = ratio of relative distance to relative speed) at the initiation of overtaking manoeu-

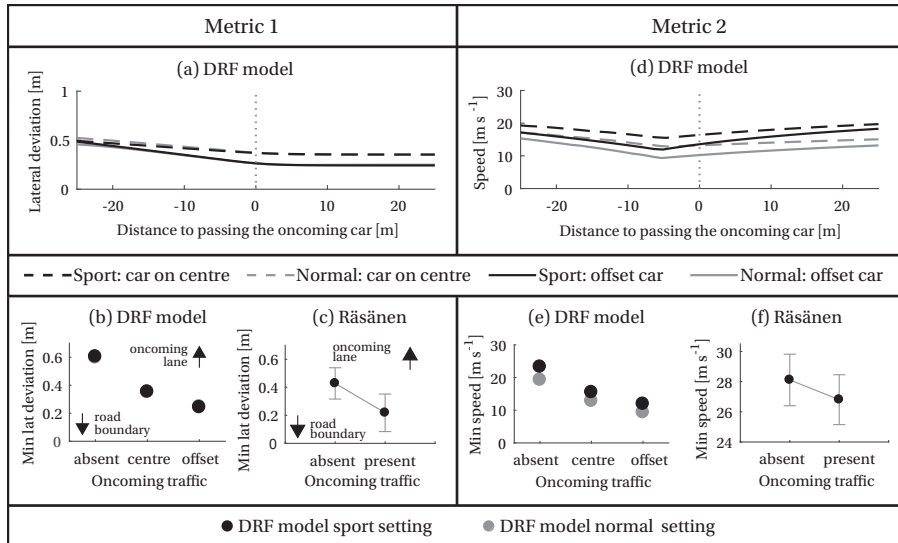


Figure 3.15: **Traffic scenario 3 - oncoming traffic:** In the two columns (Metric 1 and Metric 2), two different metrics are used to compare the DRF model predictions to those from literature (Crawford [112] and Chen et al. [113]). In the 'DRF model' subfigures, the black and grey markers represent the sport and normal parameter settings, respectively. In subfigures (b) and (c), the minimum lateral deviation is shown on the y-axis. The condition where no oncoming cars were present is indicated by 'absent'. The DRF model simulated one car that drove on the oncoming lane's centre ('centre' in subfigure (b)) and another car that was offset towards the ego lane ('offset' in subfigure (b)). In normal and sport setting the DRF model moved away from the oncoming traffic, which is in agreement with the driver's behaviour. (e) and (f) show that the DRF model slowed down, like humans (f), when it encountered oncoming traffic. In subfigures (c) and (f), the black markers indicate mean, and whiskers indicate the \pm standard deviation.

drivers either to the lead car [113] or with the oncoming car [114][115] (outside of the scope of our scenarios). The on-road study by Chen et al. [113] reported that the TTC at (start of) lane change increased with the speed of the overtaken car (Fig. 3.14 [f]). Similar behaviour is shown by the DRF model, but more interestingly, the sport setting of the DRF model maintained a lower TTC than the normal setting. In a driving simulator study, Farah [116] reported that young male drivers, generally considered sporty drivers, had smaller TTCs at lane change than adults.

ONCOMING TRAFFIC

We examined the effect of oncoming traffic's lateral position on the DRF model's choice for speed and lateral position. We simulated a narrow rural road with 2 m wide ego and oncoming lanes, without any barrier in between. Lewis-Evans and Charlton [99] reported that on a two-lane rural road, drivers drove more towards the road centre, in the absence of oncoming traffic. The DRF model also exhibits similar behaviour with a bias (≈ 50 cm) towards the road centre (Fig. 3.15 [b]): 'absent' condition). The model shows this behaviour because the paved road to the left (i.e., oncoming lane with no traffic) is less 'dangerous' than the road boundary

to the right.

Lateral position: Studies that investigated the effect of oncoming traffic [117][118][119] have reported that drivers' lateral position depends on the presence of oncoming vehicles in the adjacent lane. Räsänen [117], in an on-road study, compared driver's lateral position with and without oncoming traffic (Fig. 3.15 [c]) and reported behaviour similar to DRF model predictions, where the lateral position moves away from the lane with oncoming traffic. Additionally, it moves even further when the oncoming car is offset towards the lane position of the ego car (Fig. 3.15 [b]).

Speed: The DRF model slowed down in the presence of oncoming traffic, and slowed down more when the lateral position of the oncoming car was offset towards the ego car (Fig. 3.10 [e]). Räsänen [117] (Fig. 3.15 [f]) reported no significant difference in speed between the oncoming traffic 'absent' and 'present' conditions. However, Rosey et al. [118] reported a significant reduction in speed when drivers encountered oncoming vehicles. Moreover, they also reported a significant decrease in speed while encountering trucks as compared to cars [118], which is in line with the predictions of the DRF model.

3.4. DISCUSSION

In this study, we set out to find the underlying principle that governs human adaptations in speed and lateral position during driving, and implement this into a cost function into an operational driver model. We also evaluate the generalizability of the modelled behaviour across different traffic scenarios by comparing it to adaptations in speed and lateral position from available literature of real-world and driving simulator studies.

One of the principles that emerged from qualitative driver behaviour theories was 'perceived risk'. However, to the best of our knowledge, 'perceived risk' has not been quantified or used in a driver model to generate human-like driving behaviour. In this chapter, we operationalized the 'perceived risk' by proposing the *risk estimate* as the product of the DRF (which is assumed to account for the driver's perception-action uncertainty) and the cost map of the driving scene (which quantifies the consequence of a hazard/event). This makes the cost function 'uncertainty-aware'.

A driver's 'uncertainty-awareness' is embedded in the DRF model via four features. First, the DRF widens along the 'predicted path' and hence is wider than the car-width. Without this feature, the DRF model would not slow down on a narrow road (wider than car-width). Second, the DRF widens and elongates with increasing speed. Without this, the DRF model would not maintain constant time headways in car-following or slow down for curves. Third, the DRF widens with an increase in steering angle. Without this feature, the DRF model would not slow down more for curves with higher curvature than for curves with lower curvature, and would negotiate all the curves at the same speed. Fourth, the asymmetric widening of the DRF along the 'predicted path' (generally $k_1 < k_2$) lets the model exhibit 'curve-cutting' behaviour. Without the asymmetric widening, the model would al-

ways follow the lane centre.

Dealing with uncertainty in the ego-robot's and the external obstacles' location has been widely studied [120][22]. Several models, ranging from tentacle-like algorithms [23] to Rapidly-exploring Random Trees (RRT) [24], have been proposed for trajectory and speed planning. The methods that are closest to the cost function proposed in this chapter are based on uncertainty propagation [25]. Most of these algorithms account for the first two points mentioned in the previous paragraph, namely: widening of the uncertainty with predicted path and speed dependency of uncertainty field. Additionally, these algorithms account for the uncertainty in predicting the future location of the obstacles. This feature needs to be incorporated in the driving scene cost map of future versions of the DRF model (Fig. 3.16 [d]). However, algorithms in the literature seldom incorporate the latter two features: widening of uncertainty with steering and asymmetric uncertainty propagation; hence, existing models cannot produce 'curve-cutting' and curvature dependent speed negotiation, behaviours that are seldom required in robotic applications. In short, to generate human-like behaviour, the underlying cost function has to be 'uncertainty-aware' and incorporate the (motor-control inspired) effect of signal-dependent noise to replicate speed-accuracy trade-off that we see in driving behaviour.

Implementing a satisficing controller in a potential field has its drawbacks. The model did not return to its lane after overtaking the lead car because it can sense hazard only from physical objects (e.g., cars, road boundary) and cannot perceive the 'tactical' risk of being in an oncoming lane. Other tactical risks, such as risks that may occur when approaching an intersection or a red traffic light, are not incorporated in the model either. However, the structure of the model facilitates the addition of these 'tactical' costs to different road elements. Other limitations include the use of car-kinematic model, using a circular arc for 'predicted path' calculations, and the DRF extending only in front of the ego car. In future iterations a car-dynamic model, a spline instead of a circular arc (Fig. 3.16 [b]), and a DRF that surrounds the vehicle on all four sides (Fig. 3.16 [c]) can help generate better microscopic trajectories and generate behaviour in more scenarios (e.g., ego car being overtaken).

Satisficing behaviour becomes important when developing Advanced Driver Assistance Systems (ADAS) that physically interact with the driver, e.g., the Haptic Shared Controller (HSC) [40], which guides the driver via torques on the steering wheel. If the HSC tries to follow a reference (e.g., the lane centre), it will exert a torque and bring the driver to the centreline, even if the driver was satisfied with an off-centre lateral position. To avoid these undesired torques that can severely hamper the acceptance of the system, we need threshold-based models that can exhibit satisficing behaviour.

An important contribution of this chapter is the extensive literature-based validation. Note that in this chapter we do not compare the trajectories of steering angle, speed, and lateral deviation, but assess the behaviour of the model by comparing trends in certain metrics to those reported in the literature. Six out of the seven scenarios were validated using on-road studies or studies from driving simu-

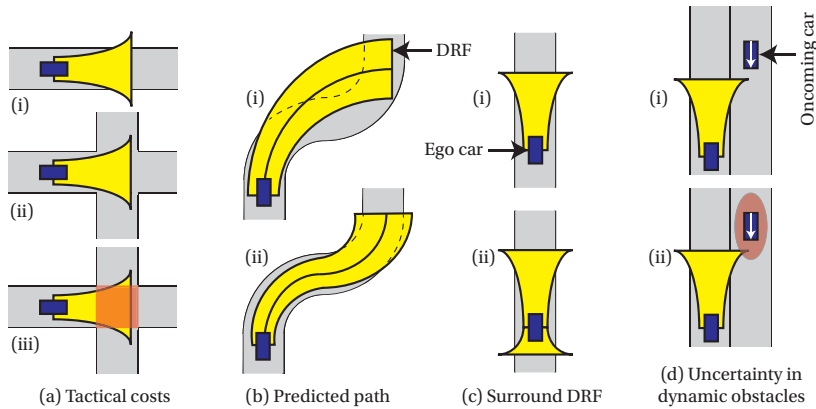


Figure 3.16: **Limitations of the model:** (a) Tactical costs: The DRF model can only perceive physical risk from objects such as cars, trees, etc. However, it cannot perceive the risk from oncoming traffic which is currently not in its field of view. Hence at an intersection, rather than slowing down, it will speed up since there is larger road-area available, which is contrary to what a human would do. This can be solved by introducing additional 'tactical costs' that artificially increase the risk of an intersection (red square). This approach can be extended to other elements such as traffic lights, or zebra crossings. (b) Predicted path: For simplicity, the DRF model currently uses a circular arc for predicting the path (for preview time t_{la} seconds). This circular path arises due to the assumption that the current steering angle (δ) and speed (v) will be held constant over the preview time. However, we can optimise for a vector of steering angles and speed (as is done in a Model Predictive Control). This allows for a flexible DRF and better prediction of microscopic trajectories. (c) Surround DRF: In this chapter, the DRF only extends in front of the vehicle (top). However, the risk field extends on all four sides. The bottom image is merely a suggestion and the shape has not been investigated. This 'surround DRF' will help predict human driving behaviour in additional scenarios such as: being followed by another car, being overtaken, lane change manoeuvres, etc. (d) Uncertainty in dynamic obstacles: The DRF represents the driver's (self) perception-action uncertainty. However, the motion of dynamic obstacles is less predictable. This uncertainty was ignored in this chapter, but will have to be accounted for in the future iterations of this model.

lators backed by on-road studies (only simulator studies found for roadside furniture: Appendix B - Supplementary Tables B.1 - B.8). In Fig. 3.9 - 3.12 (road scenarios), owing to the simplicity and 'static' nature of road elements, there was abundant literature and consensus amongst researchers as to which metric reflected human behaviour (e.g., curve-cutting: TTR, lane width: SDLP). In Fig. 3.13 - 3.15 (traffic scenarios), defining a metric that could capture human-driving characteristics was more difficult, owing to the complexity that arises due to its dynamic nature. Despite these limitations, as the results show, the strength of the *risk estimate* (cost function) and the risk threshold driver model lies in the fact that they generate human-like behaviours in different road and traffic conditions, including previously unseen scenarios. Such a generalizable model in which the behaviour emerges from an intrinsically motivated cost does not only provide understanding about human motivations for driving, but also has applications in the design of automated systems. For example, it could be used to make the automated vehicle drive in a human-like manner, which is reported to be preferred by humans

[7][119]. Machine learning algorithms could use the *risk estimate* as a feature that could be extracted from demonstrated human driving trajectories.

Our model has been developed for unassisted driving. However, since its behaviour emerges from the underlying motivations for driver adaptation, we hypothesise that it should be able to capture driver adaptations to various driving support systems. For example, drivers drove faster when their vehicle was equipped with lane-keeping assistance based on HSC than in a car without this assistance [121]. The DRF model should be able to predict this speeding behaviour, since HSC essentially provides a ‘channel’ on the road through which it guides the driver, reducing the driver’s perception-action uncertainty. This would translate to a narrower DRF, which allows a driver to drive faster before exceeding his/her risk threshold. This thought experiment illustrates that a generalizable model in which behaviour emerges from underlying cost functions, not only predicts unassisted driver behaviour but also the effect of automated and assistive technologies (on driver behaviour).

3.5. CONCLUSION

- The *risk estimate*, the driving equivalent of the sensorimotor control concept of *consequence of noise* could be formulated by combining (i) the Driver’s Risk Field (DRF) as a proxy for the *probability* of an event and (ii) a cost map of the environment, that specified the consequence of an event.
- The *risk estimate* was used as a cost function in a threshold based controller. The trends displayed by the behaviour of this controller matched the trends, in speed and lateral position adaptation in seven different scenarios, reported in the literature.
- The model can only account for the risk posed by an object due to its physical presence and cannot account for ‘tactical costs’. This combined with the *satisficing* nature of the controller meant that the model, after performing a lane change during overtaking, did not return sufficiently to its lane.
- Despite the above limitation, the DRF model can use a parametrization based on small subset of data (curves, car-following, etc.) to predict plausible adaptations in speed and lateral position of road and traffic conditions which the model has not experienced before.
- Maintaining the ‘consequence of the human’s perception-actions noise’ under a threshold level seems to be the underlying principle for driver’s adaptations in speed and lateral position to a wide variety of road and traffic conditions.

4

DRF-BASED RISK ESTIMATE: A VALIDATION STUDY IN A TEST-VEHICLE

Quantifying drivers' perceived risk is important in the design and evaluation of the automated vehicles (AVs), and to predict takeovers by the driver. A 'Driver's Risk Field' (DRF) function has been previously shown to be able to predict manual driving behaviour in several simulated scenarios. In this chapter, we test if the DRF-based risk estimate (\hat{r}) can predict manual driving behaviour and the driver's perceived risk during automated driving. To ensure that the participants perceived realistic levels of risk, the experiment was conducted in a test-vehicle. Eight participants drove 5 laps manually, and experienced 12 different laps of automated driving on a test-track. The test-track consisted of three sections (which were sub-divided into 12 sectors): curve driving (9 sectors), parked car (1 sector), and 90-degree intersections (2 sectors). If the driver verbally expressed risk or performed a takeover, that particular sector was labelled as risky. The results show that the risk estimate (\hat{r}) predicted manual driving behaviour ($\rho_{steering} = 0.69$, $\rho_{speed} = 0.64$), as well as correlated with the driver's perceived risk in curve driving ($r^2 = 0.98$) and while negotiating a car parked outside the lane boundary ($r^2 = 0.59$). In conclusion, the DRF-based risk estimate (\hat{r}) is predictive of manual driving behaviour and perceived risk in automated driving. Future research should include tactical and strategic components to the driving task.

The contents of this chapter have been published in:

S. Kolekar, S.M. Petermeijer, E.R. Boer, J.C.F. de Winter, and D. Abbink, *A risk field based metric correlates with driver's perceived risk in manual and automated driving: A test-track study*, [Transportation Research Part C: Emerging Technologies 133 \(2021\), 103428](#)

4.1. BACKGROUND

RECENT years have seen a surge in the popularity of automated vehicles (AVs). Although AVs may solve several problems, they also introduce new ones. What is acceptable driving behaviour for an AV, and when do humans takeover the AV's control? To answer these questions, it may be useful to have an estimate of the driver's perceived risk in the AV [122]. AVs will be used by drivers and passengers, and how these drivers and passengers perceive their system while driving is hardly known, yet essential to know. If drivers perceive high levels of risk, and the AV does not react appropriately and reliably, they could lose trust [123] and take over control, or reject the use of the AV altogether. Accordingly, it can be argued that new AVs need an assessment of how end-users perceive their behaviour.

Perceived risk is influenced by a variety of factors, including the environment and traffic situation, the mental state of the driver, and prior experiences. Several studies have shown a correlation between personality characteristics and risky driving behaviour [124] [125] [126] [127]. In this study, in which we provide a computational estimate of perceived risk, we consider the effect of the road environment and traffic situation only.

Summala [128] proposed four factors that need to be maintained above a certain threshold to keep drivers within their "comfort zone". These are safety margins (to road edges, obstacles or other vehicles), vehicle-road system (accelerations, road geometry), rule-following (obeying traffic laws, maintaining speed limits), and good progress of the trip (meeting one's expectations for the pace or progress of the travel). Siebert et al. [129] noted that the rule-following factor for comfort is redundant, as automated vehicles (AVs) will almost certainly follow the rules, and that good progress of the trip is dependent on traffic conditions, rather than automation state in itself. Therefore, in this chapter, we focus specifically on factors that affect the safety margins and vehicle-road system for manual and automated driving. Other researchers have investigated the acceleration-related comfort aspect of automated driving, which we do not investigate in this study [130]. Specifically, we will focus only on the perceived risk that arises due to the presence of physical objects (road curb, obstacles, cars, etc.) and exclude risks that arise due to other factors related to vehicle dynamics (loss of traction, roll over, etc.).

There have been several studies that have attempted to predict manual driving behaviour for scenarios involving road boundaries and obstacles. For example, longitudinal behaviour has been modelled using the optical edge rate on open roads [11], the time to extended tangent point in curves [12], time to collision (TTC) while approaching obstacles [13] [14], and time headway (THW) during car-following [15]. Lateral behaviour has been modelled using the two-point model [16], in which lateral and heading error were used as signals. Other models have used features such as the 'angle to the tangent point' [131] and time to lane crossing (TLC) as signals to steer the vehicle [65] [47]. Some studies have also utilised a combination of signals such as speed and acceleration (executed by the drivers) to classify manual driving behaviour into different levels of risk-taking behaviour [132][133].

All the above models used a particular measure (TLC, TTC, THW, etc.) to predict the actions of a human driver. If we abide by Nääätänen and Summala's [2] risk threshold theory, which proposes that all motivations for actions are to reduce the perceived risk and maintain it below a threshold level, these measures would represent the driver's perceived risk. However, using different measures to quantify perceived risk in different scenarios leads to a fragmented model. For example, [7] used 10 different measures for assessing the behaviour in 14 different scenarios.

Some of the problems with having separate measures for separate scenarios are that:

- (i) It is difficult to compare the estimated risk between scenarios.
- (ii) If two or more scenarios occur simultaneously it is difficult to estimate the combined risk.

(iii) The operational level driving behaviour is often influenced by higher level factors such as a driver's familiarity with a particular road, his/her mood, etc. In case of a fragmented model, one would have to tune the parameters of several models in a coherent manner. On the other hand, with a unified model one has to tune parameters of only one model.

Accordingly, a unified model that can estimate driving behaviour or generate a *risk estimate* is needed.

The first attempt of making a unified model for explaining driver behaviour in different scenarios was made by Gibson and Crooks, using their 'Field of Safe Travel' concept [1]. However, this was a qualitative description of how humans drive in different scenarios. There have been several models that utilise this concept of risk field [32] [134] [135] [136] [137]. For example, Wang et al. [32][138] tested the Driver Safety Index (DSI) in real cars on straight sections of the highway during car-following and cut-in scenarios. Rasekhipour et al. [134] proposed a path planning approach by combining the potential field approach with an optimal controller. In chapter 3, we proposed a driver model based on the 'Driver's Risk Field' (DRF) which could predict driving behaviour in a unified manner in 7 different scenarios (curve driving, obstacle avoidance, car following, etc.). Hence, we hypothesise that the DRF-based *risk estimate* (\hat{r}) is a good candidate for evaluating perceived risk during automated driving.

In chapter 3, we validated the driver model by comparing its output (i.e., steering angle and speed) to manual driving behaviour. However, we did not test if the *risk estimate* (\hat{r}), we calculated (which was used as a 'cost function' in the driver model), corresponded to the perceived risk of human drivers. Testing this is important since, if we can formulate a signal that correlates with the perceived risk by the driver, it can be a valuable tool to assess the behaviour and acceptance of automated driving systems. Also, in chapter 3, we compared the simulation results to manual driving behaviour results published in literature. Here, since we aim to quantify the driver's perceived risk, it becomes imperative that an experiment is conducted in a real vehicle to generate realistic feeling of risk.

In this chapter, we test if the DRF-based *risk estimate* (\hat{r}) correlates with the drivers' perceived risk, in a test-vehicle. We perform two main analyses. First, as an initial check, we tested if the *risk estimate* (\hat{r}) predicts the driver's behaviour

during manual driving. This is the necessary validation before performing the second step where we compared the *risk estimate* (\hat{r}) to the driver's comments and the takeovers that they performed, while being driven in an automated manner around a test-track. The test-track consisted of three scenarios: curves with different curvatures, a parked car (placed outside the lane), and intersections. The car was deliberately parked outside the lane boundary to examine if objects outside the lane boundary affect the perceived risk.

4.2. EXPERIMENTAL METHODS

4.2.1. TEST-TRACK AND TEST-VEHICLE

The experiment was conducted at a test facility in collaboration with Nissan, Japan. The test-vehicle was a 1st generation Nissan Leaf equipped with an automated driving system. The participants sat on the right side of the vehicle and drove on the left hand side of the road.

To test different scenarios we divided the test-track into three sections. The first section consisted of curves with varying curvatures and road widths. The second section, the parked car section, consisted of a Nissan NV500 van parked along the left shoulder of the road (outside the lane boundary). The third section consisted of two 90-degree intersections. We further subdivided these three sections in 12 sectors. The curve driving section was divided into 9 sectors (S1 to S9), the parked car was its own sector (PC), and the intersection segment consisted of two sectors (I1 and I2), as shown in Fig. 4.2. The intersection (I1) had a zebra crossing on it, which the participants were asked to ignore for the purpose of this experiment.

4.2.2. PARTICIPANTS AND TEST PROCEDURE

Eight male Nissan test drivers, certified to operate the automated test-vehicle, participated in the experiment (mean age = 44.1 and SD = 13.4 years). Each driver drove five laps of the test-track manually on one day, and on another day they were driven in the same car, along the same track, in an automated manner for twelve laps. The experimenter (first author) sat behind the driver's seat and an interpreter (Japanese \iff English) sat in the passenger's seat.

During the automated driving condition, the participants were requested to comment on how they felt about the driving behaviour of the vehicle. They were encouraged to specify the 'why and where' of their feedback. This was done because, first, steering or speed control data was unavailable, since the car was being driven in an automated manner. Second, we could not provide the driver's with a hand-held or foot-operated device to indicate their perceived risk level. This was in accordance with Nissan's safety committee's guidelines which required the drivers to always be able to takeover the vehicle's controls. Third, physiological measures are reliable in a laboratory setting, but in the dynamic environments of the test course, it is challenging to acquire reliable physiological data. Hence, the decision was made to ask the participants to think out loud as they were driven around the lap. The audio and video of all the laps were recorded and the participants could takeover the control of the vehicle whenever they wanted.

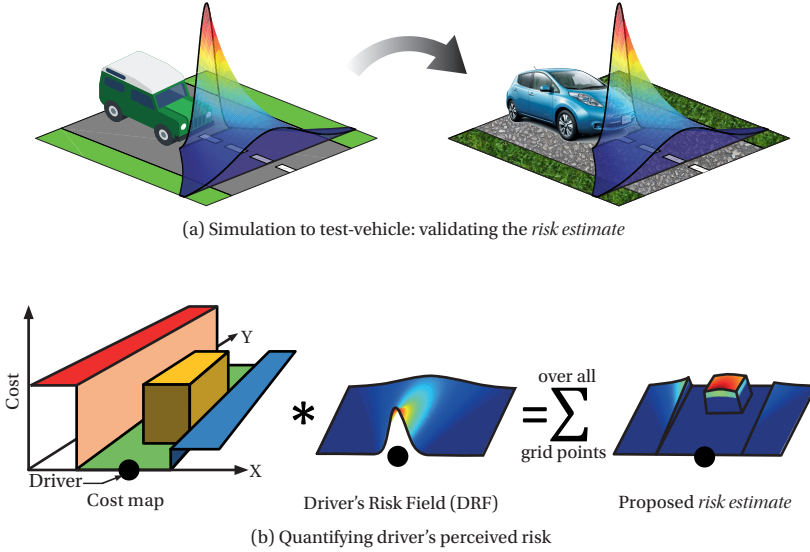


Figure 4.1: **Risk estimate:** (a) The *risk estimate* is validated in a test-vehicle to ensure the participants perceived realistic amounts of risk. (b) The driver in the ego car is indicated using the black marker. The bottom row illustrates the proposed quantification of the driver's perceived risk: the *risk estimate*. The cost of each element in the driving scene is multiplied with the Driver's Risk Field (DRF). This product summed over all grid points generates the *risk estimate* (\hat{r}).

4.2.3. DRF-BASED RISK ESTIMATE FOR EACH TRAJECTORY

The DRF-based *risk estimate* (\hat{r}) is a function of the vehicle's trajectory which is defined by the vehicle's position (x_{car} , y_{car}), heading (ϕ_{car}), steering angle (δ), and speed (v). We calculated the \hat{r} for each manual and automated lap of every participant as a product of the *probability* of the event, and the *consequence of the event* (for e.g., hitting a tree is worse compared to being on the road, see Fig. 4.1 [b]).

PROBABILITY OF THE EVENT OCCURRING

The 'probability of the event occurring' is represented by the Driver's Risk Field (DRF) (Fig. 4.1 [b]), which was empirically determined in chapter 2 [86]. The DRF is mathematically represented by a modified torus with a Gaussian cross-section, the height of which decreases and width increases, as you go further away from the ego-car (Fig. 4.1 [a]). The DRF is a dynamic field that increases its size with speed and morphs its shape with steering. Additionally, the DRF expands with steering angle (Fig. 3.4). These features, in a simplistic manner, mimic the multiplicative noise present in the driver's sensorimotor system. The DRF's shape is determined by six parameters: p , t_{1a} , k_1 , k_2 , m , and c (details in chapter 3). Although the DRF parameters are specific to each individual, in this study we decided to use the same parameter values (Table 4.1) for all the eight participants. This was done so that we could combine/average the results over all the participants.

Table 4.1: DRF and cost map parameter values

DRF parameters	p 0.04	t_{la} 3	k_1 0.02	k_2 0.05	m 0.0055	c 0.75
Cost map parameters	C_{road} 0	$C_{off-road}$ 500	$C_{oncoming-road}$ 250		$C_{parked car}$ 5000	

CONSEQUENCE OF AN EVENT

In the DRF model, the ‘consequence of an event’ is represented by a cost map that provides relative costs of colliding with different objects in the environment (for e.g., road = 0, grass off-road = 500, tree = 2000, etc.). The DRF model can generate the \hat{r} online by using the environment generated by lidar and camera systems on-board the test-vehicle. However, in this study we calculate the \hat{r} offline. We acquired a high definition map of the test-track, converted it into a cost map, and tracked the location of the car using GPS (± 5 cm accuracy). The cost of being on the road (C_{road}), cost of being off-road ($C_{off-road}$), and cost of hitting the parked car ($C_{parked car}$) were determined using manually driven trajectories (Table 4.1).

4.2.4. DATA EXCLUSION

For the automated driving conditions, participants experienced twelve different trajectories (speed and position profiles). The initial plan was to have the driver’s experience two repetitions of six different controllers (1: centreline follower, 2: manual replay, 3: manual replay with 90% speed, 4: DRF model, 5: DRF model safer (90% risk threshold) from chapter 3, and 6: ‘safe’ driver’s trajectory). However, we could not replicate these trajectories on the track. Hence, we decided not to analyse the results per controller and attribute the trajectories to any controller type. In other words, we now analyse them purely based on the trajectory that the driver’s experienced (not what the car was supposed to implement). After every lap, the participants filled up a questionnaire that evaluated the characteristics of the controllers. Since we do not draw or attribute any conclusions to the type of controller, we did not analyse the questionnaires. Additionally, due to experimenter error, the video for Lap 4 of participant 6 was not recorded and hence this lap has been excluded from the analysis.

However, between the time of submitting this chapter to a journal, and writing this thesis, a study that performs a similar experiment has emerged [139]. In this driving simulator-based experiment the participants experienced human-like and non-human-like AV driving styles, as well as the automated replay of their own manual drive. The authors conclude that humans prefer a slower human-like driving style for AV controllers that adapts its speed and lateral offset to roadside objects and furniture.

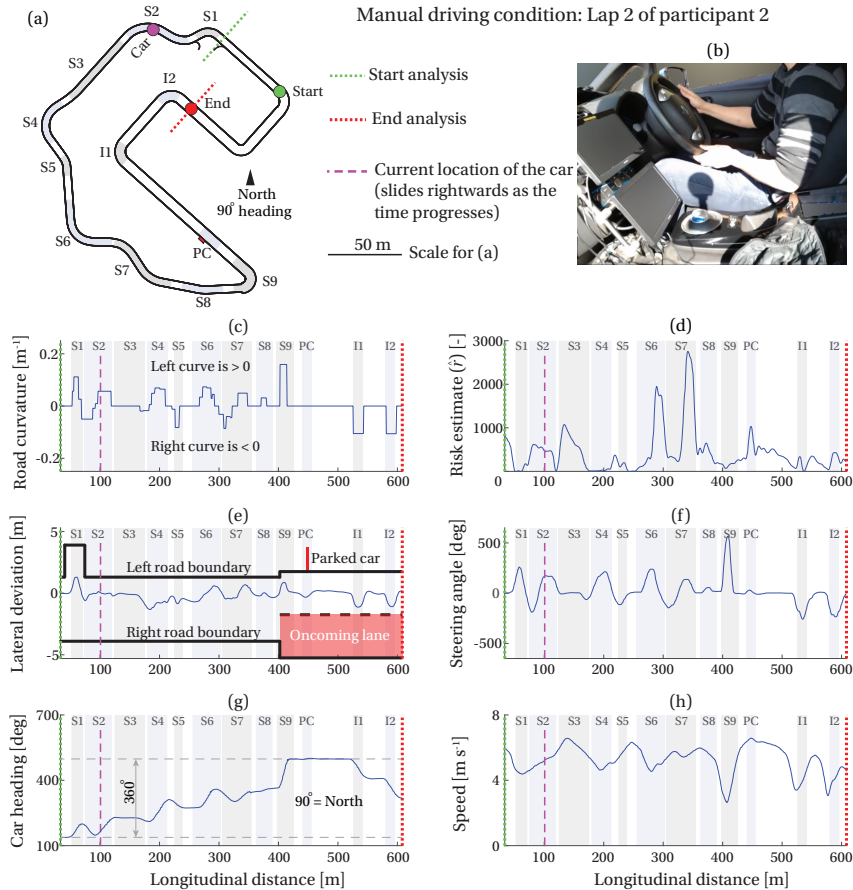


Figure 4.2: **Snapshot of manual driving condition:** The signals of lap 2 from participant 2. The dotted green and red lines indicate the start and end of the trajectory used for analysis, respectively. (a) The test-track consisted of curved section (Sectors S1 - S9), a parked car (PC), and two 90° intersections (I1, I2). The driver started every lap from the green dot and stopped at/after the red dot. In the automated driving condition, the car would need some initialisation time and hence it had to be driven manually from the green dot and it would get into automated mode by the time it crossed the green line. Hence, the green line is used as start of analysis for both manual and automated trajectories. The pink dot indicates the current (snapshot) location of the car on the track, and is indicated by the vertical dashed pink line in each of the plots. (b) A screenshot of the video recorded during the experiment. (c) Road curvature is positive for left curves, negative for right curves, and zero for straight roads. (d) The \hat{r} is the risk estimate for this particular lap. There are peaks in sectors S6 and S7, which are caused due to the car going close to the curb, as seen in the lateral deviation plot (e). Positive lateral deviation is towards the left, and negative lateral deviation is towards the right of the centreline. The thick black lines indicate the road boundaries and the translucent red box indicates the oncoming lane. The expansion in the sector S1 is due to a road joining the track as shown in test-track plot (a). Most participants used that piece of tarmac to 'cut the corner'. (f) Steering angle is positive for left turns and negative for right turns. (g) Car heading is positive counterclockwise and North direction was assumed to be 90° . (h) The speed drops at all the curves and intersections, especially at the very sharp corner in S9.

4.3. RESULTS

4.3.1. MANUAL DRIVING

For the manual driving conditions, the eight participants drove five laps of the test course. They were instructed to drive as they normally would. To test if the DRF model could predict the driver's behaviour during manual driving, we compared the predictions of the model to the steering and speed control actions performed by the driver.

DRIVER ACTIONS

To mitigate a rise in risk, the driver could perform steering corrections and speed reductions. Hence, we calculated the following signals to evaluate the DRF estimate predictions.

- Absolute steering angle ($|\delta|$): Since both positive (left turn) and negative (right turn) steering actions indicate the driver's intent to reduce risk, we calculate the absolute value of the steering angle to quantify the driver's action.
- Speed reduction ($v_{\text{reduction}}$): We assume that speed reduction is an indication of the driver's intent to reduce the risk. The reduction in speed is calculated with respect to the maximum speed at which the driver drove during that particular lap (V_{max}). Hence $v_{\text{reduction}} = V_{\text{max}} - v$. We calculate the $v_{\text{reduction}}$ with respect to V_{max} , because we think that V_{max} represents the driver's maximum willingness to incur risk, in context of this track.

DRF MODEL PREDICTIONS

The DRF-based driver model in chapter 3 generates a single *risk estimate*. However, as mentioned earlier, the driver's actions (to mitigate the rise in risk) are split mainly into two components: $|\delta|$ and $v_{\text{reduction}}$. To quantify what part of the \hat{r} corresponds to a reduction in risk due to $|\delta|$ and what part corresponds to a reduction in risk due to $v_{\text{reduction}}$, we calculate the DRF steering risk potential ($\hat{p}_{\text{steering}}$, Fig. 4.3 [b]) and DRF speed risk potential (\hat{p}_{speed} , Fig. 4.3 [c]), respectively.

$$\hat{p}_{\text{steering}} = \hat{r}_{\delta=0, v_{\text{max}}} - \hat{r}_{v_{\text{max}}} \quad (4.1)$$

$$\hat{p}_{\text{speed}} = \hat{r}_{\delta=0, v_{\text{max}}} - \hat{r}_{\delta=0} \quad (4.2)$$

The $\hat{r}_{\delta=0}$ is the \hat{r} when $\delta = 0$ and hence, indicates the \hat{r} if the driver had not taken any steering actions. Similarly, $\hat{r}_{v_{\text{max}}}$ is the \hat{r} when $v = V_{\text{max}}$ (V_{max} of that particular lap) and hence, it indicates the \hat{r} if we were to disregard the speed reductions performed by the driver. $\hat{r}_{\delta=0, v_{\text{max}}}$ is the \hat{r} when $\delta = 0$ and $v = V_{\text{max}}$ and hence, it represents the *risk estimate* if the driver had not made any speed or steering corrections.

From Fig. 4.3 [a] we can see that, for most parts, $\hat{r}_{\delta=0, v_{\text{max}}} > \hat{r}_{\delta=0}$, $\hat{r}_{v_{\text{max}}} > \hat{r}$. It indicates that, as expected, most of the steering and speed corrections performed by the driver reduced the risk. At some instances (in the neighbourhood of 300 m) the $\hat{r}_{v_{\text{max}}}$ is higher than the $\hat{r}_{\delta=0, v_{\text{max}}}$. The difference indicates that the model

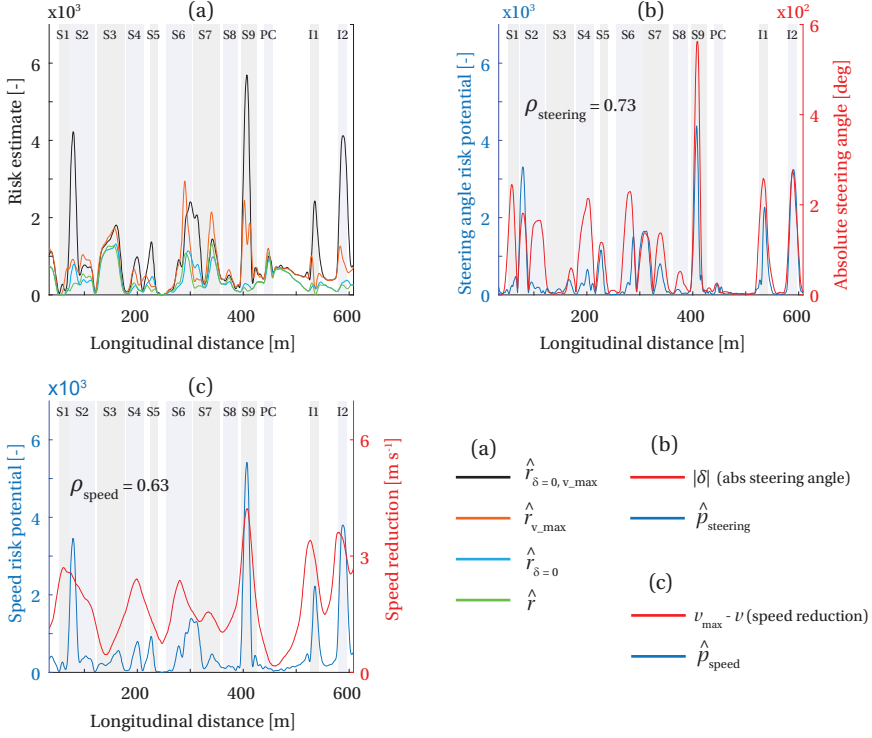


Figure 4.3: **Manual driving predictions:** The figure shows the *risk estimates*, DRF steering risk potential ($\hat{\rho}_{\text{steering}}$), and DRF speed risk potential ($\hat{\rho}_{\text{speed}}$) as a function of the distance covered along the lane centre, for Participant No. 2. All the signals are mean over the five repetitions of the manual trajectories. **(a)** The four different *risk estimates*: $\hat{r}_{\delta=0, v_{\max}}$, $\hat{r}_{v_{\max}}$, $\hat{r}_{\delta=0}$, and \hat{r} are plotted. The $\hat{r}_{\delta=0, v_{\max}}$ has the highest value, and the \hat{r} has the lowest value. In between these two are the $\hat{r}_{\delta=0}$ and $\hat{r}_{v_{\max}}$ plots. **(b)** We compare the $\hat{\rho}_{\text{steering}}$, which is the model's prediction about how much steering the driver should have implemented, to the steering angle implemented by the driver ($|\delta|$). **(c)** We compare the $\hat{\rho}_{\text{speed}}$, which is the model's prediction about how much speed reduction is needed, to the speed reduction implemented by the driver ($v_{\text{reduction}}$). The driver's speed reduction can be seen to have 'slower dynamics' compared to the model predictions. ρ indicates the Pearson's correlation coefficient. The plots for all 8 participants can be found in Appendix C.

thinks that the steering implemented by the driver at this point was 'incorrect'. Interestingly, it can be seen that the $\hat{r}_{\delta=0}$ is lower compared to the $\hat{r}_{\delta=0, v_{\max}}$, which indicates that the driver compensated for this 'steering error' by reducing the speed more than the model have expected him/her to.

The predictions of the model and the driver's steering behaviour are compared and they showed a moderate-to-strong correlation ($\rho_{\text{steering}} = 0.69 \pm 0.04$ (Mean \pm SD), Table 4.2). The peaks of the $\hat{\rho}_{\text{steering}}$ and the $|\delta|$ signals also align, indicating the steering timing also matches. In the neighbourhood of 300 m, the $|\delta|$ is higher than the $\hat{\rho}_{\text{steering}}$, which means that the driver steered more than the model expected him/her to.

Table 4.2: Correlation coefficients between DRF model predictions and manual driving behaviour

Participant No.	1	2	3	4	5	6	7	8	Mean \pm SD
ρ_{steering}	0.69	0.73	0.75	0.62	0.70	0.67	0.74	0.67	0.69 \pm 0.04
ρ_{speed}	0.77	0.63	0.63	0.61	0.67	0.64	0.65	0.52	0.64 \pm 0.07

Figure 4.3 [c] shows that the driver's speed reduction correlates moderately with the model predictions ($\rho_{\text{speed}} = 0.64 \pm 0.07$ (Mean \pm SD), Table 4.2). The peaks of the $v_{\text{reduction}}$ signal occur earlier than the peaks in the \hat{p}_{speed} , indicating that the drivers reduced their speed earlier than the model expected them to. This, we think, is due to the parameter values identified for the DRF. Specifically, the *look-ahead-time* (t_{la}) parameter of the DRF was set to 3 seconds (Table 4.1). Increasing this value will lead to the model predicting an earlier speed reduction.

Ideally, for the speed control case, we should have compared the model predictions to the brake and accelerator pedal activity since, the perceived risk of the driver is more directly related to the actions of the driver. However, the pedal activity was recorded as a binary (on/off) signal. Hence, we decided to use the speed signal, even though the car dynamics would entail that it would have a 'slower dynamics' compared to the risk metric, as can be seen in Fig. 4.3 [c]. The results hence verify that the *risk estimate* correlates well with the steering and speed reduction actions performed by the drivers during manual driving condition.

4.3.2. AUTOMATED DRIVING

Investigating if the *risk estimate* (\hat{r}) can predict the driver's subjective feeling of risk during an automated drive is the main aim of this study. To test this we compared *risk estimate* (\hat{r}) to the comments provided by the driver, and the takeovers they performed during each lap. Essentially, if the *risk estimate* captures the risk perceived by the drivers, then we should see a *Risky* comment or a takeover when the \hat{r} value was high, and a *Non-risky* comment, no comment, or no takeover when the \hat{r} value was low.

DRIVER'S COMMENTS AND TAKEOVERS

We segregated the driver's comments into two categories: *Risky* comments and *Non-risky* comments. *Risky* comments were those in which the driver indicated a sense of danger, discomfort, or risk by using words or phrases such as 'close to the curb', 'scary', etc. *Non-risky* comments are those that indicated if the drivers liked the drive, were 'OK' with it, found it too safe (boring), or did not comment at all. Table 4.3 shows a few words that, for illustration purposes, we categorised into (i) the reasoning (e.g., close, near), (ii) the object (e.g., curb), (iii) the noises participants made (e.g., woh, aaahhh), (iv) how they described the sector (e.g., risky, scary), (v) the takeovers (e.g., overtook, (steering) correct(ion)). The complete list of *Risky* and *Non-risky* comments can be found in Appendix C.

As mentioned in the methods section, we had segregated the track into 12 sectors (Curve driving: S1 - S9, Parked car: PC, Intersections: I1, and I2) because participants usually commented while referring to these salient features, after they

Table 4.3: Words mentioned in drivers' comments (8 participants x 12 laps x 12 sectors)

<i>Risky</i> comments	Count	<i>Non-risky</i> comments	Count
close, left, near, closer	105	right, close, far, clearance, larger, margin, space, wide, widely, wider, width	34
curb, edge, stone	37	curb	21
woh, aaahhh, ... (noises)	40	oh, hmmm, ooooooh (noises)	7
risk, risky, scary, hit, aggressive, immediately, wrong, bad, dangerous, harshly, intensely, jumps, rush scared, sharp, sharply, steep, suddenly, surprised, weird	45	good, ok, like, nice, fine, risk, safe, acceptable, safer, comfortable, reliable, smooth, avoid, avoided, avoiding, liked, normal, average, odd, peaceful, so-so	138
override, overrode, overshoot, correct	10	-	0

had experienced the sector. Hence using time stamps of the comments to attribute the comments to the location of the vehicle on the track would not make sense. The comments were hence attributed to each sector. If a driver complained about a particular sector being *Risky*, the trajectory for the entire sector was 'marked red' and the takeovers by the drivers were measured as a binary signal (thin black line) (Fig. 4.4).

DRF MODEL PREDICTIONS

We compared the driver's comments and takeovers to the the \hat{r} calculated during the automated trajectory. Similar to that calculated for manual driving condition, the \hat{r} in automated driving condition is unique to the trajectory of each of the 12 laps, for each of the eight participants.

Risk estimate trajectories: The \hat{r} trajectories for each participant are plotted in Fig. 4.4. Visual inspection of the plot reveals that the participants made a *Risky* comment when the \hat{r} was also calculated to be high. This points towards a good match between the driver's subjective feeling of risk and the objective *risk estimate* calculated by the DRF model. However, there are some instances in the I1 and I2 sectors (90-degree intersections) where red sectors are marked at very low *risk estimate* (\hat{r}) values.

Another interesting point is that the \hat{r} indicates a high-risk level in sectors S1 and S7, but a low-risk level in sector S9. However, in Fig 4.2 [c], we can find that the curvature in sector S9 is even higher than that of S1 and the curvature in S7 is relatively small. The reason for this high risk is due to the lateral positioning of the vehicle. The AV drove very close to the curb in S7 and S1 and hence led to a high value for \hat{r} . Several *Risky* comments from the participants also corresponded to the vehicle being too close to the curb. In S9, the AV would slow down considerably more compared to that in S1 and S7, and hence the \hat{r} is low despite the curvature being more than that in S1 and S7.

Maximum of \hat{r} per sector: We assume that the maximum risk experienced by the driver is a more valid index of perceived risk as compared to mean risk experienced during a sector. Hence, we calculate the $\max(\hat{r})$ in each sector, as a metric, to quantify the 'riskiness' of that particular sector. This metric ($\max(\hat{r})$ per sector)

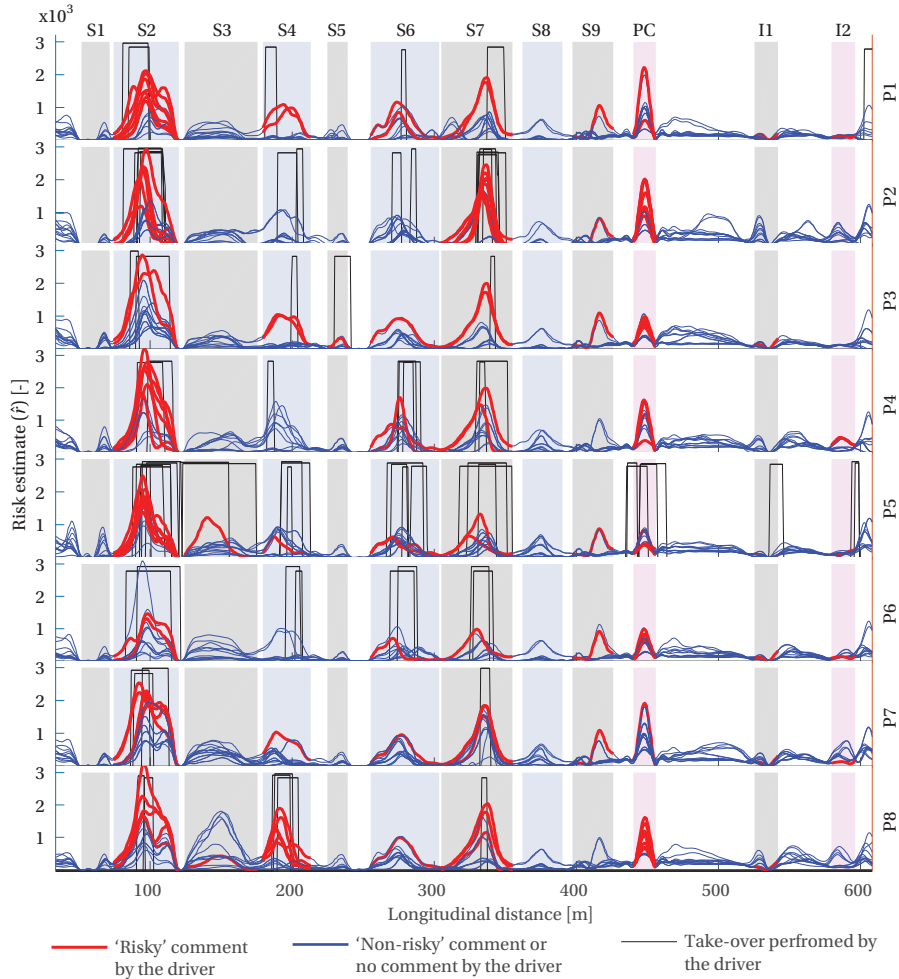


Figure 4.4: **Risk estimate for automated driving:** P1 - P8 refer to the eight participants. Each row has 12 plots corresponding to the 12 laps for each participant. The shaded rectangles indicate the 12 different sectors. S1 - S9 for the curve driving segment, PC is the parked car segment, and I1 and I2 indicate the two 90-degree intersections. The plots show the *risk estimate* (\hat{r}) for each lap. The blue parts indicate *Non-risky* sectors and the red parts indicate the *Risky* sectors. The black 'steps' indicate the steering takeover by the driver. It can be seen that, in general, the *risk estimate* (\hat{r}) is marked red when its value is high. Also, the takeovers occur when the \hat{r} peaks.

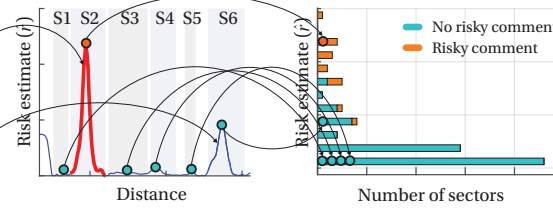
was labelled either *Risky* or *Non-risky* based on the comments, and *takeover* or *no takeover* depending on whether the participant took over the vehicle's control or not (Fig. 4.5).

Step 1: Participants commented while being driven in an automated vehicle. The comments were labeled as 'risky' or 'not risky' comments.



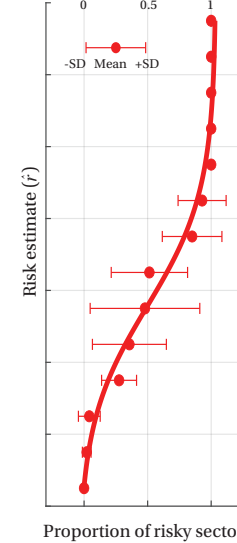
Video feed from inside the vehicle

Step 2: Entire sector is tagged 'risky' or 'not risky' depending on the driver's comment.



Step 3: Maximum value of \hat{r} from each sector is accumulated in a histogram for 12 laps of 1 participant.

Step 4: Proportion of risky (comments or take overs) averaged over 12 laps of the 8 participants.

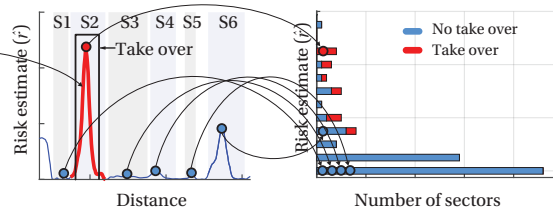


Step 1: Participants could takeover control of the vehicle if they felt the need to do so. Takeovers were recorded in the vehicle CAN data.



Video feed from inside the vehicle

Step 2: Entire sector is tagged 'take over' or 'no take over' depending on the driver's action.



Step 3: Maximum value of \hat{r} from each sector is accumulated in a histogram for 12 laps of 1 participant.

Figure 4.5: **Steps in automated driving analysis:** **Step 1:** The comments were classified into *Risky* or *Non-risky* (Table 4.3). The takeovers were recorded by the vehicle's data collection system. **Step 2:** The trajectory of the entire sector, the comment was attributed to, was tagged *Risky* or *Non-risky*. Similarly, the entire sector in which the takeover was initiated was tagged *takeover* or *no takeover*. If a takeover was initiated or comment was attributed to parts between 2 sectors, both sectors were tagged. **Step 3:** The max(\hat{r}) for each sector was chosen as a metric. The number sectors with different levels of \hat{r} were plotted in a stacked histogram. The two histograms, comments and takeovers, combined and presented in Fig. 4.6. **Step 4:** The proportion of risky comments or takeovers was calculated for each participant in each of the bins of the histogram, and then averaged over all the eight participants. The red circular markers indicate the mean, and the bars indicate \pm standard deviation (SD). The plot shown here is for the curve driving section (S1-S9). Identical analysis was performed for the parked car (PC) and intersections (I1, I2) and results are shown in Fig. 4.7.

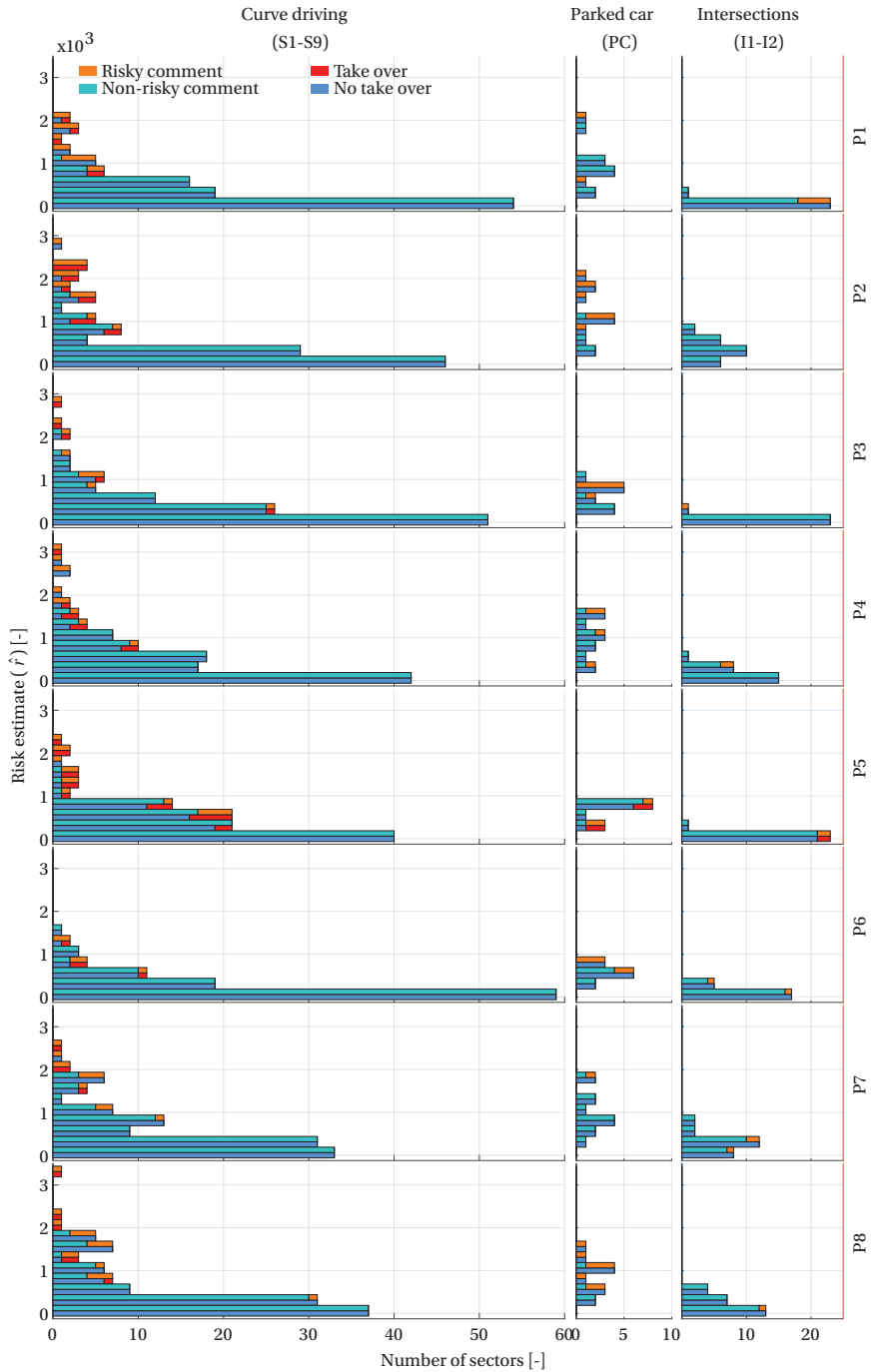


Figure 4.6: **Histogram of comments and takeovers:** P1 - P8 indicate the eight participants. The 3 columns indicate the segregation of sectors into the three segments: curve driving (S1-S9), parked car (PC), and intersections (I1-I2). The x-axis represents the number of sectors and the y-axis represents the *risk estimate*. We plot the *Risky* and *Non-risky* comments stacked on top of each other for comparison. Simultaneously, we also plot the *takeovers* and *non-takeovers* in a stacked manner. Hence the height of two adjacent bars is equal. The bar plots have 14 bins (y axes) with minimum value of 0 and maximum value of 3500, and a width of 250.

Counting the number of *Risky* and *Non-risky* sectors: We plotted a histogram for each participant (Fig. 4.6) using the $\max(\hat{r})$ for each sector (from Fig. 4.4). We compared the qualitative response - the comments provided by the driver, and a quantitative response - the takeovers performed by the drivers in a stacked histogram. Figure 4.6 shows that in the curve driving and the parked car sections, none of the participants made any *Risky* comments or performed takeovers in the lowest *risk estimate* (bin). However, in the intersections there are several instances when the participants (P1, P5, P6, P7, and P8) either made a *Risky* comment or performed a takeover. Naturalistic driving is majorly comprised of non-risky situations and a very few risky situations. A similar trend was shown by the *risk estimate* (\hat{r}), where the number of sectors decreased as the *risk estimate* increased (Fig. 4.6). Also, most of the takeovers are accompanied by a *Risky* comment.

Risk estimate as a decision variable: The main aim of this chapter was to test if the *risk estimate* could be used to detect *Risky* and *Non-risky* sectors. Since, the participants can express their 'feeling of risk' by either commenting or by taking over, we combine the two modes (using the 'or' function). Hence a sector is marked *Risky* if the participant either made a *Risky* comment, or a *takeover*, or both, and the remaining sectors are labelled *Non-Risky*.

We calculated the proportion of *Risky* sectors ($\frac{Risky}{Risky + Non-Risky}$) for each \hat{r} value (mid point of each bin) and averaged it over all the eight participants. The mean (circular markers) and standard deviation (error bars) are plotted in Fig. 4.7. The curve driving plot (Fig. 4.7 [a]), all the 14 points together, are calculated from 855 points (8 participants x 12 laps x 9 sectors - 9 sectors of lap four of participant six, which the experimenter failed to record). The parked car section plot (Fig. 4.7 [b]), all the 8 points combined, represent the mean and standard deviation over 95 points (8 participants x 12 laps x 1 sector - 1 sector of lap four of participant six). The intersection plot (Fig. 4.7 [c]), all the 9 points combined, represent the mean and standard deviation over 190 points (8 participants x 12 laps x 2 sectors - 2 sectors of lap four of participant six). We think that this difference in the number of data points explains the larger uncertainty in the parked car section and intersections compared to the curve driving section.

A logistic function was fit to the (mean) data points in all the three sections (Fig. 4.7). Instances with \hat{r} higher than 2250, and 1000 did not occur at the parked car and in the intersections, respectively. In the curve driving section, at high values of \hat{r} , the proportion of *Risky* sectors almost reaches 1, and 0 for low values.

$$x = \frac{a_1}{1 + e^{-a_2(y-a_3)}} - a_4 \quad (4.3)$$

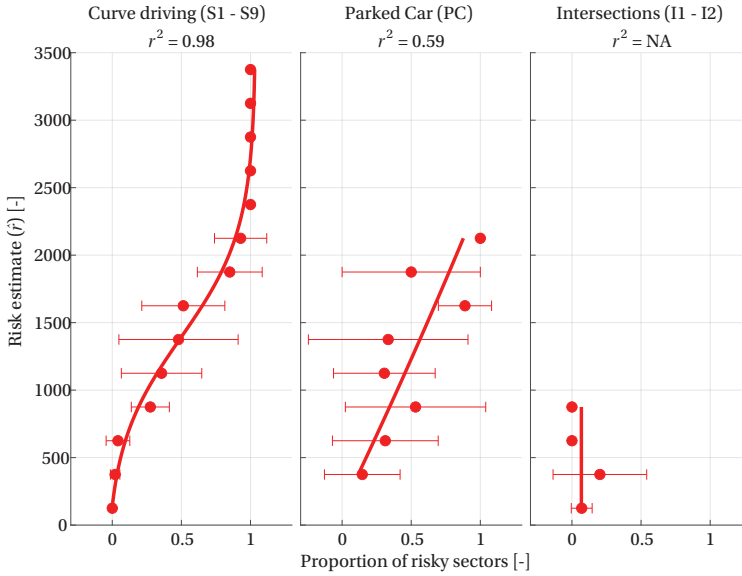


Figure 4.7: **Proportion of risky sectors:** This plot shows the mean (circular markers) and \pm SD (bars) of the proportion of risky sectors (either the comment was *Risky* or there was a *takeover*) over the 12 laps of all the 8 participants (95 laps in total, since 1 lap's video was accidentally not recorded). The sectors for the three sections: curve driving (S1-S9), parked car (PC), and intersections (I1, I2) contained 855, 95, and 190 data points respectively. A logistic function was fit to the mean (circular markers) data points (equation 4.3). The goodness of fit is indicated by the r squared (r^2) metric.

The results from Fig. 4.7 show that the *risk estimate* for the automated driving condition is correlated with the subjective feeling of risk (comments or takeovers) of the participants in curve driving and parked car sections. In the intersections however, the results are inconclusive since no instances of high \hat{r} were experienced in any of the laps.

4.4. DISCUSSION

The aim of this chapter was to test if the DRF-based *risk estimate* (\hat{r}) correlates with drivers' perceived risk. The results show that the *risk estimate* could predict the driver's manual driving behaviour - speed and steering actions. Furthermore, in automated driving, the *risk estimate*, correlated with the comments and takeovers performed by the drivers in curve driving and avoiding a car parked outside the lane boundary. In other words, the DRF, a field based risk metric, captured the perceived risk in curve driving and with a static obstacle.

The results for 90-degree intersections were inconclusive. Events with high \hat{r} did not occur (Fig. 4.6, 4.7) and the proportions of *Risky* comments were low at low \hat{r} values. It is unknown how the results extrapolate to higher values of \hat{r} . However, the fact that the current version of the DRF only accounts for the physical presence of objects suggests that the \hat{r} at intersections may be a limitation on this model.

This is because at an intersection the DRF sees a larger patch of road ('safe zone') and hence reduces the \hat{r} , which may result in speeding rather than braking at an intersection. Humans slow down at an intersection in anticipation of traffic. This kind of learned conscious behaviour will have to be integrated in future versions of the DRF.

In this study, we derived the perceived risk (indicated by the driver) as a measure of it being *Risky* or *Non-risky*. This was based only on the driver's comments and whether they took over the controls of the vehicle or not. However, while analysing the videos we found several interesting behaviours where the drivers would hover their hands near the steering wheel (presumably when they felt a high risk). This kind of bio-mechanical preparedness to takeover also contains valuable information about the risk perceived by the driver [140] and could be analysed in detail in future studies.

To put our results in the context of literature, we compare it to 'time to lane crossing' (TLC) [65]. There are several methods for calculating TLC [141], such as the 'TLC swath' approach proposed by Boer [47]. The similarities between the TLC and the \hat{r} arise from the fact that they both have an expanding arc (for TLC) or a field (for DRF). This combined with the threshold, below which these metrics need to be maintained, results in *satisficing* behaviour (a strategy that aims for a satisfactory result [e.g., stay within lane boundary], rather than the optimal solution [e.g., follow lane centre]). However, there are two key differences.

First, the expansion of the arc for the TLC is fixed, whereas the expansion of the DRF is proportional to the (absolute value of the) steering angle. This means that the DRF expands more (higher \hat{r}) for a sharper curve compared to a shallower one, and hence would want the car to drive slower for a sharper curve. The 'swath TLC' gets around this problem by having an additional 'straight line' TLC which projects straight ahead and intersects with the outer lane boundary of the curve. The added benefit of having a steering dependent expansion over a straight line TLC is that it is generalizable to scenarios other than interacting with lane boundaries.

The second difference is that, since TLC is calculated using the intersection points of the arc and the lane boundary, it cannot account for the presence of objects outside the lane boundary. For a TLC based controller driving on a road with curbs on both sides of the road is the same as driving on a road with curb on one side and an open oncoming lane on the other. The DRF being a field can expand beyond the lane boundaries and hence can account for objects outside the lane boundaries and the different levels of danger that they pose (curb is more dangerous than an open oncoming lane).

In this study, all the scenarios were static which made it easy to formulate a high definition (HD) cost map of the test-track, offline. However, multi-lane dynamic scenarios need dynamic cost maps that are updated online. Researchers, primarily using computer simulations, have suggested approaches for straight roads and intersections using the 'Conditional Random Field (CRF)' [137] and the 'Potential Field Indicator (PFI)' [136] that account for the uncertainties in behaviour of neighbouring vehicles and the noise introduced while sensing their state (e.g., position, velocity, acceleration). Lu et al. [142] also incorporate the mass of the vehicle and

Huang et al. [143] incorporate the intention of the vehicle in a mixed (manual + automated) traffic condition using long-short term memory (LSTM) networks to determine the potential field generated by external vehicles. In the future, we would like to incorporate these features into the dynamic cost-map and test the validity of \hat{r} in multi-lane dynamic scenarios with test-vehicles.

An important aspect of the DRF model is its intent to formulate a unified risk measure over a plethora of driving scenarios. Although further experimentation with other (static and dynamic) scenarios will be needed to test the validity of the model, this unified approach to express driver's perceived risk has important applications in designing the behaviour of automated systems. It can be used to assess the performance of the automated system in different scenarios and adjusted to meet the preferences of the individual drivers.

4

4.5. CONCLUSIONS

The aim of this chapter was to test if the Driver's Risk Field (DRF)-based *risk estimate* (\hat{r}) could correlate with the perceived risk of the driver. To ensure that the driver's perceived realistic levels of risk, the experiment was performed on a test-track with a Nissan Leaf test-vehicle.

- The *risk estimate* (\hat{r}) correlates with manual driving behaviour expressed in terms of steering angle and speed ($\rho_{\text{steering}} = 0.69$, $\rho_{\text{speed}} = 0.64$, Table 4.2, Fig. 4.3)
- In automated driving condition, the \hat{r} could predict the comments and takeovers performed by the drivers in the curve driving section ($r^2 = 0.98$, Fig. 4.7).
- The \hat{r} could also predict the comments and takeovers by the drivers, in the automated driving condition, while negotiating a car that was parked outside the lane boundary ($r^2 = 0.59$, Fig. 4.7).

5

CONCLUSIONS

5.1. BACKGROUND

Formulating a unified driver model that can quantitatively predict human driving behaviour in a multitude of scenarios has inspired researchers for decades. This thesis aimed to take a step towards such a unified driver model with a focus on speed and lateral position adaptations. Qualitative models that explain the motivations underlying driving behaviour in a unified manner exist, but they lack the specificity and operationalizability of quantitative models. Most quantitative driver models in literature either: (i) follow the data-driven black-box approach which provides little to no understanding about human driving behaviour, or (ii) stitch together several driver models, each using a different underlying principle and applicable to a different scenario. This has led to a fragmented understanding of the underlying motivation for driving. Moreover, stitching together different models requires an overarching *unifying* model to bring all the existing models together. The other option is to formulate a single unified model.

5.1.1. GOAL AND SCOPE OF THIS THESIS

The goal of this thesis was to formulate a unified driver model, based on a single underlying principle, from which human-like speed and lateral position adaptations would emerge in a multitude of scenarios. However, driving is a sophisticated task with sub-tasks at different levels [83]. Since, this is a preliminary step towards a unified driver model, the scope of this thesis was limited to low-level control (steering and speed) behaviour of the driver, in scenarios that involved changes to the road geometry (e.g., curvature, lane width, roadside furniture, etc.) and deterministic non-interacting traffic (e.g., car following, overtaking, etc.). Modelling the interaction between the different players in traffic is a research topic in itself [144][145] and is beyond the scope of this thesis.

5.1.2. APPROACH TO ACHIEVE THE GOAL

In order to achieve the goal mentioned above, we borrowed principles from the field of sensorimotor control. This thesis is not the first time that driver modelling researchers have borrowed from the field of sensorimotor control. Sentouh et al. [70] proposed a driver model that included visual and kinesthetic perception, as well as anticipatory and compensatory control. Markkula et al. [146] proposed a computational framework that used driver steering control as an illustration while borrowing the concepts of *motor primitives*, *neuronal evidence accumulation*, and *prediction of sensory consequences of motor actions* from the field of sensorimotor control. Both these studies focused on the microscopic trajectories of the driver's steering inputs.

The model developed in this thesis, although generated similar microscopic trajectories for steering as well as speed control, was focused on capturing the macroscopic adaptations in speed and lateral behaviour of the drivers (e.g., slowing down more and cutting the curve more for a sharper curve as compared to a shallower curve). With this intention, the following set of sensorimotor principles were borrowed: (i) presence of multiplicative noise in the perception and actions of a human [30], and (ii) balancing the reward (achieving the goal) and the *goal-relevant* cost (undesired consequences) [27]. It was also apparent that the cost (mentioned above) was generally incurred due to the undesired consequences of the noise present in our sensorimotor system. The *consequence of noise*, in the sensorimotor context, is calculated as the product of the *probability of an event* and the *consequence of that event*, and is analogous to the concept of *risk*, proposed by Näätänen and Summala [2] for the field of driving, and was used in this thesis.

The results from chapters 2, 3, and 4 show that basing a driver model on sensorimotor control theories does help in capturing speed and lateral position adaptations of a driver in a multitude of scenarios. For example, the sensorimotor principle of penalising only the *goal-relevant* costs could be seen at work in the roadside furniture scenario in chapter 3. The model (as well as human drivers) steered away from the cars parked only outside one lane boundary while not changing the speed drastically. However, when the cars were parked outside both lane boundaries, the model slowed down considerably (more than in the earlier case) and drove along the lane centre. This display of 'not slowing down when not needed' is a manifestation of the *goal-relevant* penalty in sensorimotor control. Another example where the effect of multiplicative noise becomes clear is the curve driving scenario. The DRF would expand with the increase in magnitude of the steering angle, which mimicked (in a very simplistic manner) the multiplicative noise in the driver's sensorimotor system. This led to the model having a wider DRF while negotiating a sharper curve (smaller radius), in turn incurring higher cost, leading to the model having to slow down to maintain the cost (*risk estimate*) below the threshold. This 'slowing down more for sharper curve' as compared to a shallower curve is also exhibited by human drivers.

An essential component of the driver model proposed in chapter 3 is the *risk estimate* signal that is used in conjunction with the risk threshold theory to generate speed and lateral position adaptations. The *probability* component of the *risk*

estimate, which was named the ‘Driver’s Risk Field’ (DRF), was empirically quantified in chapter 2 and was found to be wider than the ego-vehicle. The DRF was then combined with the cost map (*consequence of an event*) in chapter 3 to generate the aforementioned *risk estimate*. In chapter 4, an experiment in a real vehicle on a test-track showed that the *risk estimate* corresponded to the risk perceived by drivers during manual as well automated driving.

Each of the chapters mentioned above (chapters 2, 3, and 4) feeds into the subsequent chapters, but they have their own results and conclusions which are independently valid. However, writing this thesis presents a unique opportunity to reflect on all the three chapters, as a whole. The following section will discuss the overarching conclusions that can be drawn from this entire thesis and presents them in the context of the literature.

5.2. THREE OVERARCHING CONCLUSIONS

When all the results and conclusions of this thesis are recapitulated, three main conclusions can be drawn regarding human driving behaviour. The evidence, significance, and limitations for each these three main conclusions are discussed in the following paragraphs.

5.2.1. CONCLUSION 1: DRIVERS RESPOND TO OBJECTS BEYOND THE WIDTH OF THE CAR AND LANE BOUNDARIES

In addition to the objects within the lane boundaries, driver’s subjectively perceive and respond to the risk posed by objects outside the width of the car and the lane boundaries. This phenomenon has been observed in the literature where the presence of *roadside furniture* has been shown to affect the lateral position and speed adopted by drivers [105][106]. In this thesis, we not only provide direct evidence for this behaviour, but also quantify this *overflow of risk* (Fig. 5.1).

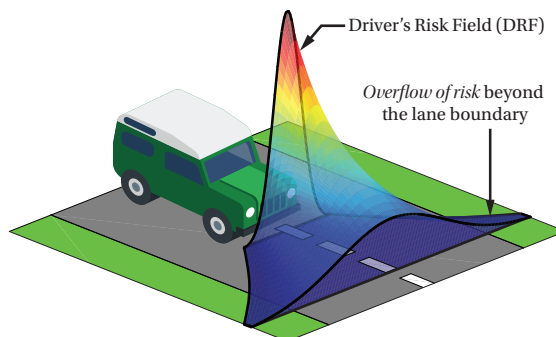


Figure 5.1: **Overflow of risk:** The Driver’s Risk Field (DRF) captures the fact that drivers care about the region beyond the car and lane boundaries.

EVIDENCE

The direct evidence for this conclusion can be found across all the three chapters. In chapter 2, all the participants of the driving simulator experiment responded to obstacles that were placed beyond the width of the ego vehicle. In this experiment, we had placed obstacles at 77 different locations in front of the driver. Only 7 out of these 77 obstacles were placed in the path of the vehicle. The remaining 70 were beyond the width of the vehicle and, in principle, did not need any action from the driver to avoid them. Yet, all the participants made steering corrections to *avoid* obstacles that were beyond the width of the vehicle.

In chapter 3, we cite literature which showed that driver's care about the objects beyond the lane boundaries. For example, Alessandro Calvi [105] found that when trees were close to the road edge, drivers decreased their speed significantly and moved towards the centreline of the road. Francesco Bella [89] found that in the presence of a shoulder on either side of the road, drivers drove faster and less towards the road centre (of a two lane road), as compared to when the shoulder was absent. Dunning et al. [106] found that participants drove slower, and away from the road edge when they encountered water as compared to grass, outside the lane boundary. In the driving simulator experiment performed in chapter 3, the single participant who drove around the track also moved away from the row of cars parked outside the left lane boundary. When cars were parked outside both lane boundaries, he slowed down.

In chapter 4, drivers complained when the automated vehicle was following a trajectory that was too close to the car parked outside the lane boundary. All these results provide sufficient direct evidence to conclude that drivers respond to objects beyond the width of the car and lane boundaries.

SIGNIFICANCE

The proposed risk metric has similarities with Time to Lane Crossing (TLC) [141], that comprises spatio-temporal safety margins towards lane boundaries and TTC [147], that comprises spatio-temporal safety margins towards objects within it. Controllers have been proposed based on these metrics [47][148][149][150]. The main difference of the *risk estimate*, lies in its ability to capture the driving behaviour as shown by the evidence mentioned above: *humans also respond to objects beyond the car and lane boundary*. Other researchers have also suggested different shapes of potential fields that extend beyond car and lane boundaries [32][136]. However, these proposed potential fields were not empirically measured, but were designed a-priori based on the understanding gained by the researcher.

The DRE, on the other hand, empirically captures this *overflow of the risk* (Fig. 5.1), as being caused by the presence and propagation of sensorimotor noise. The uncertainty about the ego vehicle's current position and speed, the uncertainty about the steering action that the driver applies, and the uncertainty in predicting the future speed and position trajectory of the ego vehicle create a probability distribution of the possible positions that the vehicle is expected to occupy in the next couple of seconds. Such uncertainty propagation has also been proposed in the field of robotics [151]. Note that, if the uncertainty was somehow removed and

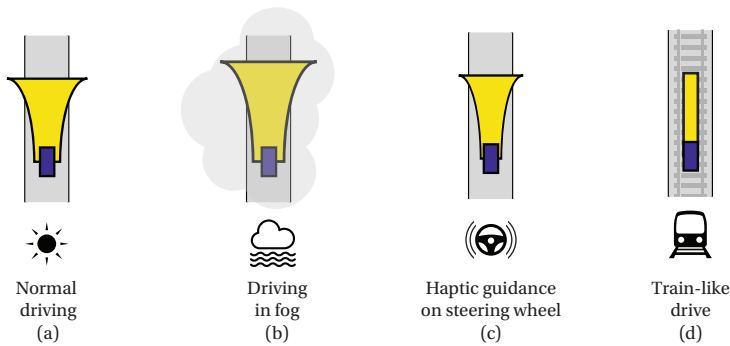


Figure 5.2: **Hypothesised effect of noise on the DRF:** We hypothesise that the DRF originates due to the noise in the sensorimotor system and its propagation. **(a)** Normal driving: This is the shape as measured in chapter 2. **(b)** We expect the size of the DRF to expand as compared to (a) in foggy weather conditions, since fog increases visual noise. **(c)** Haptic guidance on the steering can act as a ‘channel’ through which the vehicle is guided and hence reduce lateral variability. We expect the DRF to shrink laterally as compared to the DRF in (a). **(d)** In this ‘train-like’ scenario, the vehicle has Haptic guidance on the steering as well as visual cues regarding the path the vehicle is going to strictly follow. We expect this reduce the lateral variability to a negligible amount and hence expect a DRF which is of the same width as the vehicle.

the prediction of future positions of the ego vehicle was deterministic, humans would not care about objects beyond the width of the car (Fig. 5.2 [d]). A good example is that of a train. The rails of a train constrain the lateral position of the train and hence the uncertainty in this direction is negligible. The resulting behaviour is that the driver of the train can zoom past other trains, or walls of the tunnels, or station platforms, barely centimetres apart without reducing speed! The same would not be done by the driver in a car, which is not constrained to rails.

LIMITATIONS

The main limitation of this conclusion is that the direct empirical evidence for this *overflow of risk* (represented by the DRF) has been shown only for one fixed speed (experiment in chapter 2). In chapter 3, the DRF was *upgraded* to a dynamic DRF that morphed its shape and size as a function of speed and steering. However, these *upgrades* are based on assumptions that drivers tend to maintain a constant time headway [109] (hence the elongation of the DRF in the longitudinal direction with increase in speed) and that steering becomes less accurate as the steering angle increases [31]. These assumptions are yet to be experimentally verified. Experiments similar to the one conducted in chapter 2 with different levels of fixed speeds and road curvatures are recommended, to quantify the change in shape of the DRF as a function of steering and speed.

Apart from the change in shape of the DRF caused by the steering and speed, it is predicted that changes in the sensorimotor noise caused by external factors can expand or contract the DRF. One could, artificially modify the level of noise and see if the size and shape of the DRF changes (Fig. 5.2). For example, intro-

ducing fog will increase the visual noise (Fig. 5.2 [b]), introducing Haptic guidance (Fig. 5.2 [c]) and visual rails on the road could reduce noise (Fig. 5.2 [d]). We do have behavioural evidence that people drive slower in foggy conditions [152] [153] and faster with Haptic guidance [121], which suggest that the DRF expands and shrinks, respectively. However, we do not have direct evidence for this size and shape change.

These experiments recommended to address the limitations of the conclusion mentioned above will further improve our understanding of how this *overflow of risk* depends on other factors (such as steering, speed, external noise, etc.) and how drivers may adapt their behaviour to such factors.

5.2.2. CONCLUSION 2: THE *risk estimate* CONSTITUTES A SIGNAL THAT CORRELATES WITH THE RISK PERCEIVED BY THE DRIVER

The *risk estimate* proposed in this thesis, represents the driving equivalent of the sensorimotor control concept of *consequence of noise* - a product of *probability*, and the *consequence* of a risky event occurring. It constitutes a dynamic signal, which was hypothesised to correlate to the risk perceived by the driver.

5

EVIDENCE

In chapter 3, we already found indirect evidence for the above mentioned conclusion. The *risk estimate* was used as a cost function in a driver model and the behaviour of the driver model showed trends similar to human speed and lateral position adaptations in seven different scenarios. However, in chapter 4, direct evidence can be found during both manual and automated driving for the effectiveness of the *risk estimate* as a predictor for driver's perceived risk. In the manual driving condition, a peak in the *risk estimate* is observed in the vicinity of a steering and/or speed change performed by the driver (Fig. 4.3 [b][c]). This suggests that the driver perceived a large amount of risk and hence performed a corrective action to lower the risk. In the autonomous driving condition, when the value of the *risk estimate* was high, drivers either complained about the car driving in a risky manner or took over control of the vehicle.

Apart from the evidence found in this thesis, evidence can also be found in literature for *risk estimate*-like signals/metrics being able to effectively relate to driver's characteristics. For example, Woo et al. [154] and Mullakkal-Babu et al. [135] developed signals (similar to the *risk estimate* signal) based on artificial potential field approach. Woo et al. [154] developed a 'Driving Risk Feature' to assess the driving style of external drivers using a potential field based approach. Their speed dependent potential field was centred around the external road user (the DRF proposed in this thesis is attached to the ego vehicle) and generated a 'repulsive' force on the ego vehicle which could effectively classify aggressiveness of the external driver. Mullakkal-Babu et al. [135] also developed a signal based on the 'Probabilistic Driving Risk Field' which originated from the objects in the environment. The risk descriptions from their proposed approach could qualitatively reflect the narration of the situation and were in general consistent with the Time To Colli-

sion (TTC) signal. Other researchers, for example, Wei et al. [155] generated a risk-corridor based on the trajectories executed by drivers. They found that providing this corridor as a reference to the AV controller yielded a more *human-acceptable* and comfortable drive than using the road centre as reference, during curve driving and obstacle avoidance. These studies show the versatility and effectiveness of risk field/corridor based signals and metrics in predicting the characteristics of human driving.

SIGNIFICANCE

The fact that the *risk estimate* correlates with the risk perceived by a driver, provides direct evidence that even in driving (like in sensorimotor control), humans care about the *consequence of the noise*. This concept of accounting for the consequence of noise may sound familiar to those who are aware of the Kalman Filter, and indeed, both - the Kalman Filter and the DRF account for the consequence of noise. However, there is a key difference. The Kalman Filter is mainly used to estimate a *hidden* (by noise, not only non-observable) state and to propagate its uncertainties into the future, which are then used for control [156][157]. The DRF, on the other hand, also propagates uncertainties into the future, but also directly dictates the modifications in the actions depending on the magnitude of the uncertainty. This difference becomes clear when the noise in both sensing and predictions is increased proportionally. The Kalman Filter would provide the same expected value. On the other hand, the DRF would ask the controller to slow down. A more suitable way to capture the consequence of the noise on behaviour, in an 'optimal control' manner was explored by the Kolekar et al. [69] by using the *exponential Linear Quadratic Regulator* proposed by Jacobson in 1973 [158]. Here, the Taylor series expansion of the exponential of the quadratic cost automatically accounted for the variance of the signals. Another complication that arises while using 'normal' Kalman Filter while modelling driving behaviour is the presence of multiplicative noise. Todorov (2005) [159] proposed a solution to this problem, which was later then adapted by Kolekar et al. [31] into a receding horizon framework to formulate a driver steering model.

The *risk estimate*, besides improving the scientific understanding of risk perception, has several applications in automated systems of a vehicle as well. The *risk estimate* can be used to create a 'safety envelope' around an automated vehicle to ensure safe handling of critical scenarios. For example, Mobileye has proposed the Responsibility-Sensitive Safety [33] which formalises critical situations and driving rules to ensure uniform safety standards across various manufacturers. An updated version of the *risk estimate* could be useful in creating a unified 'critical situation detector' in a multitude of scenarios.

On the flip side of creating a 'safety-envelope', the *risk estimate* can also be used to monitor how risky the trajectory driven by an automated vehicle is. This could be then used to either modify the trajectory (according to the preference of the driver) or rate the automated system (safe/unsafe). The *risk estimate* can be quite effective at this because as seen in chapter 3, it could capture the trends in behaviour expressed in terms of different metrics (TLC, TTC, THW, etc.). This pro-

vides evidence that the *risk estimate* can act as a *unified metric* to quantify human behaviour in several scenarios.

LIMITATIONS

The main limitations of this conclusion arise from the nature and shape of the DRF which represents the *probability of an event* in the *risk estimate* calculations. Firstly, the *risk estimate* proposed in this thesis only accounts for the area in front of the vehicle. Hence, it cannot account for risk from the side or behind the vehicle. However, this is an important aspect of every day driving, and a ‘surround DRF’ will need to be developed. The second limitation is that the *risk estimate* can only account for the risk due to the physical presence of the object. It cannot estimate *tactical risks* which are rules that are consciously learnt by humans, for example to stop at the red light at an intersection. Hence, if the rule based behaviour is to be incorporated in this model, the ‘cost of breaking these rules’ needs to be added to the cost map using phantom obstacles. For example, a red light at an intersection

5



(a) Relaxed



(b) Instructed



(c) Ready to take-over (hovering)



(d) Take-over

Figure 5.3: **Bio-mechanical readiness of the driver during automated driving:** These are screenshots from the video recorded during the automated driving condition of the experiment in chapter 4. Drivers are expected to place their hands in a relaxed position, as shown in (a), when they do not perceive sufficient risk from the automated system’s trajectory. This screenshot is taken when the car was stationary, since the participants were instructed to keep their hands near the steering wheel, throughout the duration of the experiment, as shown in (b). When drivers perceived a high amount of risk they prepared themselves by hovering their hands above the steering wheel, as shown in (c). Finally, when the perceived risk is high enough to trigger an action from the driver, a take-over action could be seen, as shown in (d).

could be represented as a phantom barrier with a very high cost, which disappears when the light turns green. The third main limitation of this conclusion is that, in chapter 4, we could directly validate the *risk estimate* only in static scenarios (road geometry, parked car, etc.). Despite the fact that there is evidence (in chapter 3) that the trends in human behaviour match that of the driver model based on the *risk estimate*, a direct validation of the *risk estimate* in dynamic scenarios will provide valuable insights.

Apart from the above mentioned limitations, there were a few points related to this conclusion that were not tested in this thesis but could be interesting follow-up research questions. First, we did not test one of the main advantages of a unified metric, i.e. that it can estimate the ‘total risk’ when multiple scenarios occur at once. It could be an interesting experiment to test if the perceived risk of the driver correlates to the *risk estimate* when multiple scenarios (e.g., overtaking a parked car with an oncoming vehicle) occur simultaneously. Second, in chapter 4 a binary scale (*risky* or *not risky*) was used to segregate the comments and actions of the drivers. However, the video footage revealed interesting subtleties in the driver’s posture and arm movement. These could act as predictors for driver’s perceived risk. For example, the driver would occasionally hover their arms (Fig. 5.3 [c]) over the steering wheel in preparation of a take-over (Fig. 5.3 [d]). In chapter 4, we did not analyse these subtle cues because the safety regulations of the test track mandated that the participants always keep their hands near the steering wheel (Fig. 5.3 [b]). However, in naturalistic driving we can expect the drivers to relax their arms and rest them on their lap (Fig. 5.3 [a]), and then hover their hands over the steering wheel in preparation of a take-over. Such bio-mechanical readiness can give us vital information regarding the risk perceived by the driver [140]. Despite these limitations, the *risk estimate* could effectively predict the risk perceived by the driver.

5.2.3. CONCLUSION 3: HUMAN-LIKE DRIVING BEHAVIOUR EMERGES WHEN THE CONSEQUENCE OF SENSORIMOTOR NOISE IS MAINTAINED BELOW A THRESHOLD LEVEL

In sensorimotor control, it was proposed that humans try to manage the *consequence of the noise*. This principle was borrowed and applied to the field of driving. The *risk estimate* proposed in this thesis is the driving equivalent of the *consequence of noise* idea in sensorimotor control. It was hypothesised that when the *risk estimate* is used as a cost function in a driver model, that tries to maintain the *risk estimate* below a threshold level, human-like behaviour emerges in a multitude of scenarios.

EVIDENCE

The evidence for this conclusion can be found in the predictions made by the driver model in chapter 3. In seven (four road and three traffic) different scenarios, the trends in speed and lateral position adaptations matched the trends exhibited by the driver model that tried to maintain the *risk estimate* below a threshold level

(Fig. 5.4). The model could generalise its behaviour to previously seen scenarios (e.g., parameter estimation performed on a curve with radius 200 m) but with different geometric values (e.g., could generalise to driving on curves with radii 100, 300, 400 m). More importantly, the model could generalise to an unknown scenario - negotiating oncoming traffic. This scenario was not present in the parameter estimation data set, yet the model slowed down and steered away from the oncoming cars, similar to what a human would do.

In chapter 4, evidence for the presence of a risk threshold can be found. In Fig. 4.6 it can be seen that at lower values of the *risk estimate* the driver's made very few *risky comments* and performed very few take-overs. However, as the *risk estimate* increased, drivers complained and took over the control of the vehicle. The sigmoid shape of the plot in Fig. 4.7 provides evidence for the presence of a risk threshold, beyond which drivers feel the need to express or act upon the perceived risk.

SIGNIFICANCE

5

One of the important advantages of having a unified model that can predict driving behaviour in multiple scenarios is that, one does not need to stitch together several driver models that are each applicable to different scenarios. The advantage of not having to do this is clear, especially when trying to estimate the parameters of such a stitched model. The DRF based driver model could negotiate the entire track, which consisted of various scenarios, with the same set of parameters. This becomes important especially when we try to integrate higher level models of driver behaviour (mood, experience, familiarity of the road, etc.) with lower (control) level driver models. These higher level 'settings' are expected to affect the driver behaviour across scenarios. For example, if a driver is in a 'sporty' mood, he/she is likely to drive faster, cut the corners, overtake more aggressively across different scenarios. Hence, if one was to stitch together a collection of driver models, he/she would have to update their parameters separately while trying to ensure that there is no abrupt jump when the switch from one scenario to another occurs. On the contrary, if we have a unified model, we need to update only the parameters of one model and not worry about harmonising the behaviour across different models.

This unifying nature of the risk threshold based driver model has practical applications in the development of automated vehicles as well. Since the proposed DRF based driver model can generate human-like behaviour, it could act as a reference trajectory generator for the automated systems. Several researchers have shown that human's prefer technology that seems to have anthropomorphic characteristics [78]. More specifically, for automated driving trajectories, research has shown that humans prefer the trajectory they think was their own trajectory [7]. However, some research has claims opposing this idea of 'automated systems need to show human-like driving characteristics' [160]. However, it needs to be noted that this study was conducted for external road users who were watching the cars pass by them while they stood outside the lane boundaries. Essentially, apart from the zebra crossing part of the experiment, the participants did not have a lot to gain from knowing whether the car was driving in a human-like manner or not.

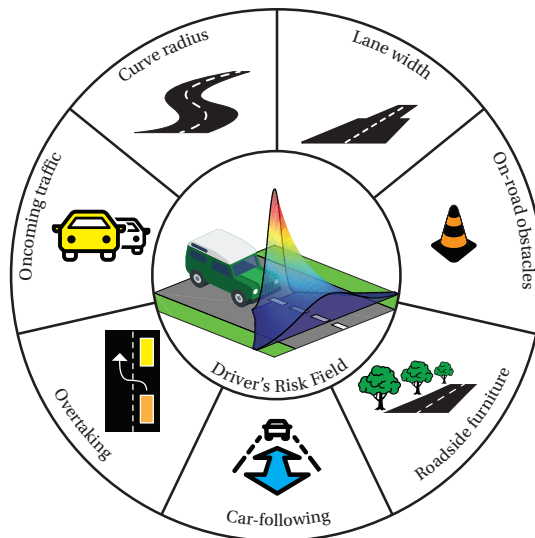


Figure 5.4: **A step towards a unified driver model:** The Driver's Risk Field (DRF) based driver model proposed in this thesis could predict human adaptations in speed and lateral position in seven different scenarios.

The second point is that, external road users observe a wide variety of driving styles. But that is not the case for a driver placed inside the vehicle. He/she is very much linked and affected by that particular vehicle's driving style. Hence, we think that automated vehicle systems need to exhibit human-like characteristics while driving (e.g., slowing down more for sharper curves, taking a larger gap towards a parked car, curve-cutting, etc.). It may not have to be completely personalised to every individual [161], but at the least, the automated vehicle systems need to behave like a non-fatigued, attentive human driver.

LIMITATIONS

One of the main limitations of this conclusion is that the validation was based on large qualitative 'trends' in speed and lateral position adaptations. The metrics that were used in calculating these trends were derived from the signals describing speed and lateral position of the driver model, in order to compare them to the metrics reported in literature. These metrics were neither used to statistically compare the difference between empirical data and the model, nor were the actual signals compared from which the metrics were determined. A follow-up study where the model's steering angle, speed and position trajectories are compared in different scenarios with human driving data, will provide valuable insights.

Note that such strengthened validation studies will not address a second major limitation of the driver model: that it is computationally inefficient, preventing the generation of vehicle control behaviour in real-time. If this model is to be used as a reference trajectory generator in automated systems, it has to be able to generate trajectories at least at real-time speed. Smarter ways to calculate the product of

the *probability* and *cost map* matrix can significantly improve the computational efficiency of the model.

Improving the computational efficiency of this model could have other benefits as well. For example, it could then be used predict the behaviour of surrounding human-driven vehicles, so that the automated ego vehicle has an estimation regarding the future paths of the agents in the scene. However, an important aspect of such a scene with multiple agents is the interaction amongst the agents. In its current form, the model cannot account for interactive and strategic level behaviour of humans. The interaction between two or more agents has been studied quite extensively [144][145] and is a field in itself. However, it could be interesting to explore the possibility of using the *risk estimate*, proposed in this thesis, as a feature/cost-function in these interaction models, especially the ones using game-theoretic approaches [162][163].

Despite the limitations mentioned above, the threshold-based driver model, formulated in chapter 3, managed to generate some interest amongst researchers from academia and industry. Discussions with these researchers revealed that there was some ambiguity regarding the physical interpretation of the different parameters used in the model. The origin of this confusion stems from the fact that decreasing the size of the DRF decreases the cost (*risk estimate*) incurred, which may seem similar to increasing the risk threshold, since the model only generates an action to mitigate the high risk when the risk threshold is exceeded. However, there is a subtle difference between decreasing the shape of the DRF and increasing the risk threshold. The difference is that the DRF is intended to capture the characteristics of a particular human, whereas increasing or decreasing the risk threshold enlarges or diminishes the impact of these characteristics on speed and position trajectories. For example, two individuals can have the same 'area' covered by the DRF but one could be a curve-cutter ($k_1 < k_2$) and another could be a curve-overshooter ($k_2 > k_1$) [164]. The model for both these individuals (with same risk threshold) will behave identically while following a car on a straight road, because the shape and size of the field will be identical for both parameter settings. However, the differences will arise during curve negotiation: the curve cutter will cut the curve and the curve-overshooter will take a trajectory is on the farther half of the lane. More importantly, increasing the risk threshold for both individuals will only exaggerate the curve-cutting and curve-overshooting behaviour, but it will not change the curve-overshooter into a curve-cutter, and vice-versa. Hence we recommend the following:

1. The parameters that define the shape of the DRF are different for different individuals. However, they are constant for an individual, irrespective of his/her mood, scenario, etc. Essentially, the DRF parameters capture the *inter-driver variability* (Fig. 5.5 [a]).
2. The risk threshold is used to modulate the behaviour of a particular driver in different 'moods'. For example, if a driver is in the mood for a relaxed drive, the risk threshold could be lowered. If the driver is in the mood for a sporty

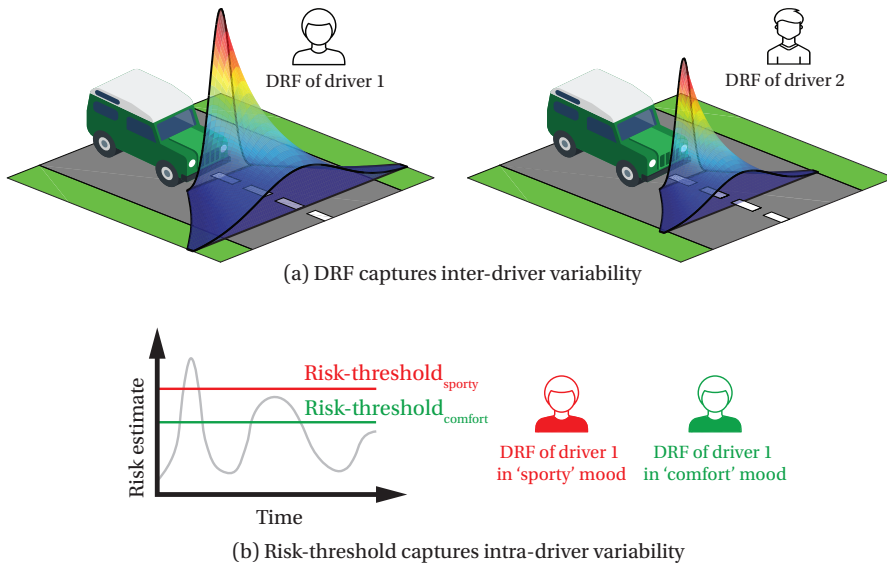


Figure 5.5: **Changing the DRF versus changing the risk threshold:** The DRF is a personalised field for each individual and captures the inter-driver variability. The risk threshold enlarges or diminishes the individual's driving characteristics defined by the DRF, for example according to the driver's mood. It captures the intra-driver variability.

drive, the risk threshold could be increased. Essentially, it captures the *intra-driver variability* (Fig. 5.5 [b]).

This clarity in the physical interpretation of the parameters can open up a few avenues of research. For example, initially the purpose of the experiment in chapter 4 was to answer the question *What type of autonomous driving trajectories do humans prefer?* A similar experiment was performed by Basu et al. [7] in a fixed base driving simulator. However, in our case, pre-programmed trajectories (e.g., a replay of participant's manual driving) could not be reproduced satisfactorily in the real vehicles. Hence, the analysis was performed on trajectories without attributing any labels (e.g., replay of manual trajectory) to them. One of the more interesting comparisons which were planned during this experiment was the trajectory generated by the DRF driver model and a 'safer DRF driver model'. The DRF driver model trajectories were generated by estimating the parameters for each driver, based on their manual driving trajectories. The 'safer DRF driver model' had a lower (90%) risk threshold as compared to the estimated parameter value. The hypothesis being that, since humans are not in control of the vehicle, they would prefer the vehicle to drive a little more safer than their driving style. However, a 'safer' trajectory can easily be implemented by merely reducing the speed of the manual trajectory. Hence, a follow-up comparison between: merely slowing down the manual trajectory, and the 'safer DRF driver model' was planned. The interesting part, in this comparison would have been the automated vehicle's trajectory near

the parked car. If the speed was merely reduced without any changes to the trajectory of the vehicle, it would drive around the parked car along the same path as in manual drive, but with a slower speed. The 'safer DRF driver model' would take a larger gap to the parked car (as compared to manual drive) and maybe slowed down, depending on the width of the lane. This distinction between merely slowing down the entire trajectory versus behavioural changes (e.g., larger gap) need to be investigated to test the need for driver model based modification of automated trajectories. Despite its limitations, this conclusion regarding human-like behaviour emerging from a risk threshold driver model can open up new avenues of research and practical solutions to defining how an automated vehicle should drive.

5.3. FUTURE WORK AND TAKE HOME MESSAGE

This thesis is just the beginning of the journey towards a unified driver model and the *risk estimate* proposed in this thesis is, to say the least, in its infancy. However, it points out the importance of looking towards and learning from other fields to gain inspiration and perspectives that can then be borrowed to solve our research questions. For example, Engström et al. [165] also took a similar approach of borrowing the *predictive processing* framework from neuroscience into the field of driving. The *predictive processing* theory essentially states that humans try to minimise the error between their own predictions about the sensory inputs they are going to receive, and the sensory inputs they actually receive. This theory especially becomes important in the current climate of automated systems where the drivers are becoming more and more detached from the act of driving and hence have lesser information to generate predictions. This can lead to a large mismatch between the expectations of a driver and the way the car drives and lead to surprise. The mathematical formulations of the DRE, the *risk estimate*, and the driver model have potential to grow and be a part of larger frameworks like the *predictive processing* framework. The *risk estimate* could act as a proxy for the level of risk generated by the behaviour of the vehicle as well as the risk expected by the driver. In the future, the model can be *upgraded* to incorporate interaction capabilities (with other agents), and can be used to explore new avenues of research that are not only practically relevant but also take us towards a quantitative unified model of human behaviour. However, for now, one thing we can be certain of is: we humans are aware of the consequence of noise in the sensorimotor system and account for it while driving, similar to while performing simple movements task.

A

APPENDIX FOR CHAPTER 2

A.1. SUPPLEMENTARY TABLE

Table A.1: **Parameters for the propagation of Gaussian width:** The table provides the values of the parameters a_9 , a_{10} , and a_{11} that define the shape of the left and right boundaries of the DRE. The values are provided for each participant (P1-P8), and according to the rules mentioned in Fig. 2.7, are used to classify the shapes into Types (1 to 4). The top and bottom blocks provide the values for the subjective and objective DRE, respectively. The results are shown in Fig. 2.11.

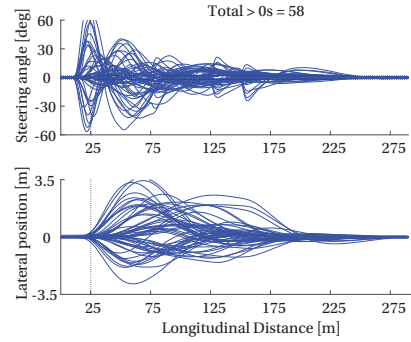
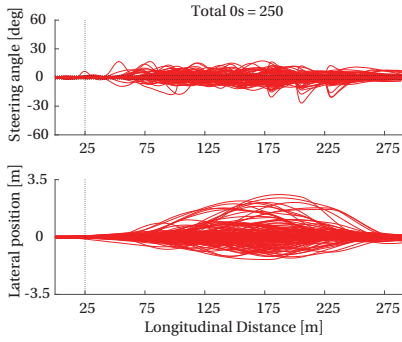
	Parameter	P1	P2	P3	P4	P5	P6	P7	P8
Subjective	$a_9 \times 10^{-4}$	1.9346	0.5172	1.075	3.1583	1.1236	0.6673	-0.1808	1.5271
	a_{10}	55.9150	83.9591	78.9046	88.8631	59.0451	71.8177	15.9020	95.7857
	a_{11}	0.9251	1.3207	1.5260	1.7744	1.1113	0.8433	1.3983	1.6816
Objective	$a_9 \times 10^{-4}$	0.3939	0.5058	1.2518	2.1292	0.1546	3.0247	1.1487	1.0856
	a_{10}	108.6883	90.4710	62.2331	102.6379	224.1546	78.3114	73.4117	103.8128
	a_{11}	0.9248	1.3974	1.3158	1.0962	0.7956	0.9746	1.1534	1.5344

A.1.1. STEERING ANGLE AND LATERAL DEVIATION TRAJECTORIES

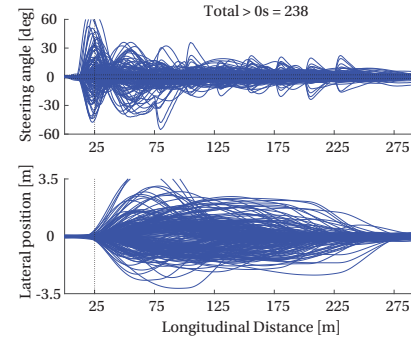
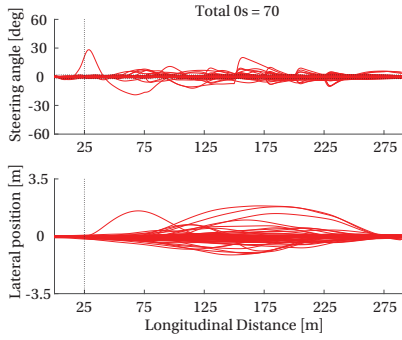
The following plots show the steering angle, and lateral deviation trajectories as a function of the longitudinal distance covered by the vehicle along the lane centre. The left plots (red) show all the trajectories that had a corresponding subjective measure of '0'. Hence indicating a 'no steering action' by the participant. The right plots (blue) show all the trajectories that had a corresponding subjective measure of > 0 , hence indicating a steering action by the participant. The horizontal black dotted lines indicate ± 2 degree in the steering angle plots. The vertical dotted line indicates the 25 m longitudinal distance mark.

A

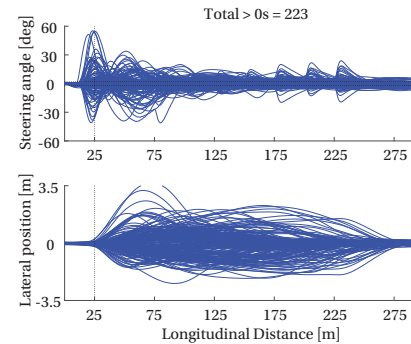
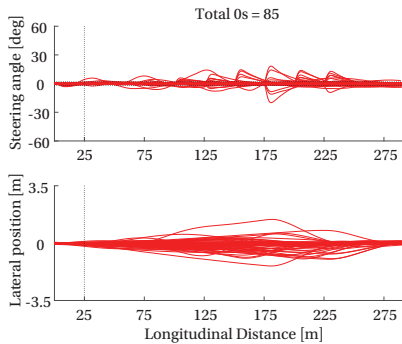
Participant 1



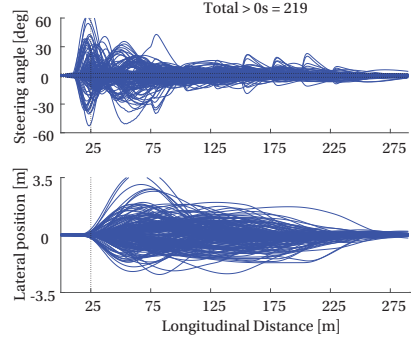
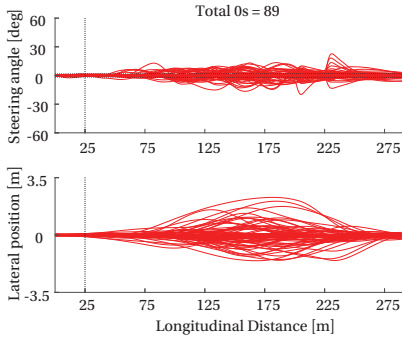
Participant 2



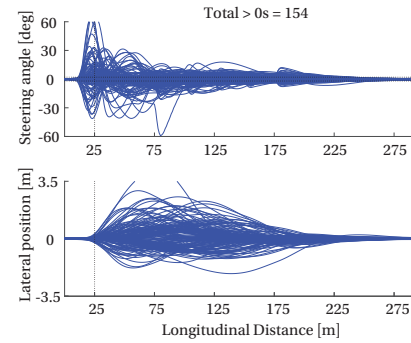
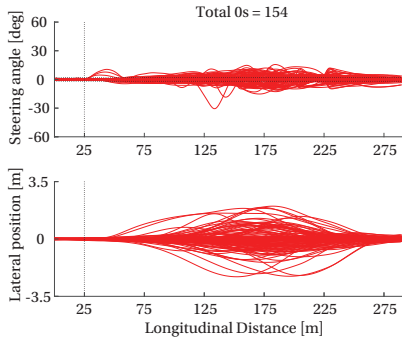
Participant 3



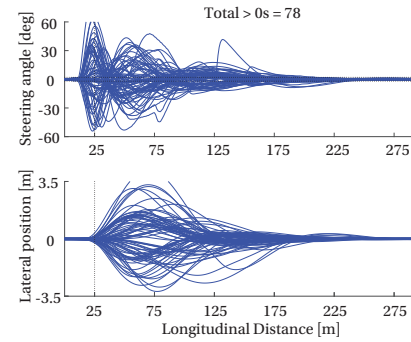
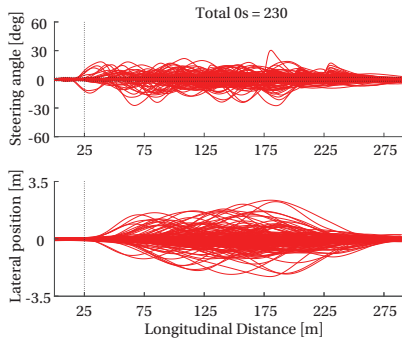
Participant 4



Participant 5



Participant 6



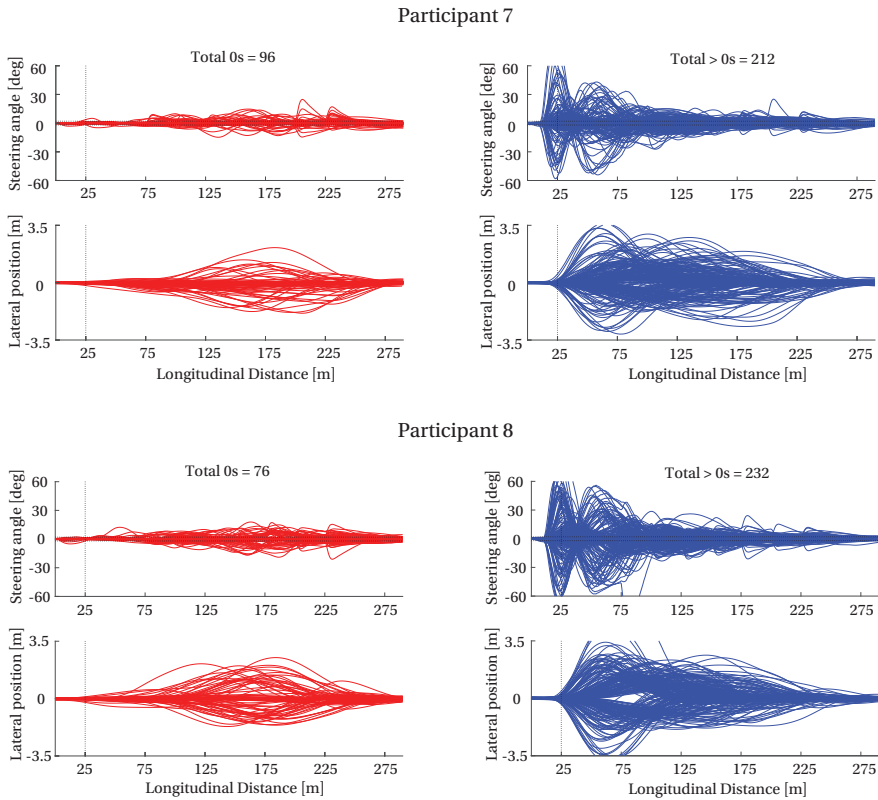


Figure A.1: **Steering angle and lateral deviation trajectories:** The plots show the steering angle, and lateral deviation trajectories as a function of the longitudinal distance covered by the vehicle along the lane centre.

A.2. DATA AVAILABILITY AND SUPPLEMENTARY MEDIA

DATA AVAILABILITY:

The data and the accompanying MATLAB code used to perform the analysis is available in the 4TU.Centre for Research Data with the identifiers: <http://doi.org/10.4121/uuid:921b56a0-7ae0-4d5e-a8a1-bda219a00048>

SUPPLEMENTARY MEDIA:

A video of the experiment is available at: <https://ars.els-cdn.com/content/image/1-s2.0-S0003687018307373-mmc3.mp4>. The video is also included in the data folder whose link is provided above.

A.2.1. GENERAL INFORMATION ABOUT THE DATA FOLDER

SET-UP OF THE FILES AND FOLDERS

1. Extract the files and folders from the compressed file in a folder of your choice.

2. The extracted data should contain the following folders
 - (a) `AnalysisCode`: Contains all the MATLAB code.
 - (b) `ExptSetup`: Contains the data regarding the experimental setup (`.mat` files).
 - (c) `Objective`: Contains the data recorded from driving the simulator for each participant
 - (d) `Subjective`: Contains the subjective answers provided by the participants
 - (e) `ParticipantDetails`: Contains the driving details of participants (anonymous)
3. In `AnalysisCode` folder should contain the following files
 - (a) `Results_figures_from_article.m`: This file you need to run to generate the results (plots) presented in chapter 2 (Fig. 2.8, 2.9, 2.10, 2.11, 2.12).
 - (b) `Data_extraction.m`: This file that will help you extract the separate trials (4 repetitions) corresponding to each of the 77 obstacles, of every participant (8 participants).
 - (c) All the other functions are ‘called’ from the above two files (3.(a) and 3.(b))

DATA EXTRACTION GUIDE: BASIC GUIDE

1. We have made a simple file so that you can extract all the data that you need of each trial of each subject (`Data_extraction.m`).
2. The `Plot_data_extraction.m` will help you plot the subjective and corresponding objective metrics in one figure for 3 signals (steering torque, steering angle, lateral position)
3. If you want to extract other signals (for e.g. yaw rate, heading angle etc.) please open `Objective_Analysis.m` file and refer to lines 66 to 72, 76 to 82, and 90 to 96, while not forgetting to ‘output’ the new signals on the first line in the function.
4. The driving simulator logs 69 signals at 100 Hz. Some of these signals may not be useful to the readers, but it is necessary to know the names and convention of the signals if you want to extract them (as mentioned in the step (3) above). A summary and sign conventions of the signals are provided in the document `DRF_DS_sign_conv.pdf`

DATA EXTRACTION GUIDE: ADVANCED GUIDE

1. If readers want to delve deeply into the data, we have provided all the raw `.mat` files for every participant in the `Subjective` and `Objective` folders.

2. Subjective data: `S1_subjective_answers.mat` contains the subjective answers of participant number 1.
3. Loading this file will provide a `S1ME` (Subject 1 Magnitude Estimation) matrix (26 x 12) matrix.
4. The 12 columns refer to the 12 sub-blocks of the experiment. The 26 rows correspond to the 26 obstacles that the participant encountered during each sub-block.
5. Since the obstacles popped at random, they are uniquely identified by their `ObsID` (Obstacle ID) . The order in which each obstacle appeared during a sub-block is provided in the `ExptSetup` folder in the `ObsID1to12.mat` file.
6. When you load `ObsID 1 to 12 .mat` it should generate the variables `ObsID 1`, `ObsID 2`,... `ObsID 12` in the MATLAB workspace. Each is a row vector of 26 elements. The numbers specify the Obstacle ID, hence specifying the order in which the obstacles popped up.
7. For example: `ObsID 1` contains the following numbers '32, 40, 22, 34,...'. It means that the 1st obstacle that popped up was with `ObsID 32`, the 2nd obstacle that popped up has `ObsID 40`, and so on.

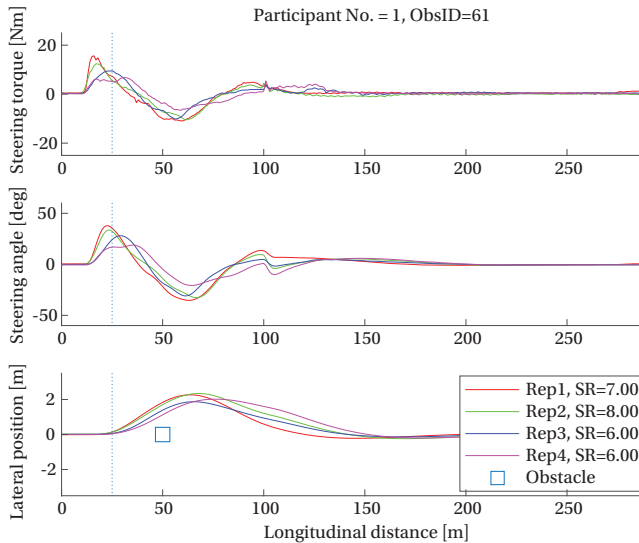


Figure A.2: **Data extraction guide:** The figure shows the 4 repetitions (Rep1 = 1st repetition) of objective data (signals of steering torque, steering angle, lateral position) when participant number 1 encountered the obstacle with ID (ObsID) = 61. The position and corresponding Obstacle IDs can be found in the 'Data_extraction.png' image file. SR = Subjective response provided by the participant for the corresponding trials. All the signals are plotted as a function of the Longitudinal Distance (x axis) covered by the vehicle along the lane centre (for further clarification check the end of this document).

8. The relation between ObsID and the position of the obstacle is provided in the `Data_extraction.png`.
9. Objective data: `S1data.mat` contains the subjective driving simulator data of participant number 1.
10. Loading this file load variables `S1B1log` (Subject 1 sub-block1), `S1B2log`,... `S1B12log` (Subject 1 sub-block12) in the MATLAB workspace.
11. Each of these log files contain 69 signals recorded at 100Hz, in addition to the initial conditions (`inco`) of the experiment. A summary and sign conventions of the signals are provided in the document `DRF_DS_sign_conv.pdf`
12. The `S1B1log.ObstacleNumber` signal will provide you information about which obstacle popped up, as a function of simulation time. Then using this information and the information from `ObsID1`, you can arrive at the obstacle position.
13. General advice would be to always plot/analyse the signals with respect to the longitudinal distance travelled by the car along the lane centre (as done in our analysis). For this you will need to use `S1B1log.nearest_rp_idx` signal. Please refer to the `Data_extraction.m` and `Plot_data_extraction.m` files, or for further help please contact Sarvesh Kolekar (s.b.kolekar@tudelft.nl / kolekar.sarvesh380@gmail.com).
14. Subjects performed the 12 sub-blocks in different orders. The following table details out the order in which each participant performed the sub-blocks.

Table A.2: **Sub-block order for each participant**

Sub-blocks --	1	2	3	4	5	6	7	8	9	10	11	12
P1	ObsID1	ObsID2	ObsID3	ObsID4	ObsID5	ObsID6	ObsID10	ObsID11	ObsID12	ObsID7	ObsID8	ObsID9
P2	ObsID4	ObsID5	ObsID6	ObsID7	ObsID8	ObsID9	ObsID1	ObsID2	ObsID3	ObsID10	ObsID11	ObsID12
P3	ObsID7	ObsID8	ObsID9	ObsID10	ObsID11	ObsID12	ObsID4	ObsID5	ObsID6	ObsID1	ObsID2	ObsID3
P4	ObsID10	ObsID11	ObsID12	ObsID1	ObsID2	ObsID3	ObsID7	ObsID8	ObsID9	ObsID4	ObsID5	ObsID6
P5	ObsID1	ObsID2	ObsID3	ObsID4	ObsID5	ObsID6	ObsID10	ObsID11	ObsID12	ObsID7	ObsID8	ObsID9
P6	ObsID4	ObsID5	ObsID6	ObsID7	ObsID8	ObsID9	ObsID1	ObsID2	ObsID3	ObsID10	ObsID11	ObsID12
P7	ObsID7	ObsID8	ObsID9	ObsID10	ObsID11	ObsID12	ObsID4	ObsID5	ObsID6	ObsID1	ObsID2	ObsID3
P8	ObsID10	ObsID11	ObsID12	ObsID1	ObsID2	ObsID3	ObsID7	ObsID8	ObsID9	ObsID4	ObsID5	ObsID6

B

APPENDIX FOR CHAPTER 3

B.1. SUPPLEMENTARY FIGURES

B.1.1. SHAPE OF THE DRF AND SATISFICING

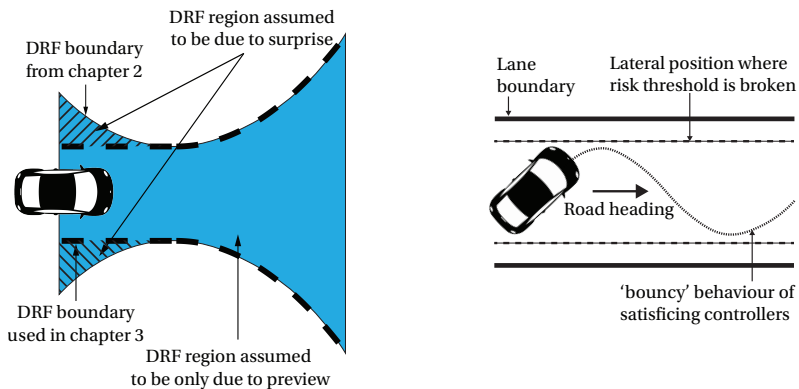


Figure B.1: **Shape of the DRF and satisficing:** (a) In chapter 2, it is reported that the hatched region was only 'active' when the obstacle appeared instantaneously, or approached from the rear of the vehicle. In this paper, the DRF model focuses on previewed objects and hence the hatched region is neglected. (b) 'Bouncing' behaviour exhibited by *satisficing* controllers since there is no correction until the risk threshold is crossed. The dashed line represents the lateral position at which the risk threshold is broken. That's when a correction (steering) is made.

B.1.2. METRICS USED TO COMPARE DRIVER MODEL TO LITERATURE

The following figures (Fig. B.2 - B.8) refer to the figures in chapter 3 (Fig. 3.9 - 3.15) and provide details regarding the calculations of the metrics.

The two figures below explain the calculations for the metrics used while comparing the **curve radius** and **lane width** scenarios with results from literature. For more details regarding the TTR metric shown in Fig. B.2, please refer to Xu et al. [26].

B

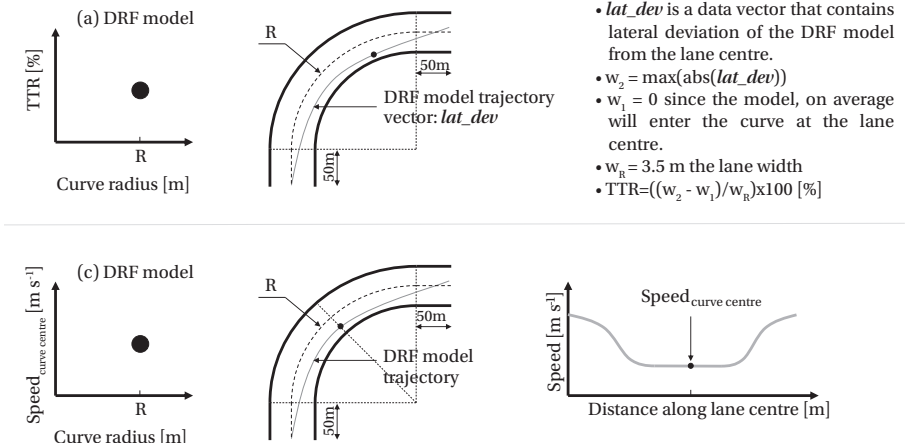


Figure B.2: **Road scenario - curve radius:** This figure explains the calculations of the metrics used in the subfigures (a) and (c) in Fig. 3.9 of the main text.

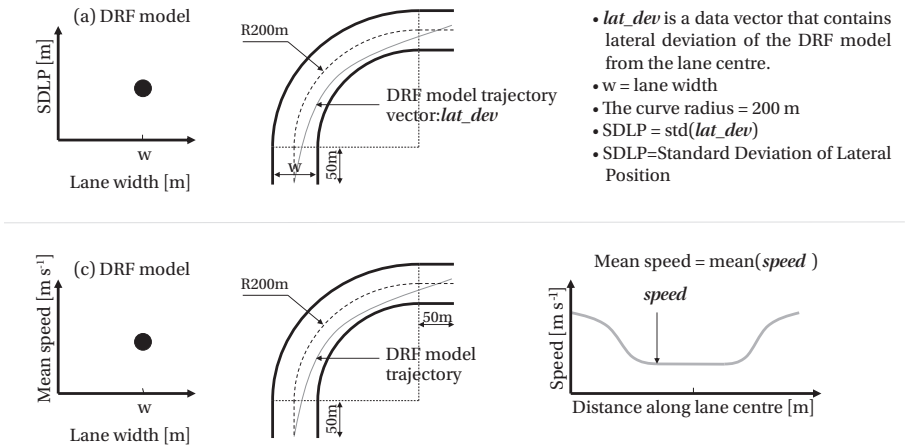


Figure B.3: **Road scenario - lane width:** This figure explains the calculations of the metrics used in the subfigures (a) and (c) in Fig. 3.10 of the main text.

The two figures below explain the calculations for the metrics used while comparing the road scenarios: **on-road obstacles** and **roadside furniture**, with results from literature. In Fig. B.5, we expect the trajectory in the *symmetric* case to be along the lane centre. However, the trajectory shown in the image is merely for illustration purposes.

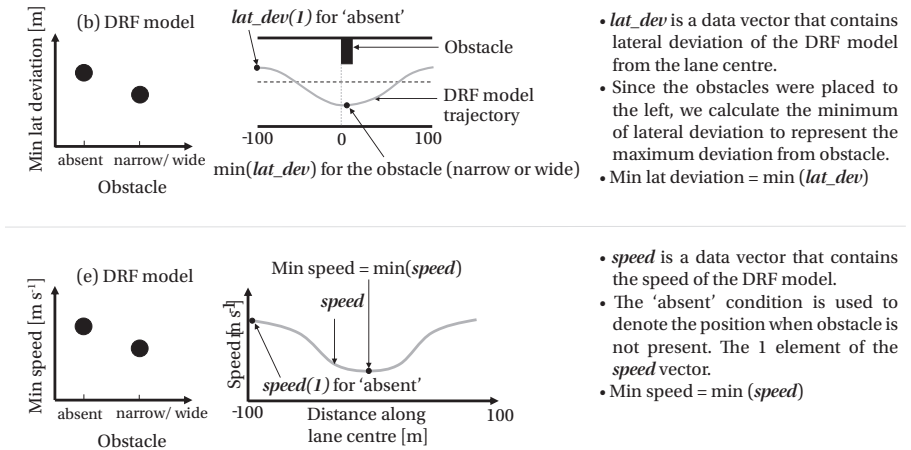


Figure B.4: **Road scenario - on-road obstacles:** This figure explains the calculations of the metrics used in the subfigures (b) and (e) in Fig. 3.11 of the main text.

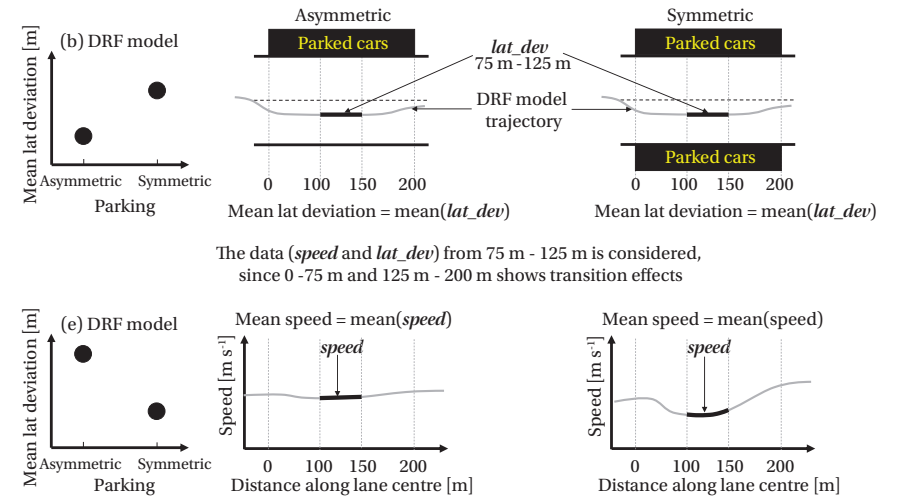


Figure B.5: **Road scenario - roadside furniture:** This figure explains the calculations of the metrics used in the subfigures (b) and (e) in Fig. 3.12 of the main text.

B

The two figures below explain the calculations for the metrics used while comparing the traffic scenarios: **car following** and **overtaking**, with results from literature. In Fig. B.7, the start (d_1) and end (d_2) of an overtaking manoeuvre is calculated using lateral velocities since we staged the overtaking manoeuvre of a straight road. Hence we assume that any lateral velocity $> 0.2 \text{ m s}^{-2}$ is due to the overtaking manoeuvre.

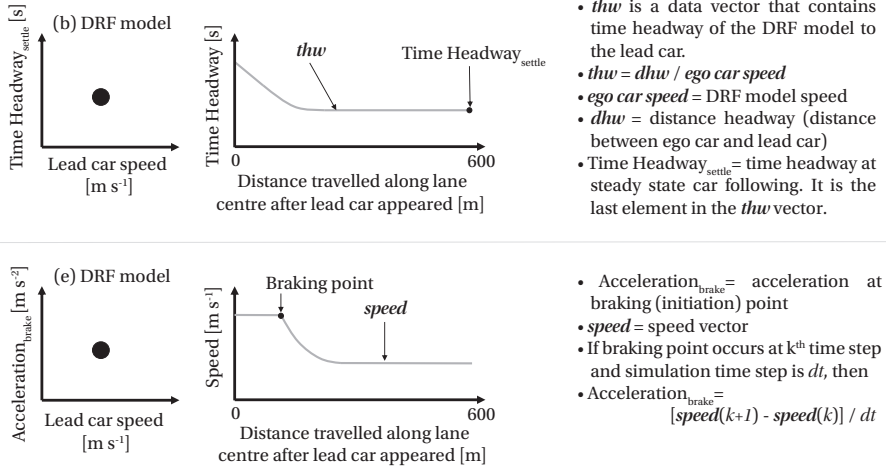


Figure B.6: **Traffic scenario - car following:** This figure explains the calculations of the metrics used in the subfigures (b) and (e) in Fig. 3.13 of the main text.

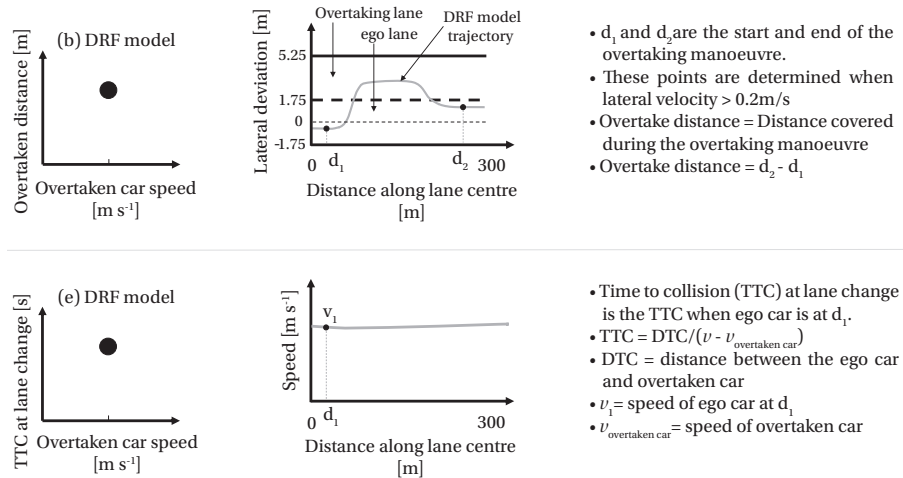


Figure B.7: **Traffic scenario - overtaking:** This figure explains the calculations of the metrics used in the subfigures (b) and (e) in Fig. 3.14 of the main text.

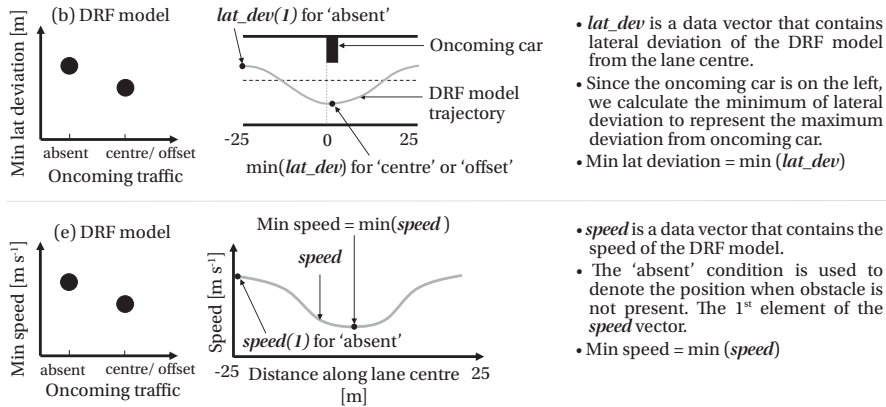


Figure B.8: **Traffic scenario - oncoming traffic:** This figure explains the calculations of the metrics used in the subfigures (b) and (e) in Fig. 3.15 of the main text.

B.2. SUPPLEMENTARY TABLES

In chapter 3, studies were selected based on the similarity of the conditions they tested, to those simulated for the DRF model. This meant that in some scenarios studies performed in a simulator were chosen ahead of an on-road study. The Tables B.1-B.8 provide a brief description of the experimental setup of the selected studies, and in scenarios where simulator based studies were used, at least one on-road study which supports the findings of the simulator based study (except for roadside furniture scenario, where a similar quantified on-road study was not found).

Table B.1: **Curve radius - metrics 1 and 2**

The effect of curve radii on curve cutting behaviour (metric 1) and speed (metric 2) was validated using the on-road study of Xu et al., 2018 [26] and Taragin & Leisch, 1954 [90], respectively.

Paper	Setup	Description	Conclusion
Xu et al. [26]	On-road	(N=4) Field driving experiments were performed on four two-lane mountain highways in China, and vehicle trajectories under natural driving conditions were acquired. The road lengths were 26.8 km, 45.2 km, 74.8 km, 121.9 km, and participants had to drive them on them twice. Cars used: Mitsubishi ASX, Buick Firstland GL8 Business, Mercedes Benz Vito Business.	Curve cutting reduced as the curve radius increased (Fig. 3.9 [b]).
Taragin & Leisch [90]	On-road	(N=8400) The study was conducted on two-lane highways mainly in Maryland, New York, South Carolina, Illinois, and Minnesota. 8400 free moving passenger cars were observed on 35 different curves.	Speed increases with curve radius, and reaches an asymptote approaching straight road speed for a large radius (Fig. 3.9 [d]).

Table B.2: Lane width - metric 1

The effect of lane width on standard deviation of lateral position (SDLP) was validated using the driving simulator based study of Godley et al., 2004 [94]. The simulator has a motion platform and has been validated for use in research. We also cite the on-road study of De Waard et al., 1995 [97] who found similar results that validate the DRF model's predictions. However, we used the simulator based study of Godley et al., 2004 [94] since the conditions they used (lane widths) were similar to those simulated for the DRF model.

Paper	Setup	Description	Conclusion
Godley et al. [94]	Simulator	(N=28) Experiment was conducted in the Monash University Accident Research Centre driving simulator, in Australia. This simulator has been validated for its use in examining road-based speeding countermeasures [166]. The driving simulator consisted of a Ford Falcon cabin. The simulator also contained a three-dimensional sound system reproducing tyre and engine noises, and a vertical motion platform providing road feel for accelerating, braking, cornering, and raised road objects.	Standard Deviation of Lateral Position (SDLP) which denotes the swerving behaviour of a car is reported to increase with lane width (Fig. 3.10 [b]).
De Waard et al. [97]	On-road	(N=28) The experiment was conducted on 12 km of woodland road and 10 km of moorland roads in the Netherlands. The test vehicle was a modified Volvo 245 station wagon.	"More important, the SD of the lateral position, which reflects swerving behaviour, is lower on the experimental (narrow sections" (Section 3.1 of De Waard et al. [97])

Table B.3: Lane width - metric 2

The effect of lane width on speed (metric 2) was validated using the driving simulator based study of Liu et al., 2016 [98]. The simulator has a motion platform and has been validated for use in research. We also cite the on-road study of Fitzpatrick et al., 2000 [100] who found similar results that validate the DRF model's predictions. However, we used the simulator based study of Liu et al., 2016 [98] since the conditions they used (lane widths) were similar to those simulated for the DRF model.

Paper	Setup	Description	Conclusion
Liu et al. [98]	Simulator	(N=24) The driving simulator of Tongji University - China is a motion-base simulator. A real car is placed in the middle of the experimental cabin as the test vehicle. This simulator has been validated in published literature([167][168]).	Speed increased with lane width (Fig. 3.10 [d]).
Fitzpatrick et al. [100]	On-road	(N=100) In this on-road study, the speed data was collected between April 1998 and June 1999 during daylight, off-peak periods, and under dry weather conditions. Speed profiles for approximately 100 free-flowing vehicles were taken at each site (several sites in Texas, USA). Vehicle type was identified by observation. The speed profiles were collected using laser guns positioned on the side of the roadway. Techniques used to hide the technicians from passing motorists include the truck blind and locating behind a tree or bushes were used.	Speed increased with lane width (Fig. 8-6 of Fitzpatrick et al.[100]).

Table B.4: **On-road obstacles - metric 1 and 2**

The effect of on-road obstacles (parked cars on the road) was validated using the simulator study of Edquist et al., 2012 [104]. Results similar to that predicted by the DRF model and Edquist et al. [104] in terms of speed adaptation are also found in the on-road study of Daisa Peers, 1997 [101]. We chose the simulator study of Edquist et al. [104] over Daisa Peers [101] because it examined both speed and lateral position effect of parked cars.

Paper	Setup	Description	Conclusion
Edquist et al. [104]	Simulator	(N=29) The experiment used an EF-X by Eca-Faros driving simulator with modified software for research purposes. Twenty-nine drivers (15 male) with an average number of years participants had been driving was 9.8 (SD = 8.0); all participants were regular drivers with at least one year of licensed driving experience.	The mean lateral position of the vehicles shifted away from the parked cars (Fig. 3.11 [c]). The mean speed reduced in the presence of parked cars (Fig. 3.11 [f]).
Ivan et al. [102]	On-road	(N=6900) Two sections of the same road about a mile apart in the same town (Rte. 77 in Guilford). The pavement widths are different, as one location has on-street parking but the other does not. However, the pavement width at the site without parking is about the same as the width of the travel lanes at the site with parking.	Speed decreased with increase in parking density (Fig. 6-3 of Ivan et al., [102]).

Table B.5: **Roadside furniture - metric 1 and 2**

The effect of roadside furniture was validated using the simulator study of Dunning et al., 2015 [106]. Results similar to that predicted by the DRF model and Dunning et al. [106], in terms of speed and lateral deviation adaptation are also found in another simulator study of Calvi, 2015 [105]. We chose the simulator study of Dunning et al. [106] over Calvi [105] because it examined both symmetric and asymmetric roadside furniture. Calvi [105] only examined asymmetric roadside furniture (Trees on one side and oncoming lane on the other).

Paper	Setup	Description	Conclusion
Dunning et al. [106]	Simulator	(N=12) In the experiment, subjects maintained one-dimensional "steering" control of a vehicle in a driving simulation. The goal of the game was to complete each trial as quickly as possible, where the speed of the car was determined solely by position on a two-lane road.	Lateral position of the participants shifted towards the less dangerous grass in the asymmetric case and remained in the centre in the symmetric case (Fig. 3.12 [c]). Participants, on average, drove slower in the symmetric case (Fig. 3.12 [f]).
Calvi [105]	Simulator	(N=44) The experiments were performed with the fixed-base CRISS driving simulator at Roma Tre University. The apparatus consisted of a real car with a force-feedback steering wheel, brake pedal, and accelerator. The system was widely validated in previous studies [169][170] and used for evaluating driving performance in terms of speed, acceleration, and trajectory under various driving conditions and road environments.	"When trees were closer, drivers saw the trees as a risk, slowed down, and moved further away from them." (Abstract and Table 2 of Calvi [105]).

As mentioned in chapter 3, only in the **roadside furniture** (Table B.5, above) scenario on-road quantitative studies which could be readily compared to the DRF model simulation scenario were not found. In all other scenarios at least one on-road study was reported. It is recommended that this scenario be tested in an on-road test, but the trends in speed and lateral position behaviour from these simulator studies can be assumed to be similar to on-road behaviour.

Table B.6: **Car following - metric 1 and 2**

The effect of car following on Time Headway (metric 1) was validated using the on-road study of He et al., 2002 [109]. The effect on acceleration at braking point (metric 2) was validated using the on-road study of Van der Horst, 2004 [111].

Paper	Setup	Description	Conclusion
He et al. [109]	On-road	(N=184,546) Data in both constrained and free flow traffic were collected. By using a set of traffic flow measuring apparatus based on switch sensors, more than 196,000 field data, with flow varying from 50 to 1900 veh/h/lane, had been collected at JingShi, Jinghua and Guang Fuo highway, located at Beijing and Guangdong province, China. After data validation process, 184,546 pairs data of vehicle pairs can be used in the study, only 5.87% of data was eliminated.	The preferred time headway under steady-state car following (THW_{pref}) is almost constant and independent of the lead car speed (Fig. 3.13 [c]).
Van der Horst [111]	On-road	(N=12) The experiment was conducted on a former runway 540 m long and 60 m wide in Vancouver, Canada. Participants drove an instrumented car which approached a Styrofoam model of a car. The instrumented car used in the experiment was a front wheel drive Dodge Mini Ram.	Braking intensity (deceleration at the onset of braking) increased as the approach-speed increased (Fig. 3.13 [f]).

Table B.7: **Overtaking - metric 1 and 2**

The effect of overtaking on overtake distance (metric 1) was validated using the on-road study of Crawford, 1963 [112]. The effect on time to collision (TTC) at lane change (metric 2) was validated using the on-road study of Chen et al., 2015 [113].

Paper	Setup	Description	Conclusion
Crawford [112]	On-road	(N=8) The experiment was carried out on a straight two-lane road 22 ft wide laid out along the edge of an airfield runway 2000 yd long. Participants drove a 2.25 litre (engine displacement) saloon car.	Overtake distance increased with the speed of the overtaken car (Fig. 3.14 [c]).
Chen et al. [113]	On-road	(N=45) The 100-Car study was a landmark large-scale naturalistic driving study (NDS) conducted by the Virginia Tech Transportation Institute-USA from 2001 to 2004. A total of 46,250 trips from 45 drivers were used in this study. A total of 326,238 lane changes were found in the 46,250 trips. The distribution of left side and right side lane changes was essentially even.	TTC at (start of) lane change increased with the speed of the overtaken car (Fig. 3.14 [f]).

Table B.8: **Oncoming traffic - metric 1 and 2**

The effect of oncoming traffic on lateral deviation away from the oncoming traffic (metric 1) and speed (metric 2) was validated using the on-road study of Räsänen., 2005 [117].

Paper	Setup	Description	Conclusion
Räsänen. [117]	On-road	(N=6599) This study was conducted along a curve on a two-lane road section of main road 4 in Finland where the barrier line was worn out due to encroachment by cars. The length of the left turning curve was 467 m, radius of curvature 990 m and speed limit 100 km h ⁻¹ .	Lateral position of ego car moves away from the oncoming traffic (Fig. 3.15 [c]). No significant difference in the speed between the oncoming traffic 'absent' and 'present' conditions (Fig. 3.15 [f]).

As it can be seen, 6 out of the 7 scenarios have results from on-road/test-track based studies from published literature that support the predictions of the DRF model. Also, the simulator based studies used for validation are mostly performed in previously validated high-fidelity simulators. Hence we think that the results found in these studies are valid indications of on-road human driving behaviour.

B.3. SUPPLEMENTARY NOTES

These notes explain which figures/ data, from the corresponding literature, were used and the unit conversions (for example, km h⁻¹ to m s⁻¹) that we performed.

B.3.1. ROAD SCENARIOS

- **Note 1 - Main text Fig. 3.9 [b]. Xu et al. (2018) [26]:** This figure is adopted from Fig. 10 on page 13.
- **Note 2 - Main text Fig. 3.9 [d]. Taragin & Leisch (1954) [90]:** This figure is created from the data of Taragin & Leisch (1954) [90] and adopted from Fig. 9 of McLean (1974) [93]. That figure contains data points from Taragin & Leisch (1954) [90] and the Department of Main Roads-NSW, (1969) [171]. We only plot the data points from Taragin & Leisch (1954) [90].
- **Note 3 - Main text Fig. 3.10 [b]. Godley et al. (2004) [94]:** This figure is adopted from Fig. 5. We arranged the lane widths in the ascending order, while in the original figure it is in the descending order.
- **Note 4 - Main text Fig. 3.9 [d]. Liu et al. (2016) [98]:** This figure shows the data from Table. 2 [98]. We only show speed for 0.5 m shoulder width right lane.
- **Note 5 - Main text Fig. 3.11 [c]. Edquist et al. (2012) [104]:** This figure is adopted from Fig. 4 of the corresponding paper [104]. We reversed the direction of the Y axis since in the original plot negative values of lateral deviation from lane centre indicate to the left of the lane centre. In the DRF model's convention (which is maintained consistent throughout the paper). We plot

only the ‘No lead vehicle’ case, since that’s the most relevant to our discussion.

- **Note 6 - Main text Fig. 3.11 [f]. Edquist et al. (2012) [104]:** This figure is adopted from Fig. 2 of the corresponding paper. We only plot the ‘Mean speed’ condition for empty and full parking, since that’s the most relevant for our discussion.
- **Note 7 - Main text Fig. 3.12 [c]. Dunning et al. (2015) [106]:** This figure was adopted from Fig. 3 of the corresponding paper [106]. Out of the 13 lateral position distribution figures we only show 2 plots. The plots for ‘Standard Deviation of Motor Noise = 8’ for ‘Symmetric-High cost’ and ‘Asymmetric case’.
- **Note 8 - Main text Fig. 3.12 [f]. Dunning et al. (2015) [106]:** This figure was adopted from Fig. 5 of the corresponding paper [106]. Out of the 13 box plots we only show 2 plots. The plots for ‘Standard Deviation of Simulated Motor Noise = 8’ for ‘Symmetric-High cost’ and ‘Asymmetric case’.

TRAFFIC SCENARIOS

- **Note 9 - Main text Fig. 3.13 [c]. He et al. (2002) [109]:** This figure is adopted from Fig. 3 [109]. The X axis is plotted in m s^{-1} rather than km h^{-1} .
- **Note 10 - Main text Fig. 3.13 [f]. Van der Horst (2004) [111]:** This figure is adopted from Fig. 3 (the bottom subplot). Only plot the ‘no occlusion’ case is plotted, since the DRF model did not simulate any occluded conditions.
- **Note 11 - Main text Fig. 3.14 [c]. Crawford (2007) [112]:** This figure is adopted from Fig. 5 [112]. Only the ‘Average overtaking distance’ condition is plotted, while the ‘Average of each driver’s best performance’ condition is omitted.
- **Note 12 - Main text Fig. 3.14 [f]. Chen et al. (2015) [113]:** This figure is adopted Fig. 3 [113]. All the points and the 50 percentile line are plotted. The 10 percentile line is not plotted.
- **Note 13 - Main text Fig. 3.15 [c]. Räsänen (2005) [117]:** This figure is plotted from Table 3 of the corresponding paper. The data of only the ‘Before’ condition (which refers to the road before lane dividing measures were taken) for passenger cars was plotted. The DRF model also did not simulate a lane divider. To convert the original data (say x) provided in the table into the same convention as used for DRF model (say y), the following steps were taken:
 1. Convert cm to m : $x_1 = x/100$
 2. Räsänen (2005) [117] measured the lateral distance from lane edge to left tyre. Hence an average vehicle width of 1.8 m : $x_2 = x_1 + 1.8/2$, was assumed.
 3. To state the distance from lane centre the (lane width)/2 was subtracted : $x_3 = x_2 - 3.4/2$ (Lane width they used was 3.4 m)

4. To make left of lane centre means positive lateral deviation values multiplied by -1 : $x_4 = -x_3$
 5. Data plotted in Results figure of DRF model : $y = x_4$
- **Note 14 - Main text Fig. 3.15 [f]. Räsänen (2005) [117]:** This figure is plotted from Table 3 of the corresponding paper [117]. The data of only the 'Before' condition (which refers to the road before lane dividing measures were taken) for passenger cars is plotted. The DRF model also did not simulate a lane divider. km h^{-1} was converted to m s^{-1} .

B.4. DATA AVAILABILITY AND SUPPLEMENTARY MEDIA

B.4.1. DATA AVAILABILITY:

The driving simulator experiment data, the simulation data that support the findings of this study, and the source data for Figs. 3.9 - 3.15 are available in the 4TU.Centre for Research Data with the identifier: <https://doi.org/10.4121/uuid:8132bccd-e900-4ba0-942e-c3114502bda2>.

B.4.2. CODE AVAILABILITY

The DRF Model MATLAB code that supports the findings of this study and a MATLAB GUI that helps explain the DRF are available in the 4TU.Centre for Research Data with the identifiers:

DRF model: <https://doi.org/10.4121/uuid:ec0f2742-e665-4af9-bf37-8fe1761a8a62>

DRF GUI: <https://doi.org/10.4121/uuid:1230ca50-4120-47b2-b6de-35d41c0a4d8a>.

B.4.3. SUPPLEMENTARY MEDIA:

Supplementary movie 1: This video shows the track and scenarios implemented in the fixed base driving simulator. https://static-content.springer.com/esm/art%3A10.1038%2Fs41467-020-18353-4/MediaObjects/41467_2020_18353_MOESM4_ESM.mp4.

Supplementary movie 2: This videos shows the simulation of the DRF model with 'normal' parameter settings. https://static-content.springer.com/esm/art%3A10.1038%2Fs41467-020-18353-4/MediaObjects/41467_2020_18353_MOESM5_ESM.mp4.

Supplementary movie 3: This videos shows the simulation of the DRF model with 'sport' parameter settings. https://static-content.springer.com/esm/art%3A10.1038%2Fs41467-020-18353-4/MediaObjects/41467_2020_18353_MOESM6_ESM.mp4.

C

APPENDIX FOR CHAPTER 4

C.1. DRIVER COMMENTS DURING AUTOMATED DRIVING

Below is a list of all the comments made by the eight participants during the automated driving condition. The comments were mostly made in Japanese which were then translated into English by an interpreter. This translation was done offline by watching the videos recorded during each lap. Only the red and blue coloured text are included in formulating Table 4.3 from chapter 4. We have added some grey text to these comments to clarify what the participant was trying to say. These grey parts of the text are not included in formulating Table 4.3.

C.1.1. RISKY COMMENTS

1. "When the car came close to the lane boundary (left curb), I feel a bit of risk, while approaching the curve. My driving line would be the same, but I felt different since the car is automated. Maybe it is because I am not used to it."
2. "I felt risk, so I over ride the steering. It comes very intensely and jumps suddenly. I feel the car drive into the edge stone very sharply."
3. "The car drove lot more left compared to the last trial."
4. "The car drove lot more left compared to the last trial."
5. "The car drove lot more left compared to the last trial."
6. "At the gas station, car went wide. It overshoot. And the come back from overshoot was not human-like."
7. "This right turn I would have made this very slowly (creep). It felt scary"
8. "It is slow. This is better than previous trials. But it will be better to be slow earlier"

9. "Distance to parked car was fine. But the steering just turned left and then I immediately felt the risk and felt to take over!"
10. "I felt risk and prepared to take over. It was too close to curb stone. I guess I do similar stuff in manual driving, but in autonomous driving the car is not under my control so I feel a bit risk. So if something happens, I immediately have to take over."
11. "This is not mine. The way it slows here, its not mine."
12. "The way to stop near the intersection is weird."
13. "At this point sometimes I feel the risk. It drives really slow, but I still could feel the risk"
14. "I am overriding. I feel it is aggressive. It accelerated when it turned. At this point too (feel risk and it accelerated when it turned)!"
15. "Too close to the left side."
16. "Ooooooohhhooohhoo! (Car hit the curb). I felt that it will not hit, but...."
17. "In the first curve it goes close to the side stone. I feel risk"
18. "When it goes close to curb I feel risk behind the building."
19. "Everyone (all trials) drove close to the curb stone in the corner"
20. "This time it drives very close to the curb stone"
21. "Parked car: The distance to parked car was close. The risk level was ummmm.. ok, but I felt it was close."
22. "It is close to the curb."
23. "Close to the curb here."
24. "It is too close (to the curb). I override a little bit."
25. "I feel little bit close to the car."
26. "Woh woh woh. This is too close! Its like tracing the curb!"
27. "Little bit close to the curb."
28. "Oh!!"
29. "Parked Car: This is too close."
30. "Very close to the curb."
31. "Parked car: It behaves as if there is no car parked there. It just goes straight."
32. "It is little bit close. But less close compared to previous trial."

33. "Parked car: It is close to the car. It drove as if there was nothing (no parked car)."
34. "Little bit close."
35. "Parked Car: Its little bit close."
36. "This one is too close."
37. "This one is close close close!"
38. "Wooooh! Too close!"
39. "So close!"
40. "Parked Car: This is close to the car."
41. "A little bit close. As usual (almost all the trials were close)."
42. "Parked Car: This is too close."
43. "Oh no! This is wrong! Here it is wrong!"
44. "Parked Car: Ah! this is not my trajectory. I am not going to do that close."
45. "It was a little bit left (close to the curb)."
46. "Oooh! Here I feel risk. Very close (to curb)."
47. "Here also too much left."
48. "Oh! It went too much left (Post trial comment: (right) (took the curve wide))."
49. "Parked Car: Oh! A little bit close."
50. "Parked Car: It is close."
51. "Parked Car: (Distance is) not so good."
52. "Parked Car: Hmm... too close"
53. "Oh no!"
54. "Too much left and too close."
55. "Too much left and too close"
56. "Oh.(My comment: Hands touching the steering wheel)"
57. "Too close and too fast."
58. "Parked Car: Too close."
59. "No deceleration."
60. "Parked Car: bad"

61. "In the first corner speed is fast. the car drove too left."
62. "The distance form the car is fine. But it comes back to the lane too early."
63. "The car went too much left."
64. "It was not scary but it was a bit too close to the left side."
65. "Parked car: The car drove too close to parked car."
66. "Oooooo.. That was scary! Very risky"
67. "It was left. If there was an oncoming car I might take that trajectory."
68. "Parked Car: Since at the steep corner, the car went too much outside, at the parking car, the distance is ok,but the angle at which it approaches the Parking car, it is not ok."
69. "Oooooo! It went straight (in) to the curb.In the first section the speed is little bit faster. On the first left corner, the car accelerated. He never did this. So he is surprised."
70. "I override. Since it hit the curb. Since it already hit the curb once, I overrode more earlier."
71. "I override. Since it already hit the curb once, I overrode more earlier."
72. "Too much left. Thinks a lot about oncoming car."
73. "Ooooo...."
74. "Ooo.. (Override). Dangerous point. It is little bit fast here."
75. "Parked car: Distance from Parking car, close."
76. "Decelration is not enough."
77. "It did not stop at intersection!"
78. "It was going very close to the curb, but I may do it as well."
79. "Oooooh!! (Car hit the curb)"
80. "Because it hit the curb (in Sector2), so now I am a bit scared"
81. "Ohohoh.. (My comment: Went too close to left boundary)"
82. "I would go closer to edge. (encroaching oncoming lane)"
83. "It is too close to the edge."
84. "It is too close to the edge."
85. "It is too close to the edge."

86. "It is making a very big circle."
87. "Parked Car: The car was pointing to wards the parked car, hence he corrected."
88. "Hmm.."
89. "(My comment: Says something, not clearly audible)"
90. "I slowed it down and steered. The car tends to rush. Car steered too early."
91. "Parked Car: This car tends to approach the parked car.The distance was still good, but after the sharp curve, the car went too wide, and to correct it, it came inside and that i did not like."
92. "The car follows the curb too much. It is too fast."
93. "Speed was slow, but car started steering too early. So it was a mismatch."
94. "Parked Car: Timing of steering was too late.I would steer to the right earlier."
95. "Car started steering too early and it was too close to the edge"
96. "Parked Car: Distance is close."
97. "Hmm..but ok.. maybe little bit near."
98. "(No comments: I accidentally did not record the video!)"
99. "Close"
100. "Parked Car: It is little near."
101. "Parked Car: It is little bit near."
102. "Waauiww! Wow! wow! I override!."
103. "Close!"
104. "Override again. It is too risky!"
105. "Woh woh woh (My comment: It took a big circle.)"
106. "Parked Car: It is near."
107. "No brake!"
108. "Very close."
109. "It is offset to the left. It is a bit faster than I drive."
110. "It was close to the left curb."
111. "It was little bit close."

112. "Should have slowed down earlier."
113. "Close to the left curb."
114. "That corner was close to the curb."
115. "This corner also close to the curb."
116. "Here also close to the curb."
117. "This goes too much to (road) centreline (wide turn)."
118. "Intersection: This corner is not well modulated. There is no deceleration control!"
119. "It goes to the left."
120. "In this corner, it is close to the curb."
121. "It is close to left curb and speed is high. This is very different from my drive. If I drive this close, I drive slower."
122. "Here it is close."
123. "Too much left."
124. "Different trajectory from my drive."
125. "Here also steering return timing is early. So it always goes to the right."
126. "Ooooo! (Car hits the left curb)"
127. "Parked Car: Close. He did not think it was avoiding the parked car. It just goes. It is like a robot."
128. "Here car was aggressive."
129. "Parked Car: This trajectory he felt like the car was not avoiding the parked car. It just went straight. Because there is no avoiding reaction near the parking car, he felt it is like a robot."
130. "Too fast and too aggressive."
131. "Scary!!"
132. "Parked Car: Scary!! (Distance too close)"
133. "Too close to left curb."
134. "Too close to the curb."
135. "Woh woh woh! (Too close to curb)"
136. "Ahh ahhh ahhh ooh! This is aggressive (Too close to curb)"

137. "AAAhhh aaahhh! (Hit the curb)"
138. "Why is this steering so harshly? Interviewer then explains that, since you corrected it went away from its reference trajectory and now it wants to come back to its reference trajectory."
139. "Ooo Oh! (Hit the curb)"
140. "Parked Car: Too close to the car."
141. "A bit close"
142. "Oh! A little bit close"
143. "Parked Car: This is scary."
144. "Intersection: It goes left before the right turn.It is robot like. Humans will not do this."
145. "Parked car: It is near."
146. "It was close to the left curb."
147. "Parked Car: That was close."
148. "Parked Car: Distance is close."

C.1.2. NON-RISKY COMMENTS

1. "That curve was ok."
2. "Probably the car drove close to the left side. But I could predict that the car would turn right. That is why I did not feel a lot of risk"
3. "Probably the car drove close to the left side. But I could predict that the car would turn right. That is why I did not feel a lot of risk"
4. "The distance to parked car was ok."
5. "The distance to parked car was more than last time. Larger space is safer. The risk level was still acceptable but it is better to have some margin."
6. "I did not feel any high risk. So it is good"
7. "I did not feel any high risk. So it is good"
8. "In the widening section it is close to my trajectory."
9. "In the widening section it is close to my trajectory."
10. "It is not my trajectory, but it is fine."
11. "The car also tried to avoid the parked car.That part I feel safe."
12. "Parked car: It is completely fine.It is close to my sense."

- C
13. "Parked car: It had enough clearance. And the way it passed by was also very smooth."
 14. "Ooooooh. It is good"
 15. "Parked car: It is completely fine. Maybe because I (have) drive a Leaf, I know (its dimensions) that this kind of clearance is completely fine."
 16. "That behaviour was very much like a human. Because the lateral movement. This person has that. I do not say it is bad, but there is lateral movement."
 17. "I like that it keeps distance from the curb. It feels more safe."
 18. "Here also it keeps distance. I like this one. It is same like my drive."
 19. "Parked Car: I like the distance from the car."
 20. "It is a little bit offset to the right (towards the road centre)."
 21. "This section is ok. A lot of distance from the curb."
 22. "Car speed is ok"
 23. "I like this trajectory here. Nice distance from the curb."
 24. "This is good. No problem. (My comment: But he overrides!)"
 25. "Keeps distance from the curb. Nice!"
 26. "I like this distance from the curb"
 27. "Hmm... nice! Oh I like this!"
 28. "Nice!"
 29. "Nice trajectory. But car speed is very slow."
 30. "This is nice."
 31. "This is nice. Very reliable drive."
 32. "Car speed is slow. Distance from the curb is nice. Reliable drive."
 33. "This section is nice. A little bit far from the curb. Needs to be a bit closer."
 34. "This is nice."
 35. "Hmmm.. nice! This is much safer. This is like robot! Overall this is robot!"
 36. "Oh! This supposed to be inside"
 37. "Parked Car: Oh! Yeah this is robot. You are robot now! Distance to parked car was completely fine."

38. "Very comfortable speed. I like this one."
39. "Hmmm, nice... This is like human"
40. "Hmm... ok."
41. "Parked Car: I like it."
42. "This distance is ok. It is comfortable for me."
43. "Nice distance."
44. "Speed is good. Distance from curb is also good."
45. "This drives very slow."
46. "Nice and safe."
47. "This is nice."
48. "It keeps the distance. This is like a robot! It is safer."
49. "Parked Car: This is robot. It keeps safe distance form the car."
50. "Oh I like this. Speed and trajectory."
51. "So far I like this. Speed and trajectory."
52. "This is my drive isn't it?."
53. "Parked Car: It is ok."
54. "It is ok."
55. "It is ok."
56. "Very peaceful."
57. "Parked Car: Distance is ok."
58. "Thats good."
59. "Thats good."
60. "Parked Car: Distance is very good."
61. "Thats ok."
62. "Thats very good."
63. "It is a little bit fast behind xx building."
64. "Parked Car: That is good."
65. "It slows down more. I get time to check around."

66. "Very slow. Trajectory is good."
67. "Hmm.. That was good. Speed is just a little bit fast"
68. "Not so much risk."
69. "Very slow!"
70. "No risk. But, I do not like (went wide)."
71. "That is good. Speed is also very nice."
72. "Parked Car: Its ok."
73. "Parked Car: Distance is very good."
74. "This deceleration timing is very good."
75. "It is ok."
76. "Hmm... here it is not good (too much right)."
77. "(No comment)"
78. "This behaviour is preferred."
79. "(No Comment)"
80. "Similar to my driving"
81. "It is slow. I would drive bit more to the left"
82. "I would drive more left. I want to follow the curb, but car goes outside (away from curb)."
83. "Parked Car: Its fine"
84. "I would steer more towards the left."
85. "The car is bit to the right. Similar to previous one."
86. "Here the car is going more right."
87. "Parked car: Distance is totally fine."
88. "It is good. It is more similar to mine (as compared to Lap 1 and 2)"
89. "It was smooth"
90. "Parked car: Distance is ok."
91. "The car is too far from my trajectory"
92. "Parked Car: Distance is ok."
93. "The car is too far from the curb (going towards road centre)"

94. "Parked Car: Distance to the parked car is a bit too wide."
95. "This part is similar to my driving."
96. "It is similar to me."
97. "Parked Car: Car did not approach the parked car.It was straight."
98. "The car should go a bit to left."
99. "Here its different from me. Car starts steering too late.Here it assumes as if the road is one way. It steers too widely,and goes into the oncoming lane"
100. "Here, timing of steering is good. But I would steer more."
101. "Here, timing of steering is good. But I would steer more.The car fully uses the width of the road."
102. "I would steer more. It did not follow the curve. (It went to road centre)."
103. "(My comment: Take over. It went to road centre,he wanted it to be more towards the left, nearer to the curb.)"
104. "This part was similar to what I do. It is not exactly like me, but I may do like this. (Steering correction)"
105. "This part is similar to me. (Steering correction)"
106. "Parked Car: Distance is ok."
107. "Braking before intersection was good."
108. "It is ok."
109. "It is ok."
110. "It is ok."
111. "Parked Car: Yes it (distance) is ok."
112. "Parked Car: Distance is ok."
113. "Parked Car: Distance is ok."
114. "Nice nice."
115. "Parked Car: Distance is nice."
116. "It went a little bit over to the right."
117. "Little bit too much steer."
118. "It is little over the centreline. It is not close to the curb but a bit more offset to the right. compared to his drive"

- C
119. "It is little over the centreline. It is not close to the curb but a bit more offset to the right. compared to his drive"
 120. "Parked car: Distance is good."
 121. "Timing of deceleration is good."
 122. "So far this is the best. Distance between car and curb is also good."
 123. "That corner was slightly different."
 124. "Parked Car: This is my drive."
 125. "Beginning of the corner is similar to my drive."
 126. "Parked Car: Distance to parked car is little narrow."
 127. "Here also goes to the left."
 128. "Last corner was bit towards the road centre."
 129. "Around this corner is good."
 130. "Speed and distance from curb is good."
 131. "This corner also good."
 132. "Parked Car: Slightly closer, but ok."
 133. "It is little bit slower than me."
 134. "Beginning of the corner is slightly different from me."
 135. "Distance from the curb is ok."
 136. "Car went towards the centre. But I might drive like this"
 137. "Parked Car: Distance is good."
 138. "Angle is towards the left."
 139. "Distance from the curb is good."
 140. "This goes inside (cuts the curve more)."
 141. "Parked Car: Distance is so-so."
 142. "This trajectory is similar to his drive."
 143. "Parked Car: Distance is narrow. Hmm..but acceptable."
 144. "It felt a bit odd. Deceleration timing little bit late"
 145. "Trajectory around this corner is good."
 146. "This curved section is very good."

147. "Little bit different from my drive."
148. "Goes to the right (road centre)."
149. "Parked Car: Little bit close. But it is acceptable."
150. "Distance from curb is good."
151. "Here it is good."
152. "Speed and distance from curb is good, so far."
153. "Little bit right side (towards road centre)."
154. "Parked Car: Distance is wider."
155. "Deceleration is quite good."
156. "Beginning of the corner is completely different from his drive."
157. "Distance from curb and speed is good."
158. "Distance from curb is more."
159. "It is keeping more distance from the curb on purpose."
160. "It went a little centre (road centre)"
161. "Parked Car: Distance is normal/average."
162. "Steering return timing is early."
163. "Parked Car: It was avoiding the car."
164. "Parked Car: This car avoided the parking car. So this is the best trajectory so far."
165. "It went to the left before the turn. I liked it."
166. "I like this speed."
167. "That corner was good."

C.2. SUPPLEMENTARY FIGURE

The predictions of the DRF model were compared to the steering and speed adaptations made by the drivers during manual driving in chapter 4. This figure below (Fig. C.1) is an expansion of Fig. 4.3 from the main text. Each row corresponds to a participant (P1 to P8). **Left column:** Compares the four different types of risk estimates. **Middle column:** Comparing steering risk potential ($\hat{p}_{\text{steering}}$) to the absolute steering angle ($|\delta|$). **Right column:** Comparing speed risk potential (\hat{p}_{speed}) to the speed reduction ($v_{\text{reduction}}$).

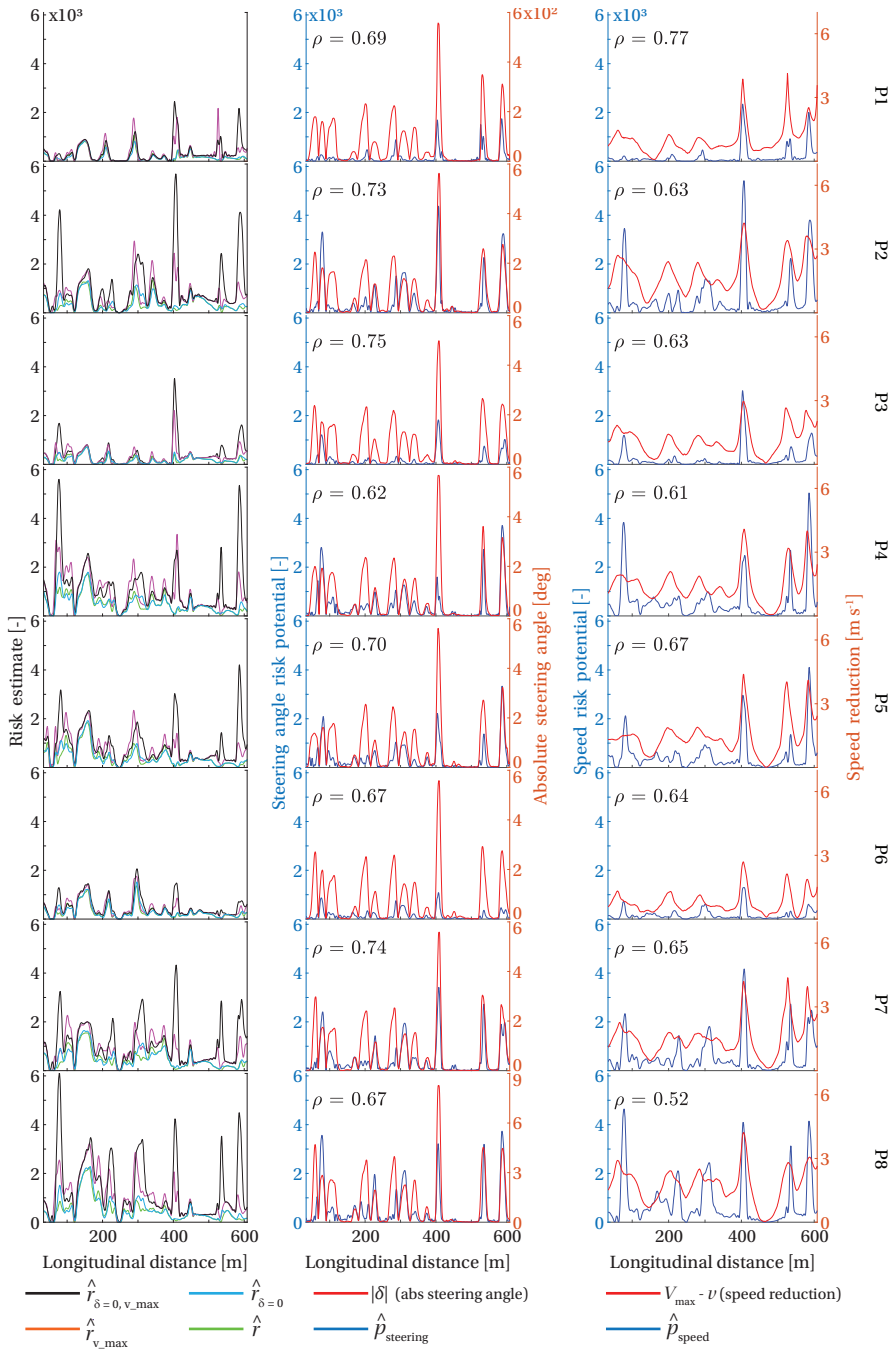


Figure C.1: **Manual driving predictions:** Each row corresponds to a participant (P1 - P8).

BIBLIOGRAPHY

- [1] J. J. Gibson and L. E. Crooks, “A theoretical field-analysis of automobile-driving”, *The American journal of psychology*, vol. 51, no. 3, pp. 453–471, 1938.
- [2] R. Näätänen and H. Summala, “Road-user behaviour and traffic accidents”, *Publication of: North-Holland Publishing Company*, 1976.
- [3] R. Fuller, “Motivational determinants of control in the driving task”, in *Modelling driver behaviour in automotive environments*, Springer, 2007, pp. 165–188.
- [4] G. J. Wilde, “The theory of risk homeostasis: Implications for safety and health”, *Risk analysis*, vol. 2, no. 4, pp. 209–225, 1982.
- [5] T. A. Ranney, “Models of driving behavior: A review of their evolution”, *Accident Analysis & Prevention*, vol. 26, no. 6, pp. 733–750, 1994.
- [6] N. Kalra and S. M. Paddock, “Driving to safety: How many miles of driving would it take to demonstrate autonomous vehicle reliability?”, *Transportation Research Part A: Policy and Practice*, vol. 94, pp. 182–193, 2016.
- [7] C. Basu, Q. Yang, D. Hungerman, M. Sinahal, and A. D. Draqan, “Do you want your autonomous car to drive like you?”, in *2017 12th ACM/IEEE International Conference on Human-Robot Interaction (HRI)*, IEEE, 2017, pp. 417–425.
- [8] P. Koopman and M. Wagner, “Autonomous vehicle safety: An interdisciplinary challenge”, *IEEE Intelligent Transportation Systems Magazine*, vol. 9, no. 1, pp. 90–96, 2017.
- [9] C. Rudin, “Stop explaining black box machine learning models for high stakes decisions and use interpretable models instead”, *Nature Machine Intelligence*, vol. 1, no. 5, pp. 206–215, 2019.
- [10] V. Papakostopoulos, N. Marmaras, and D. Nathanael, “The “field of safe travel” revisited: Interpreting driving behaviour performance through a holistic approach”, *Transport reviews*, vol. 37, no. 6, pp. 695–714, 2017.
- [11] G. G. Denton, “The influence of visual pattern on perceived speed”, *Perception*, vol. 9, no. 4, pp. 393–402, 1980.
- [12] V. Gruppelaar, R. Van Paassen, M. Mulder, and D. Abbink, “A perceptually inspired driver model for speed control in curves”, in *2018 IEEE International Conference on Systems, Man, and Cybernetics (SMC)*, IEEE, 2018, pp. 1257–1262.

- [13] D. N. Lee, "A theory of visual control of braking based on information about time-to-collision", *Perception*, vol. 5, no. 4, pp. 437–459, 1976.
- [14] T. Kondoh, T. Yamamura, S. Kitazaki, N. Kuge, and E. R. Boer, "Identification of visual cues and quantification of drivers' perception of proximity risk to the lead vehicle in car-following situations", *Journal of Mechanical Systems for Transportation and Logistics*, vol. 1, no. 2, pp. 170–180, 2008.
- [15] W. V. Winsum and A. Heino, "Choice of time-headway in car-following and the role of time-to-collision information in braking", *Ergonomics*, vol. 39, no. 4, pp. 579–592, 1996.
- [16] D. D. Salvucci and R. Gray, "A two-point visual control model of steering", *Perception*, vol. 33, no. 10, pp. 1233–1248, 2004.
- [17] R. Van Auken, J. Zellner, D. Chiang, J. Kelly, J. Silberling, R. Dai, P. Broen, A. Kirsch, and Y. Sugimoto, "Advanced crash avoidance technologies program—final report of the honda-dri team volume vi: Appendix r (part 1 of 2)", Tech. Rep., 2011.
- [18] B. D. Anderson, T. Brinsmead, D. Liberzon, and A. Stephen Morse, "Multiple model adaptive control with safe switching", *International journal of adaptive control and signal processing*, vol. 15, no. 5, pp. 445–470, 2001.
- [19] D. Liberzon and A. S. Morse, "Basic problems in stability and design of switched systems", *IEEE Control Systems Magazine*, vol. 19, no. 5, pp. 59–70, 1999.
- [20] H. Peng and M. Tomizuka, "Preview control for vehicle lateral guidance in highway automation", 1993.
- [21] M. A. Goodrich, W. C. Stirling, and E. R. Boer, "Satisficing revisited", *Minds and Machines*, vol. 10, no. 1, pp. 79–109, 2000.
- [22] G. S. Aoude, B. D. Luders, D. S. Levine, and J. P. How, "Threat-aware path planning in uncertain urban environments", in *2010 IEEE/RSJ International Conference on Intelligent Robots and Systems*, IEEE, 2010, pp. 6058–6063.
- [23] F. Von Hundelshausen, M. Himmelsbach, F. Hecker, A. Mueller, and H.-J. Wuensche, "Driving with tentacles: Integral structures for sensing and motion", *Journal of Field Robotics*, vol. 25, no. 9, pp. 640–673, 2008.
- [24] S. M. LaValle, J. J. Kuffner, B. Donald, *et al.*, "Rapidly-exploring random trees: Progress and prospects", *Algorithmic and computational robotics: new directions*, vol. 5, pp. 293–308, 2001.
- [25] S.-Y. Chung and H.-P. Huang, "Robot motion planning in dynamic uncertain environments", *Advanced Robotics*, vol. 25, no. 6-7, pp. 849–870, 2011.
- [26] J. Xu, X. Luo, and Y.-M. Shao, "Vehicle trajectory at curved sections of two-lane mountain roads: A field study under natural driving conditions", *European Transport Research Review*, vol. 10, no. 1, pp. 1–16, 2018.
- [27] E. Todorov, "Optimality principles in sensorimotor control", *Nature neuroscience*, vol. 7, no. 9, pp. 907–915, 2004.

- [28] T. Flash and N. Hogan, "The coordination of arm movements: An experimentally confirmed mathematical model", *Journal of neuroscience*, vol. 5, no. 7, pp. 1688–1703, 1985.
- [29] H. P. Clamann, "Statistical analysis of motor unit firing patterns in a human skeletal muscle", *Biophysical journal*, vol. 9, no. 10, pp. 1233–1251, 1969.
- [30] C. M. Harris and D. M. Wolpert, "Signal-dependent noise determines motor planning", *Nature*, vol. 394, no. 6695, pp. 780–784, 1998.
- [31] S. Kolekar, W. Mugge, and D. Abbink, "Modeling intradriver steering variability based on sensorimotor control theories", *IEEE Transactions on Human-Machine Systems*, vol. 48, no. 3, pp. 291–303, 2018.
- [32] J. Wang, J. Wu, and Y. Li, "The driving safety field based on driver–vehicle–road interactions", *IEEE Transactions on Intelligent Transportation Systems*, vol. 16, no. 4, pp. 2203–2214, 2015.
- [33] P. Koopman, B. Osyk, and J. Weast, "Autonomous vehicles meet the physical world: Rss, variability, uncertainty, and proving safety", in *International Conference on Computer Safety, Reliability, and Security*, Springer, 2019, pp. 245–253.
- [34] D. A. Abbink, *Delft haptics lab*, May 2015. [Online]. Available: <https://delfthapticslab.nl/programme/vidi-research/>.
- [35] B. Reimer, "Driver assistance systems and the transition to automated vehicles: A path to increase older adult safety and mobility?", *Public Policy & Aging Report*, vol. 24, no. 1, pp. 27–31, 2014.
- [36] P. G. Neumann, "Automated car woes—whoa there!", *Ubiquity*, vol. 2016, no. July, pp. 1–6, 2016.
- [37] S. Faltaous, M. Baumann, S. Schneegass, and L. L. Chuang, "Design guidelines for reliability communication in autonomous vehicles", in *Proceedings of the 10th international conference on automotive user interfaces and interactive vehicular applications*, 2018, pp. 258–267.
- [38] H. Muslim and M. Itoh, "A theoretical framework for designing human-centered automotive automation systems", *Cognition, Technology & Work*, vol. 21, no. 4, pp. 685–697, 2019.
- [39] D. Niu, J. Terken, and B. Eggen, "Anthropomorphizing information to enhance trust in autonomous vehicles", *Human Factors and Ergonomics in Manufacturing & Service Industries*, vol. 28, no. 6, pp. 352–359, 2018.
- [40] D. A. Abbink, M. Mulder, and E. R. Boer, "Haptic shared control: Smoothly shifting control authority?", *Cognition, Technology & Work*, vol. 14, no. 1, pp. 19–28, 2012.
- [41] N. Kauffmann, F. Winkler, F. Naujoks, and M. Vollrath, "What makes a cooperative driver?" identifying parameters of implicit and explicit forms of communication in a lane change scenario", *Transportation research part F: traffic psychology and behaviour*, vol. 58, pp. 1031–1042, 2018.

- [42] T. Melman, D. A. Abbink, M. M. Van Paassen, E. R. Boer, and J. C. De Winter, "What determines drivers' speed? a replication of three behavioural adaptation experiments in a single driving simulator study", *Ergonomics*, vol. 61, no. 7, pp. 966–987, 2018.
- [43] O. Lappi and C. Mole, "Visuomotor control, eye movements, and steering: A unified approach for incorporating feedback, feedforward, and internal models.", *Psychological bulletin*, vol. 144, no. 10, p. 981, 2018.
- [44] A. J. McKnight and B. B. Adams, "Driver education task analysis. volume ii: Task analysis methods. final report.", 1970.
- [45] H. Godthelp, P. Milgram, and G. J. Blaauw, "The development of a time-related measure to describe driving strategy", *Human factors*, vol. 26, no. 3, pp. 257–268, 1984.
- [46] H. Godthelp, "Vehicle control during curve driving", *Human Factors*, vol. 28, no. 2, pp. 211–221, 1986.
- [47] E. R. Boer, "Satisficing curve negotiation: Explaining drivers' situated lateral position variability", *IFAC-PapersOnLine*, vol. 49, no. 19, pp. 183–188, 2016.
- [48] Y. Rasekhipour, "Prioritized obstacle avoidance in motion planning of autonomous vehicles", 2017.
- [49] K. Smith and J.-E. Källhammer, "Experimental evidence for the field of safe travel", in *Proceedings of the Human Factors and Ergonomics Society Annual Meeting*, SAGE Publications Sage CA: Los Angeles, CA, vol. 56, 2012, pp. 2246–2250.
- [50] X. Hu, L. Chen, B. Tang, D. Cao, and H. He, "Dynamic path planning for autonomous driving on various roads with avoidance of static and moving obstacles", *Mechanical Systems and Signal Processing*, vol. 100, pp. 482–500, 2018.
- [51] E. E. Kadar and R. E. Shaw, "Toward an ecological field theory of perceptual control of locomotion", *Ecological psychology*, vol. 12, no. 2, pp. 141–180, 2000.
- [52] D. M. Wolpert and M. S. Landy, "Motor control is decision-making", *Current opinion in neurobiology*, vol. 22, no. 6, pp. 996–1003, 2012.
- [53] M. Land and J. Horwood, "Which parts of the road guide steering?", *Nature*, vol. 377, no. 6547, pp. 339–340, 1995.
- [54] N. E. Du Toit and J. W. Burdick, "Robot motion planning in dynamic, uncertain environments", *IEEE Transactions on Robotics*, vol. 28, no. 1, pp. 101–115, 2011.
- [55] R. S. Jurecki and T. L. Stańczyk, "Driver reaction time to lateral entering pedestrian in a simulated crash traffic situation", *Transportation research part F: traffic psychology and behaviour*, vol. 27, pp. 22–36, 2014.

- [56] B. Lewis-Evans, D. De Waard, and K. A. Brookhuis, "That's close enough—a threshold effect of time headway on the experience of risk, task difficulty, effort, and comfort", *Accident Analysis & Prevention*, vol. 42, no. 6, pp. 1926–1933, 2010.
- [57] S. S. Stevens, *Psychophysics: Introduction to its perceptual, neural and social prospects*. Routledge, 1975.
- [58] E. Johansson, J. Engström, C. Cherri, E. Nodari, A. Toffetti, R. Schindhelm, and C. Gelau, "Review of existing techniques and metrics for ivis and adas assessment", *Adaptive Integrated Driver Vehicle Interface (AIDE) Product number: IST-1-507674-IP*, 2004.
- [59] G. Markkula and J. Engström, "A steering wheel reversal rate metric for assessing effects of visual and cognitive secondary task load", in *Proceedings of the 13th ITS World Congress*, Leeds, 2006.
- [60] S. Petermeijer, P. Bazilinskyy, K. Bengler, and J. De Winter, "Take-over again: Investigating multimodal and directional tors to get the driver back into the loop", *Applied ergonomics*, vol. 62, pp. 204–215, 2017.
- [61] T. F. Coleman and Y. Li, "An interior trust region approach for nonlinear minimization subject to bounds", *SIAM Journal on optimization*, vol. 6, no. 2, pp. 418–445, 1996.
- [62] C. Gold, D. Damböck, L. Lorenz, and K. Bengler, "take over!" how long does it take to get the driver back into the loop?", in *Proceedings of the human factors and ergonomics society annual meeting*, Sage Publications Sage CA: Los Angeles, CA, vol. 57, 2013, pp. 1938–1942.
- [63] F. W. Siebert, M. Oehl, and H.-R. Pfister, "The influence of time headway on subjective driver states in adaptive cruise control", *Transportation research part F: traffic psychology and behaviour*, vol. 25, pp. 65–73, 2014.
- [64] R. Tscharn, F. Naujoks, and A. Neukum, "The perceived criticality of different time headways is depending on velocity", *Transportation Research Part F: Traffic Psychology and Behaviour*, vol. 58, pp. 1043–1052, 2018.
- [65] W. Van Winsum and H. Godthelp, "Speed choice and steering behavior in curve driving", *Human factors*, vol. 38, no. 3, pp. 434–441, 1996.
- [66] B. R. Fajen, W. H. Warren, S. Temizer, and L. P. Kaelbling, "A dynamical model of visually-guided steering, obstacle avoidance, and route selection", *International Journal of Computer Vision*, vol. 54, no. 1, pp. 13–34, 2003.
- [67] K. Chu, M. Lee, and M. Sunwoo, "Local path planning for off-road autonomous driving with avoidance of static obstacles", *IEEE Transactions on Intelligent Transportation Systems*, vol. 13, no. 4, pp. 1599–1616, 2012.
- [68] M. Werling, J. Ziegler, S. Kammel, and S. Thrun, "Optimal trajectory generation for dynamic street scenarios in a frenet frame", in *2010 IEEE International Conference on Robotics and Automation*, IEEE, 2010, pp. 987–993.

- [69] S. Kolekar, J. de Winter, and D. Abbink, "A human-like steering model: Sensitive to uncertainty in the environment", in *2017 IEEE International Conference on Systems, Man, and Cybernetics (SMC)*, IEEE, 2017, pp. 1487–1492.
- [70] C. Sentouh, P. Chevrel, F. Mars, and F. Claveau, "A sensorimotor driver model for steering control", in *2009 IEEE International Conference on Systems, Man and Cybernetics*, IEEE, 2009, pp. 2462–2467.
- [71] L. Saleh, P. Chevrel, F. Mars, J.-F. Lafay, and F. Claveau, "Human-like cybernetic driver model for lane keeping", *IFAC Proceedings Volumes*, vol. 44, no. 1, pp. 4368–4373, 2011.
- [72] O. Benderius and G. Markkula, "Evidence for a fundamental property of steering", in *Proceedings of the human factors and ergonomics society annual meeting*, SAGE Publications Sage CA: Los Angeles, CA, vol. 58, 2014, pp. 884–888.
- [73] S. Schnelle, J. Wang, H. Su, and R. Jagacinski, "A driver steering model with personalized desired path generation", *IEEE Transactions on Systems, Man, and Cybernetics: Systems*, vol. 47, no. 1, pp. 111–120, 2016.
- [74] B. Shi, L. Xu, J. Hu, Y. Tang, H. Jiang, W. Meng, and H. Liu, "Evaluating driving styles by normalizing driving behavior based on personalized driver modeling", *IEEE Transactions on Systems, Man, and Cybernetics: Systems*, vol. 45, no. 12, pp. 1502–1508, 2015.
- [75] S. Barendswaard, D. M. Pool, and D. A. Abbink, "A method to assess individualized driver models: Descriptiveness, identifiability and realism", *Transportation research part F: traffic psychology and behaviour*, vol. 61, pp. 16–29, 2019.
- [76] J. D. Lee and K. A. See, "Trust in automation: Designing for appropriate reliance", *Human Factors*, vol. 46, no. 1, pp. 50–80, 2004.
- [77] M. T. Dzindolet, S. A. Peterson, R. A. Pomranky, L. G. Pierce, and H. P. Beck, "The role of trust in automation reliance", *International journal of Human-Computer Studies*, vol. 58, no. 6, pp. 697–718, 2003.
- [78] A. Waytz, J. Heafner, and N. Epley, "The mind in the machine: Anthropomorphism increases trust in an autonomous vehicle", *Journal of Experimental Social Psychology*, vol. 52, pp. 113–117, 2014.
- [79] P. C. Cacciabue, *Modelling driver behaviour in automotive environments: critical issues in driver interactions with intelligent transport systems*. Springer, 2007.
- [80] G. Markkula, O. Benderius, K. Wolff, and M. Wahde, "A review of near-collision driver behavior models", *Human Factors*, vol. 54, no. 6, pp. 1117–1143, 2012.
- [81] C. J. Nash, D. J. Cole, and R. S. Bigler, "A review of human sensory dynamics for application to models of driver steering and speed control", *Biological Cybernetics*, vol. 110, no. 2-3, pp. 91–116, 2016.

- [82] R. Fuller, "Towards a general theory of driver behaviour", *Accident Analysis & Prevention*, vol. 37, no. 3, pp. 461–472, 2005.
- [83] J. A. Michon, "A critical view of driver behavior models: What do we know, what should we do?", in *Human behavior and traffic safety*, Springer, 1985, pp. 485–524.
- [84] H. H. Van der Molen and A. M. Bötticher, "A hierarchical risk model for traffic participants", *Ergonomics*, vol. 31, no. 4, pp. 537–555, 1988.
- [85] J. De Winter and R. Happee, "Modelling driver behaviour: A rationale for multivariate statistics", *Theoretical Issues in Ergonomics Science*, vol. 13, no. 5, pp. 528–545, 2012.
- [86] S. Kolekar, J. De Winter, and D. Abbink, "Which parts of the road guide obstacle avoidance? quantifying the driver's risk field", *Applied Ergonomics*, vol. 89, p. 103 196, 2020.
- [87] E. Felipe and F. Navin, "Automobiles on horizontal curves: Experiments and observations", *Transportation Research Record*, vol. 1628, no. 1, pp. 50–56, 1998.
- [88] V. Gawron and T. Ranney, "Curve negotiation performance in a driving simulator as a function of curve geometry", *Applied Ergonomics*, vol. 21, no. 1, pp. 33–38, 1990.
- [89] F. Bella, "Driver perception of roadside configurations on two-lane rural roads: Effects on speed and lateral placement", *Accident Analysis & Prevention*, vol. 50, pp. 251–262, 2013.
- [90] A. Taragin and L. Leisch, "Driver performance on horizontal curves", in *Highway Research Board Proceedings*, vol. 33, 1954.
- [91] G. Reymond, A. Kemeny, J. Droulez, and A. Berthoz, "Role of lateral acceleration in curve driving: Driver model and experiments on a real vehicle and a driving simulator", *Human Factors*, vol. 43, no. 3, pp. 483–495, 2001.
- [92] A. M. Odhams and D. J. Cole, "Models of driver speed choice in curves", in *Proceedings of the 7th International Symposium on Advanced Vehicle Control*, Citeseer, 2004.
- [93] J. McLean, "Driver behaviour on curves-a review", in *Australian Road Research Board (ARRB) Conference, 7th, 1974, Adelaide*, vol. 7, 1974.
- [94] S. T. Godley, T. J. Triggs, and B. N. Fildes, "Perceptual lane width, wide perceptual road centre markings and driving speeds", *Ergonomics*, vol. 47, no. 3, pp. 237–256, 2004.
- [95] P. Green, "Driver workload as a function of road geometry: A pilot experiment", Tech. Rep., 1994.
- [96] C. Dijksterhuis, K. A. Brookhuis, and D. De Waard, "Effects of steering demand on lane keeping behaviour, self-reports, and physiology. a simulator study", *Accident Analysis & Prevention*, vol. 43, no. 3, pp. 1074–1081, 2011.

- [97] D. D. Waard, M. Jessurun, F. J. Steyvers, P. T. Reggatt, and K. A. Brookhuis, "Effect of road layout and road environment on driving performance, drivers' physiology and road appreciation", *Ergonomics*, vol. 38, no. 7, pp. 1395–1407, 1995.
- [98] S. Liu, J. Wang, and T. Fu, "Effects of lane width, lane position and edge shoulder width on driving behavior in underground urban expressways: A driving simulator study", *International Journal of Environmental Research and Public Health*, vol. 13, no. 10, p. 1010, 2016.
- [99] B. Lewis-Evans and S. G. Charlton, "Explicit and implicit processes in behavioural adaptation to road width", *Accident Analysis & Prevention*, vol. 38, no. 3, pp. 610–617, 2006.
- [100] K. Fitzpatrick, P. J. Carlson, M. D. Wooldridge, and M. A. Brewer, "Design factors that affect driver speed on suburban arterials", Tech. Rep., 2000.
- [101] J. M. Daisa and J. Peers, "Narrow residential streets: Do they really slow down speeds?", in *Institute of Transportation Engineers 67th annual Meeting Institute of Transportation Engineers (ITE)*, 1997.
- [102] J. N. Ivan, N. W. Garrick, and G. Hanson, "Designing roads that guide drivers to choose safer speeds", Tech. Rep., 2009.
- [103] S. Biswas, S. Chandra, and I. Ghosh, "Effects of on-street parking in urban context: A critical review", *Transportation in Developing Economies*, vol. 3, no. 1, p. 10, 2017.
- [104] J. Edquist, C. M. Rudin-Brown, and M. G. Lenné, "The effects of on-street parking and road environment visual complexity on travel speed and reaction time", *Accident Analysis & Prevention*, vol. 45, pp. 759–765, 2012.
- [105] A. Calvi, "Does roadside vegetation affect driving performance?: Driving simulator study on the effects of trees on drivers' speed and lateral position", *Transportation Research Record*, vol. 2518, no. 1, pp. 1–8, 2015.
- [106] A. Dunning, A. Ghoreyshi, M. Bertucco, and T. D. Sanger, "The tuning of human motor response to risk in a dynamic environment task", *PloS one*, vol. 10, no. 4, e0125461, 2015.
- [107] H. Ota, "Distance headway behavior between vehicles from the viewpoint of proxemics", *IATSS Research*, vol. 18, no. 2, pp. 5–14, 1994.
- [108] A. Heino, H. H. Van der Molen, and G. J. Wilde, "Risk perception, risk taking, accident involvement and the need for stimulation", *Safety Science*, vol. 22, no. 1-3, pp. 35–48, 1996.
- [109] M. He, X. Liu, and J. Rong, "Driver's preferred time headway selection: Experimental findings", in *Traffic and Transportation Studies (2002)*, 2002, pp. 889–894.
- [110] L. Evans and P. Wasielewski, "Risky driving related to driver and vehicle characteristics", *Accident Analysis & Prevention*, vol. 15, no. 2, pp. 121–136, 1983.

- [111] R. Van der Horst, "Occlusion as a measure for visual workload: An overview of tno occlusion research in car driving", *Applied Ergonomics*, vol. 35, no. 3, pp. 189–196, 2004.
- [112] A. Crawford, "The overtaking driver", *Ergonomics*, vol. 6, no. 2, pp. 153–170, 1963.
- [113] R. Chen, K. D. Kusano, and H. C. Gabler, "Driver behavior during overtaking maneuvers from the 100-car naturalistic driving study", *Traffic Injury Prevention*, vol. 16, no. sup2, S176–S181, 2015.
- [114] S. Leung and G. Starmer, "Gap acceptance and risk-taking by young and mature drivers, both sober and alcohol-intoxicated, in a simulated driving task", *Accident Analysis & Prevention*, vol. 37, no. 6, pp. 1056–1065, 2005.
- [115] S. J. Levulis, P. R. DeLucia, and J. Jupe, "Effects of oncoming vehicle size on overtaking judgments", *Accident Analysis & Prevention*, vol. 82, pp. 163–170, 2015.
- [116] H. Farah, "Age and gender differences in overtaking maneuvers on two-lane rural highways", *Transportation Research Record*, vol. 2248, no. 1, pp. 30–36, 2011.
- [117] M. Räsänen, "Effects of a rumble strip barrier line on lane keeping in a curve", *Accident Analysis & Prevention*, vol. 37, no. 3, pp. 575–581, 2005.
- [118] F. Rosey, J.-M. Auberlet, O. Moisan, and G. Dupré, "Impact of narrower lane width: Comparison between fixed-base simulator and real data", *Transportation Research Record*, vol. 2138, no. 1, pp. 112–119, 2009.
- [119] P. Rossner and A. C. Bullinger, "Do you shift or not? influence of trajectory behaviour on perceived safety during automated driving on rural roads", in *International Conference on Human-Computer Interaction*, Springer, 2019, pp. 245–254.
- [120] S. M. LaValle and R. Sharma, "On motion planning in changing, partially predictable environments", *The International Journal of Robotics Research*, vol. 16, no. 6, pp. 775–805, 1997.
- [121] T. Melman, J. De Winter, and D. A. Abbink, "Does haptic steering guidance instigate speeding? a driving simulator study into causes and remedies", *Accident Analysis & Prevention*, vol. 98, pp. 372–387, 2017.
- [122] T. Zhang, D. Tao, X. Qu, X. Zhang, R. Lin, and W. Zhang, "The roles of initial trust and perceived risk in public's acceptance of automated vehicles", *Transportation research part C: emerging technologies*, vol. 98, pp. 207–220, 2019.
- [123] H. Azevedo-Sa, H. Zhao, C. Esterwood, X. J. Yang, D. M. Tilbury, and L. P. Robert Jr, "How internal and external risks affect the relationships between trust and driver behavior in automated driving systems", *Transportation research part C: emerging technologies*, vol. 123, p. 102973, 2021.

- [124] B. A. Jonah, "Sensation seeking and risky driving: A review and synthesis of the literature", *Accident Analysis & Prevention*, vol. 29, no. 5, pp. 651–665, 1997.
- [125] P. Ulleberg and T. Rundmo, "Personality, attitudes and risk perception as predictors of risky driving behaviour among young drivers", *Safety science*, vol. 41, no. 5, pp. 427–443, 2003.
- [126] E. R. Dahlen and R. P. White, "The big five factors, sensation seeking, and driving anger in the prediction of unsafe driving", *Personality and individual differences*, vol. 41, no. 5, pp. 903–915, 2006.
- [127] M. A. Machin and K. S. Sankey, "Relationships between young drivers' personality characteristics, risk perceptions, and driving behaviour", *Accident analysis & prevention*, vol. 40, no. 2, pp. 541–547, 2008.
- [128] H. Summala, "Towards understanding motivational and emotional factors in driver behaviour: Comfort through satisficing", in *Modelling driver behaviour in automotive environments*, Springer, 2007, pp. 189–207.
- [129] F. W. Siebert, M. Oehl, R. Höger, and H.-R. Pfister, "Discomfort in automated driving—the disco-scale", in *International Conference on Human-Computer Interaction*, Springer, 2013, pp. 337–341.
- [130] F. Hartwich, M. Beggiano, and J. F. Krems, "Driving comfort, enjoyment and acceptance of automated driving—effects of drivers' age and driving style familiarity", *Ergonomics*, vol. 61, no. 8, pp. 1017–1032, 2018.
- [131] E. R. Boer, "Tangent point oriented curve negotiation", in *Proceedings of Conference on Intelligent Vehicles*, IEEE, 1996, pp. 7–12.
- [132] L. Eboli, G. Mazzulla, and G. Pungillo, "Combining speed and acceleration to define car users' safe or unsafe driving behaviour", *Transportation research part C: emerging technologies*, vol. 68, pp. 113–125, 2016.
- [133] L. Eboli, G. Mazzulla, and G. Pungillo, "How to define the accident risk level of car drivers by combining objective and subjective measures of driving style", *Transportation research part F: traffic psychology and behaviour*, vol. 49, pp. 29–38, 2017.
- [134] Y. Rasekhipour, A. Khajepour, S.-K. Chen, and B. Litkouhi, "A potential field-based model predictive path-planning controller for autonomous road vehicles", *IEEE Transactions on Intelligent Transportation Systems*, vol. 18, no. 5, pp. 1255–1267, 2016.
- [135] F. A. Mullahkal-Babu, M. Wang, X. He, B. van Arem, and R. Happee, "Probabilistic field approach for motorway driving risk assessment", *Transportation research part C: emerging technologies*, vol. 118, p. 102716, 2020.
- [136] L. Li, J. Gan, Z. Yi, X. Qu, and B. Ran, "Risk perception and the warning strategy based on safety potential field theory", *Accident Analysis & Prevention*, vol. 148, p. 105805, 2020.

- [137] L. Guofa, Y. Yifan, Z. Tingru, Q. Xingda, C. Dongpu, C. Bo, and L. Keqiang, "Risk assessment based collision avoidance decision-making for autonomous vehicles in multi-scenarios", *Transportation research part C: emerging technologies*, vol. 122, p. 102 820, 2021.
- [138] J. Wang, J. Wu, X. Zheng, D. Ni, and K. Li, "Driving safety field theory modeling and its application in pre-collision warning system", *Transportation research part C: emerging technologies*, vol. 72, pp. 306–324, 2016.
- [139] F. Hajiseyedjavadi, E. Boer, R. Romano, E. Paschalidis, C. Wei, A. Solernou, D. Forster, and N. Merat, "Effect of environmental factors and individual differences on subjective evaluation of human-like and conventional automated vehicle controllers", 2021.
- [140] B. Zhang, Z. Lu, R. Happee, J. de Winter, and M. Martens, "Compliance with monitoring requests, biomechanical readiness, and take-over performance: Video analysis from a simulator study", in *13th ITS European Congress*, 2019.
- [141] W. van Winsum, K. A. Brookhuis, and D. de Waard, "A comparison of different ways to approximate time-to-line crossing (tlc) during car driving", *Accident Analysis & Prevention*, vol. 32, no. 1, pp. 47–56, 2000.
- [142] B. Lu, G. Li, H. Yu, H. Wang, J. Guo, D. Cao, and H. He, "Adaptive potential field-based path planning for complex autonomous driving scenarios", *IEEE Access*, vol. 8, pp. 225 294–225 305, 2020.
- [143] H. Huang, J. Wang, C. Fei, X. Zheng, Y. Yang, J. Liu, X. Wu, and Q. Xu, "A probabilistic risk assessment framework considering lane-changing behavior interaction", *Science China Information Sciences*, vol. 63, no. 9, pp. 1–15, 2020.
- [144] L. Sun, W. Zhan, M. Tomizuka, and A. D. Dragan, "Courteous autonomous cars", in *2018 IEEE/RSJ International Conference on Intelligent Robots and Systems (IROS)*, IEEE, 2018, pp. 663–670.
- [145] D. Sadigh, S. Sastry, S. A. Seshia, and A. D. Dragan, "Planning for autonomous cars that leverage effects on human actions.", in *Robotics: Science and Systems*, Ann Arbor, MI, USA, vol. 2, 2016.
- [146] G. Markkula, E. Boer, R. Romano, and N. Merat, "Sustained sensorimotor control as intermittent decisions about prediction errors: Computational framework and application to ground vehicle steering", *Biological cybernetics*, vol. 112, no. 3, pp. 181–207, 2018.
- [147] R. Van Der Horst and J. Hogema, "Time-to-collision and collision avoidance systems", in *Proceedings of the 6th ICTCT workshop: Safety evaluation of traffic systems: Traffic conflicts and other measures*, 1993, pp. 109–121.
- [148] H. M. Zwaan, S. M. Petermeijer, and D. A. Abbink, "Haptic shared steering control with an adaptive level of authority based on time-to-line crossing", *IFAC-PapersOnLine*, vol. 52, no. 19, pp. 49–54, 2019.

- [149] S. Oudshoorn, S. Kolekar, D. Abbink, and S. Petermeijer, "Design of time-to-lane-crossing based haptic steering guidance", in *Proceedings of the Human Factors and Ergonomics Society Europe Chapter 2018 Annual Conference*, Human Factors and Ergonomics Society, 2018.
- [150] L. Wang, H. Zhang, H. Meng, and X. Wang, "A model based on ttc to describe how drivers control their vehicles", *The European Physical Journal B*, vol. 66, no. 1, pp. 149–153, 2008.
- [151] A. W. Berning, A. Girard, I. Kolmanovsky, and S. N. D'Souza, "Rapid uncertainty propagation and chance-constrained path planning for small unmanned aerial vehicles", *Advanced Control for Applications: Engineering and Industrial Systems*, vol. 2, no. 1, e23, 2020.
- [152] P. Pretto, J.-P. Bresciani, G. Rainer, and H. H. Bühlhoff, "Foggy perception slows us down", *Elife*, vol. 1, e00031, 2012.
- [153] X. Yan, X. Li, Y. Liu, and J. Zhao, "Effects of foggy conditions on drivers' speed control behaviors at different risk levels", *Safety Science*, vol. 68, pp. 275–287, 2014.
- [154] H. Woo, Y. Ji, Y. Tamura, Y. Kuroda, T. Sugano, Y. Yamamoto, A. Yamashita, and H. Asama, "Dynamic state estimation of driving style based on driving risk feature", *International Journal of Automotive Engineering*, vol. 9, no. 1, pp. 31–38, 2018.
- [155] C. Wei, R. Romano, N. Merat, Y. Wang, C. Hu, H. Taghavifar, F. Hajiseyedjavadi, and E. R. Boer, "Risk-based autonomous vehicle motion control with considering human driver's behaviour", *Transportation research part C: emerging technologies*, vol. 107, pp. 1–14, 2019.
- [156] D. L. Kleinman, S. Baron, and W. Levison, "An optimal control model of human response part i: Theory and validation", *Automatica*, vol. 6, no. 3, pp. 357–369, 1970.
- [157] S. Baron, D. Kleinman, and W. Levison, "An optimal control model of human response part ii: Prediction of human performance in a complex task", *Automatica*, vol. 6, no. 3, pp. 371–383, 1970.
- [158] D. Jacobson, "Optimal stochastic linear systems with exponential performance criteria and their relation to deterministic differential games", *IEEE Transactions on Automatic control*, vol. 18, no. 2, pp. 124–131, 1973.
- [159] E. Todorov, "Stochastic optimal control and estimation methods adapted to the noise characteristics of the sensorimotor system", *Neural computation*, vol. 17, no. 5, pp. 1084–1108, 2005.
- [160] P. Bazilinskyy, T. Sakuma, and J. de Winter, "What driving style makes pedestrians think a passing vehicle is driving automatically?", *Applied Ergonomics*, vol. 95, p. 103 428, 2021.
- [161] S. Barendswaard, "Modelling individual driver trajectories to personalise haptic shared steering control in curves", Ph.D. dissertation, 2021.

- [162] X. Na and D. J. Cole, "Game-theoretic modeling of the steering interaction between a human driver and a vehicle collision avoidance controller", *IEEE Transactions on Human-Machine Systems*, vol. 45, no. 1, pp. 25–38, 2014.
- [163] J. F. Fisac, E. Bronstein, E. Stefansson, D. Sadigh, S. S. Sastry, and A. D. Dragan, "Hierarchical game-theoretic planning for autonomous vehicles", in *2019 International Conference on Robotics and Automation (ICRA)*, IEEE, 2019, pp. 9590–9596.
- [164] S. Barendswaard, D. M. Pool, E. R. Boer, and D. A. Abbink, "A classification method for driver trajectories during curve-negotiation", in *2019 IEEE International Conference on Systems, Man and Cybernetics (SMC)*, IEEE, 2019, pp. 3729–3734.
- [165] J. Engström, J. Bårgman, D. Nilsson, B. Seppelt, G. Markkula, G. B. Piccinini, and T. Victor, "Great expectations: A predictive processing account of automobile driving", *Theoretical issues in ergonomics science*, vol. 19, no. 2, pp. 156–194, 2018.
- [166] S. T. Godley, T. J. Triggs, and B. N. Fildes, "Driving simulator validation for speed research", *Accident analysis & prevention*, vol. 34, no. 5, pp. 589–600, 2002.
- [167] Y. Chen and S. Zheng, "Mechanism analysis of vehicles operating characteristic affected by visual environment of underground road", *Journal of Tongji University (Natural Science)*, no. 7, p. 13, 2013.
- [168] C. Changbin, W. Junhua, and L. Yangming, "Driving simulator validation for research on driving behavior at entrance of urban underground road", in *2015 International Conference on Transportation Information and Safety (ICTIS)*, IEEE, 2015, pp. 147–150.
- [169] F. Bella, "Validation of a driving simulator for work zone design", *Transportation Research Record*, vol. 1937, no. 1, pp. 136–144, 2005.
- [170] F. Bella, "Driving simulator for speed research on two-lane rural roads", *Accident Analysis & Prevention*, vol. 40, no. 3, pp. 1078–1087, 2008.
- [171] N. S. W. Department of Main Roads, "The behaviour of drivers on horizontal curves", *Main Roads*, vol. 34, no. 4, pp. 127–128, 1969.

CURRICULUM VITÆ

Sarvesh KOLEKAR

22-02-1991 Born in Alnavar - India.

EDUCATION

1996–2006 Primary and Secondary schooling
St. Joseph's Institute, Vasco-Da-Gama, Goa - India

2008–2012 B.Tech in Mechanical Engineering
National Institute of Technology Karnataka, Surathkal - India

2013–2016 MSc (cum-laude) in Mechanical Engineering
Delft University of Technology - The Netherlands

2016–2021 Ph.D. Driver behaviour modelling
Delft University of Technology - The Netherlands

AWARDS

2013–2016 GS-2013 grant of \$20000
Government of Goa - India

EXPERIENCES

2019 Visiting researcher
Nissan Advanced Technical Centre, Kanagawa - Japan

2014–2015 Visiting intern
University of Cambridge - England

2012–2013 Research Assistant
Indian Institute of Science, Bangalore - India

2010–2012 Formula Student engineer
NITK Racing - India (FSAE - Michigan 2011, FS Hungary 2012)

LIST OF PUBLICATIONS

JOURNAL PUBLICATIONS

1. **S. Kolekar**, S.M. Petermeijer, E.R. Boer, J.C.F. de Winter, and D. Abbink, *A risk field based metric correlates with driver's perceived risk in manual and automated driving: A test-track study*, [Transportation Research Part C: Emerging Technologies](#) **133** (2021), 103428
2. **S. Kolekar**, J.C.F. de Winter, and D. Abbink, *Human-like driving behaviour emerges from a risk-based driver model*, [Nature communications](#) **11.1** (2020), 1-13
3. **S. Kolekar**, J.C.F. de Winter, and D. Abbink, *Which parts of the road guide obstacle avoidance? Quantifying the driver's risk field*, [Applied ergonomics](#) **89** (2020), 103196
4. **S. Kolekar**, W. Mugge, and D. Abbink, *Modeling intradriver steering variability based on sensorimotor control theories*, [IEEE Transactions on Human-Machine Systems](#) **48.3** (2018), 291-303

PEER-REVIEWED CONFERENCE PAPERS

1. T. Melman, **S. Kolekar**, E. Hogerwerf, and D. Abbink, *How road narrowing impacts the trade-off between two adaptation strategies: reducing speed and increasing neuromuscular stiffness*, [2020 IEEE International Conference on Systems, Man, and Cybernetics \(SMC\) 2020 Oct 11](#) (pp. 3235-3240)
2. S. Oudshoorn, **S. Kolekar**, D. Abbink, and S.M. Petermeijer, *Design of time-to-lane-crossing based haptic steering guidance*, [Proceedings of the Human Factors and Ergonomics Society Europe Chapter, Annual Conference 2018](#)
3. **S. Kolekar**, J.C.F. de Winter, and D. Abbink, *A human-like steering model: Sensitive to uncertainty in the environment*, [2017 IEEE International Conference on Systems, Man, and Cybernetics \(SMC\) 2017 Oct 5](#) (pp. 1487-1492)

OPEN DATASETS

1. **S. Kolekar**, J.C.F. de Winter, and D. Abbink, *Driver's Risk Field (DRF) - Model Matlab Code*, [4TU.ResearchData. Dataset](#) (2020)
2. **S. Kolekar**, J.C.F. de Winter, and D. Abbink, *Driver's Risk Fields (DRF) - Graphical User Interface*, [4TU.ResearchData. Dataset](#) (2020)
3. **S. Kolekar**, J.C.F. de Winter, and D. Abbink, *Driver's Risk Field (DRF) - Model data*, [4TU.ResearchData. Dataset](#) (2020)

4. **S. Kolekar**, J.C.F. de Winter, and D. Abbink, *Driver's Risk Field (DRF) - Model videos*, [4TU.ResearchData. Dataset \(2020\)](#)
5. **S. Kolekar**, J.C.F. de Winter, and D. Abbink, *Driver's Risk Field (DRF) - Simulator Experiment*, [4TU.ResearchData. Dataset \(2020\)](#)

PROPOSITIONS

1. Drivers perceive and act upon the risk posed by objects beyond the lane boundaries (*this thesis*).
2. Humans have a veridical perception of objective risk, i.e., the product of the probability and consequence of an adverse event (*this thesis*).
3. Human-like adaptations emerge when the driver's perceived risk is maintained below a threshold (*this thesis*).
4. Models from which human-like behaviour emerges are the only means to make predictions about human driving behaviour in previously unseen scenarios (*this thesis*).
5. A term similar to 'jaywalker' will be invented to shame the driver of a manually driven car.
6. Autonomous vehicles would have emerged even in a world with zero road accidents.
7. No one knows the absolute truth; everything in quantitative science is a correlation.
8. All the wars in the world are due to local optima; every side thinks they are right.
9. A person can only perceive themselves through their interaction with others.
10. It is a certainty that humans care about uncertainty.

These propositions are considered opposable and defensible, and have been approved as such, by the promoters prof. dr. ir. D.A. Abbink and dr. ir. J.C.F. de Winter.